The Effect of Structure, Actuator, and Sensor on the Zeroes of Controlled Structures

by

Farla Mindy Fleming

S.B. Massachusetts Institute of Technology (1988)

SUBMITTED TO THE DEPARTMENT OF
AERONAUTICS AND ASTRONAUTICS
IN PARTIAL FULFILLMENT OF THE
REQUIREMENTS FOR THE DEGREE OF

Master of Science
in
Aeronautics and Astronautics
at the
Massachusetts Institute of Technology
February 1991

Signature of Author _____
Department of Aeronautics and Astronautics
December 21, 1990

Certified by _____
Professor Edward F. Crawley
Thesis Supervisor, Department of Aeronautics and Astronautics

Certified by _____
Professor Michael Athans
Thesis Co-Supervisor, Department of Electrical Engineering and Computer Science

Accepted by _____
Professor Harold Y. Wachman
Chairman, Department Graduate Committee

The Effect of Structure, Actuator, and Sensor on the Zeroes of Controlled Structures

by

Farla Mindy Fleming

Submitted to the Department of Aeronautics and Astronautics on December 21, 1990 in partial fulfillment of the requirements for the Degree of Master of Science in Aeronautics and Astronautics

ABSTRACT

Effects on the zero frequencies of single input single output systems of design and modelling decisions are explored. The pole-zero patterns of transfer functions from input to output are studied as a function of sensor and actuator choice, namely type and impedance, and location. A variety of zero definitions are used for the studies. Where possible infinite order models are adopted to explore the design decisions so that the effects of finite order modelling are removed. The design studies are parametric in nature, so that the effects of impedance and location may be better understood. Examples focus on point or localized actuators and sensors and simple uniform structures. The sensitivity of the zero frequencies to changes in the sensor and actuator location for both collocated and non-collocated cases are presented. Non-minimum phase behavior is visible in only certain non-collocated situations. In addition to the design decisions, the zeroes are shown to be a function of the modelling technique used to model the structural response for collocated and dual systems. Methods for improving the zero predictions in the control bandwidth are suggested.

Thesis Supervisor: Dr. Edward F. Crawley

Title: Professor of Aeronautics and Astronautics

Co-Thesis Supervisor: Dr. Michael Athans

Title: Professor of Systems Science and Engineering

ACKNOWLEDGEMENTS

There are many people who have contributed to my experience as a graduate student.

To Ed, I have learned a lot from your structured approach, from both an organizational and a research level. I also haven't forgotten my pilot endeavors. Thanks for taking me up to Montpelier. See you in the Bush!

To Mike, thanks for your helpful comments and ideas along the way. Andy, thanks for your advice in my earthsattering (or not-so-earth-shattering) decisions.

To all of the Space Engineering Research Center students and staff, I wish you all the best, although I'm not dropping off the face of the earth! Javier, your experiment still lives on. Your voice of experience has been of great help to me.

To my office mates in particular, good luck. Without support, companionship, suggestions, and an audience for our ideas, where would we all be? Bob, from sleeping on countertops to wake up calls, we've worked and helped each other along. Remember today is the last day to turn in your reg day material!

Massi, thanks for everything, especially for drawing some of my figures.

To my parents. Yes, my "paper" is done. Want to read it? Thanks for your unquestioning support in all of my endeavors.

Contents

List of Figures

Chapter 1

Introduction

Although open loop zeroes are a key indicator of the eventual performance achievable in control system design, they have not received the attention given to other aspects of the controlled structures problem. Among the influential features, the transient response of systems, namely overshoot and response time, are affected greatly by the zeroes. Zeroes are critical in the disturbance rejection and isolation problems where the sensitivity transfer function becomes unity at the frequencies of the undamped zeroes. Systems with non-minimum phase zeroes have significant performance limitations. These non-minimum phase zeroes set the bandwidth limitations on both disturbance rejection and command following [1].

Zeroes effectively encapsulate in a different form information regarding the input to output characteristics of a system. For controlled structures in particular, the zeroes are closely related to the modal residues, an inner product of modal controllability and observability, as defined in Chapter 2. The focus of this effort is on the behavior of the zeroes, rather than the residues, for numerous practical reasons. Firstly, the zeroes may be found directly from experimental data and identification methods. The zeroes also allow for a direct assessment in the frequency domain of the impact on performance of various design and modelling issues. Finally, the zeroes are a concept that is easily abstracted from the single input single output to the multi input multi output case.

The zeroes need not be considered fixed parameters in the design of controlled

structures. Design of the actuator sensor system allows wide lattitude in placement of zero locations and the resulting closed loop performance. For the case of single input/ single output (SISO) feedback control of structures, collocated and dual actuator sensor pairs yield alternating pole zero patterns [2,3] which have good stability robustness properties. The pole zero spacing of these alternating pole-zero patterns can actually be controlled by choices of sensors and actuators and their location. Constant gain feedback effectiveness can thereby be improved by understanding the contributing factors to zero locations. It has been shown through experiment [4] and analysis [5] that these alternating pole-zero patterns are more robust to parameter variations than non-collocated systems where the alternating pole-zero patterns no longer exist. By understanding the nature of the greater sensitivity of non-collocated systems designers may be encouraged to leave the safe haven of positive real systems [6].

In addition to design decisions regarding the actuators and sensors, a control design relies heavily on the modelling effort to adequately capture the features of the plant dynamics. Efforts aimed at improving the model fidelity in the bandwidth and crossover region reduce the uncertainty environment in which a controller must operate. Multiplicative errors in the vicinity of zeroes may be very large and 180 degrees phase uncertainty may exist for lightly damped structures [7,8]. Most control techniques involving dynamic compensation rely on accurate models of the plant poles and zeroes in the control bandwidth [9]. These methods consist of inverting the plant dynamics and substituting desired dynamics in their stead. Experimental efforts of control design and implementation show the modelling efforts ability to predict zeroes to be a difficult problem in the control of lightly damped structures [10, 11]. Finite order modelling techniques must therefore be evaluated on their ability to predict poles *and* zeroes adequately. Control system design often requires a reduced order model consisting of only a few modes. Such model reduction techniques must also be examined for the consequences on the zeroes.

Knowledge of the zeroes is important as well in identification efforts. Modes may be made unobservable or uncontrollable corresponding to pole-zero cancellation by unwise placement of actuators and sensors. Modes which would contribute strongly to a particular performance metric should be made observable, for good characterization, and observable and controllable for closed loop performance. Knowledge of the zeroes can allow disturbance sources to be located so as to minimize performance degradation.

The research on zeroes in the controlled structures community has provided helpful insight for the controlled structure designer. deLuis [12] addressed sensor and actuator choice in a study of the optimal measurement to make with a highly distributed sensing and actuation system to produce the most banded static controller. Fanson [13] addressed the issue of actuator impedance relative to the structure to explain the feedthrough nature of the collocated open loop transfer function from active piezoelectric truss element to collocated accelerometer measurement. Williams [14] addressed transmission zero bounds for the limited case of collocated and dual systems. The zero frequencies in the s-plane are bounded by the properties of the poles of the system. His method relies on a discretized finite model of the structure. A transcendental transfer function approach was used by Wie [15]. He solved for the zero frequencies exactly, but his solution procedure has some limitations because actuation must be introduced at the boundaries of the structure. Spector and Flashner [16] carried these efforts further with a locus of the zero frequencies from the same transcendental transfer function models where actuation must be introduced at the boundaries. Their solution method does not allow determination of the zero directions, a modal controllablity and observability measure. Trends were shown of non-minimum phase behavior for a pinned-free beam as the sensor was moved successively further from the actuated hub. A few examples show the transfer function magnitude and phase to be sensitive to sensor location as the non-collocation destroys the alternating pole zero pattern.

There has been limited research into the effects on the zeroes of various modelling methods. Wie [15] and Spector and Flashner [16] address the options of structural models based on both products and summations to determine which yield more accurate dynamic response. Most modelling efforts for complicated structures however consist of finite element or Rayleigh Ritz assumed modes models. Wie [15] showed that consistent mass finite element models and lumped mass models yielded very disparate results for predicting the zero frequencies. Williams proved that for Ritz models with actuators and sensors which are physically collocated and acting along the same axis, the zeroes converge with Rayleigh convergence characteristics as the model order is increased. For non-collocated systems, the zeroes predicted by finite order models become more questionable as pointed out in an example by Wie [15]. Models of systems which physically are minimum phase may contain non-minimum phase zeroes due to truncation.

The first objective of this work is to explore the effects of the zero frequencies of the design decisions of sensor and actuator type, impedance relative to the structure, and location. Studies of the effects of these decisions are performed parametrically and finite order modelling issues are decoupled from such studies when possible.

In addition as a second objective, the effect on the zero frequencies of finite order modelling methods are examined, and methods for improving the structural models to improve the zero predictions are explored.

The issues explored in this work are done so for the single input single output case. Clearly, if the control system were to use successive loop closure from individual inputs to outputs these analyses would still be valid. For the general multi input multi output case however these results need to be extended, just as Williams [14] extended the results of Gevarter [2] regarding alternating poles and zeroes for systems with collocated sensors and actuators acting along the same axis.

In this study, a variety of definitions of a zero are used, depending on the nature of the model and the information to be determined. Hence, Chapter 2 introduces an

array of accepted or proposed definitions of zeroes as well as secondary information to be found from these definitions. These definitions are based on a transfer function description, a residue expansion description, a transmission blocking description, and a root locus description. The additional information to be found from these definitions consists of controllability and observability tests, one of which is the zero direction. The equivalence of the various definitions is established so that results based on one definition are uniformly valid for zeroes in general. A sensitivity analysis based on the transmission zero definition is performed to examine the sensitivity of the zeroes to actuator and sensor location. The sensitivity of the controllability and observability tests may also be explored.

In chapter 3, three basic design issues are addressed which directly influence the zero frequencies. The design issues are actuator and sensor type, impedance relative to the structure, and location. Each of these issues is individually discussed with reference to the pole-zero pattern which they produce. The design decisions of sensor and actuator (S/A) choice and placement are coupled as well to the nature of the structure on which the sensors and actuators act. While collocated and dual sensors and actuators produce alternating pole-zero patterns irrespective of the structure, a class of sensor and actuator pairs, referred to as pseudo-dual, which guarantee alternating poles and zeroes on particular structures are identified. The issue of impedance of a sensor and actuator pair is studied by means of a static model of an actuator whose stiffness may be parameterically varied so that the actuator trasitions uniformly from a force to a displacment actuator. The sensor is similarly varied as a mixture of a force and displacment measurement. The resulting zero loci are presented. A study of the location of the sensor and actuator is performed via a solution scheme based on the zeroes as a limiting high gain solution of system poles. Both zero frequencies and directions for infinite order systems may be derived using this method. The zero loci as a function of the collocated and non-collocated sensor and actuator pair are presented for a variety of structures. The sensitivity of the

zeroes to parameter variations for both collocated and non-collocated cases are studied parametrically. The sensitivity of the zeroes for both collocated and non-collocated systems may be larger at different locations on the structure.

In chapter 4, the effects on the zeroes of structural modelling are examined. The convergence behavior of the zeroes is explored given a particular modelling technique as a function of the number of degress of freedom in the model. The prediction of the zeroes in the control bandwidth are affected by two finite order modelling techniques, truncation and discretization. The ability to improve zero predictions by including information other than the open loop dynamic modes is explored. It is desired to determine what information to include in a low order model to best predict the poles and zeroes with fidelity in the control bandwidth.

Chapter 2

Zero Definitions

In this chapter several definitions of zeroes for both the single input single output (SISO) and multi input multi output (MIMO) cases are presented. It is desired to establish that all the zero definitions for the SISO case yield numerically equivalent zeroes and likewise that all of the MIMO zero definitions yield numerically equivalent zeroes. This equivalence of zeroes will be necessary to abstract the results based on a particular zero definition to results for zeroes in general. These zero definitions are compared not only for the equivalence of zeroes predicted but on the ability of the definitions to provide other useful information such as observability and/ or controllability tests.

The most basic concept highlighted by all of the definitions presented is the fact that the zeroes are clearly a function not only of the homogeneous system, but of the nature of actuation and sensing as well. While the homogeneous behavior of a system is described only by the A matrix, the zeroes are a function of the A, B, C, and D matrices. The B matrix captures information about the type of actuators and their location, a measure of how effectively the control inputs can influence the states of the structure. Similarly, the C matrix embodies the type of sensors and their ability to measure the activity of the states. The D matrix captures the direct static feedthrough from the actuators to the sensors. It is obvious that modelling and design efforts which attempt to capture the zero information adequately must concentrate equally on the structural model and the actuation and measurement mechanisms.

Building on this fundamental concept is the notion of the zeroes as a controllability and observability measure. Often coupled to the solution of the zeroes is a test for modal controllability and observability. A weakly controllable or observable mode is characterized by near pole-zero cancellation. The limiting case of this is a pole-zero cancellation which is a necessary condition for a loss of controllability or observability. Often these poorly observable or controllable modes are truncated from a model as in model reduction techniques such as Modal Cost Analysis [17]. Instead of this truncation process, the placement of the zeroes can be incorporated in the design process to ensure good modal controllability and observability if there is an understanding in design of how to control zero placement. These zero definitions therefore must yield the necessary design information.

With these fundamental concepts in mind, the zero definitions are presented first for the SISO case and then extended to the MIMO case. Before any definitions are given the criteria for a comparison of the zero defintions are explained. The highlights and implications of the individual definitions are discussed as each definition is presented. The equivalence of the various definitions in predicting the zeroes is determined. Finally, a sensitivity analysis of the zeroes which highlights the effects of various parameters on the zeroes is performed based on one of the zero definitions.

2.1 Zero Definitions for the SISO Case

There are numerous possibilities for mathematically defining a zero, all of which provide a different prespective on the physical implication of zeroes. The goal here is to present four commonly cited definitions of zeroes and show that they all provide numerically equivalent information. Some definitions capture more of the physical information such as observability and controllability tests. Others, due to the nature of the mathematics, do not yield explicit values for the zeroes.

The four definitions chosen for discussion here are based on common system response descriptions or on operational definitions. Two of the zero definitions are

based on a description of a system response in the frequency domain, a product expansion and a summation expansion. There are also two operational definitions of zeroes presented , based on a transmission blocking property of zeroes and on the root locus definition of zeroes as a limiting high gain feedback location of closed loop poles. Of these four definitions, three assume a response with no initial conditions. The fourth, the transmission blocking definition, incorporates the initial condition response as well. Yet all of the four definitions for the SISO case implicitly or explicitly yield numerically equivalent values for the zeroes. All of these four definitions are discussed first for the SISO case in this section and then extended to the MIMO case in the next section.

While the zeroes calculated by the methods are numerically equivalent, each of the zero definitions provides a different framework for understanding the effect of the zeroes and for calculating them. These numerically equivalent zeroes may be categorized as *transmission* zeros and *pole cancellation* zeroes. Transmission zeroes derive their name from the the transmission blocking property of zeroes. The transmission zeroes can be thought of as an interference of all the modal contributions. A limiting case of these *interference* zeroes is a pole cancellation zero, but the pole cancellation zeroes are always maintained as a distinct group separate from the transmission zeroes [18]. Pole cancellation zeroes have also been referred to as input or output or input-output decoupling zeroes [18]. While all of the definitions capture the effect of the transmission zeroes and the limiting case pole cancellation zeroes, the definitions do not always provide a means for calculating them explicitly. In particular, pole cancellation zeroes must be found before being cancelled by a pole which would result in the pole and zero both being unobservable. Pole-zero cancellation is often desirable, and hence the definitions are compared for their ability to numerically predict such occurences.

In addition to the ability of the definitions to predict the pole cancellation zeroes, the definitions can be compared and contrasted for their ability to provide further

information about the controlled and observed system. A zero that cancels a pole implies that there is a loss of observability and/ or controllability of the mode associated with the pole. Certain zero definitions produce explicitly the discriminating evidence of which of the modal controllability or observability has been lost. For the other definitions this information can be obtained but it requires additional calculations to find the modal observability and controllability. One method for determining the character of the pole cancellation zero is by looking at its corresponding direction. Just as poles have a direction known as an eigenvector, the zeroes have a corresponding zero direction. This zero direction provides information about whether the interference is at the limiting case of a pole cancellation zero. The zero direction can also be used to discern when a pole-zero cancellation is due to a loss of observability versus a loss of controllability or in fact due to both. Only certain definitions can provide this zero direction information which is clearly valuable.

To provide a consistent framework for presenting the various definitons, a state space description of the system is adopted,

$$\begin{aligned} \dot{x} &= Ax + bu \\ y &= cx \end{aligned} \tag{2.1}$$

where $x \in R^n$, $u \in R^1$, $y \in R^1$. For this SISO system, the plant is square. The performance variable (or output) is denoted by y. The system matrix A has right and left eigenvectors given by V and W respectively, where each column of V, v_i, and each row of W, w_i^T, correspond to the eigenvectors of a given mode. The input-output relation from $u(s)$ to $y(s)$ is given by $g(s)$.

$$g(s) = \frac{y(s)}{u(s)} \tag{2.2}$$

The zero definitions are presented and discussed consecutively, beginning first with the transfer function and residue expansion definitions. The transmission blocking and root locus definitions then follow.

The response of a system with no initial conditions can be represented as a ratio of products of factors of a numerator and denominator polynomial. This is referred to as a transfer function description.

Transfer Function Definition 1 *The transfer function from input u to performance variable (or output) y is a scalar and is given by*

$$\begin{aligned} g(s) &= c(sI - A)^{-1}b \\ &= \frac{cQ(s)b}{det(sI - A)} \\ &= \frac{\psi(s)}{\phi(s)} \\ &= \prod_{i}^{n} \frac{(s - z_i)}{(s - p_i)} \end{aligned} \tag{2.3}$$

where $Q(s)$ is the matrix of cofactors of $(sI - A)$and z_i, p_i are the i^{th} zero and pole respectively. The numerator and denominator, $\psi(s)$ and $\phi(s)$, are polynomials in s. The zeroes are the roots of $\psi(s)$ while the poles are the roots of $\phi(s)$.

The calculation of the transmission zeroes, or the interference zeroes, and the limiting case of the pole cancellation zeroes, are possible from this definition because the numerator and denominator are solved separately. This definition does not explicitly provide for a discriminating test to determine whether a pole-zero cancellation corresponds to a loss of observability or controllability or both. This information can only be found by a separate calculation of V and W and then a test of the modal controllability $\mathcal{C}_i = w_i^T b$ and modal observability $\mathcal{O}_i = cv_i$. Zero directions, another observability and controllability test, can not be found from this system description.

The transfer function definition of zeros lends itself to one possible physical interpretation of zeroes. The transfer function, as expressed in a block diagram form, is a serial processing of an input $u(s)$ through successive filters, namely the poles and zeroes. There is however no specified order or grouping of these filters specified by the transfer function description.

As opposed to a product expansion, the residue expansion zero definition uses a summation expansion description of the response with no initial conditions.

Residue Expansion Definition 1 *The performance variable (or output) is described by a summation of the response of each mode weighted by its modal residue, where the modal residue is the product of the modal observability, cv_i, and modal controllability, $w_i^T b$.*

$$g(s) = \sum_{i=1}^{n} \frac{r_i}{(s - p_i)} = \sum_{i=1}^{n} \frac{cv_i w_i^T b}{(s - p_i)} \tag{2.4}$$

The pole cancellation zeroes which signify a loss of observability or controllability or both occur at those p_i at which the modal residue $r_i = 0$. The other zeroes, the transfer function or interference zeroes are those frequencies at which the contributions of each mode sum to zero.

The zeroes predicted from this system description are numerically equivalent to those zeroes defined via a transfer function approach. The residue expansion is simply a partial fraction expansion of the transfer function definition.

Pole cancellation zeroes can be found in the expanded form, where each individual residue is calculated so that a zero residue is accounted for. If instead $g(s)$ is evaluated on a frequency by frequency basis, the pole cancellation zero is invisible, as is the pole at the same frequency. Unless the poles of the system are known *a priori*, the pole cancellation zeroes are not detected. This is similar to the case of the transfer function definition, where teh numerator and denominator polynomial must be evaluated separately. Once the response is evaluated on a frequency by frequency basis, the pole cancellation is invisible. Modal observability and controllability are available directly and hence the zero definition does allow for the classification of a pole cancellation zero as one due to a loss of observability and/ or controllability. Unfortunately, the interference or transmission zeroes are not easily calculated. They cannot be observed explicitly as in the transfer function system description, but must be solved for either by evaluating the summation on a frequency by frequency basis or by combining the expansion under a common denominator if possible. Zero directions,

as one particular observability or controllability measure cannot be found from this definition.

This form has the ability to directly represent the SISO system response as a modal decomposition and as such provides a modal description of the manifestation of zeroes. A mode that is almost uncontrollable or unobservable can easily be noticed by its small modal residue. The residue expansion description infers that the transmission zeroes, i.e. the zeroes that do not cancel poles, arise due to the effective summing to zero of all the modal responses. Thus the zeroes capture both the observability and controllability of an individual mode as reflected by a pole-zero cancellation, and they are simultaneously an aggregate quantity, a function of all the modal controllabilities and observabilities. It is using this definition that W. B. Gevarter proved that flexible systems with collocated and dual sensors and actuators have alternating pole-zero patterns which result from all positive modal residues [2].

It is easy to see from a modal summation how the damping of the zeroes may or may not be affected by the damping of the poles. The frequency domain representation of a second order response is a function of the damping only within a narrow region about ω_n. Outside of this region, the response is largely independent of damping. When the individual modal responses are summed together, the damping of the zero will depend on the damping of the pole only if the pole-pole spacing is small. These results are consistent with [14] for the case of general modal damping. The damping of the zeroes is bounded by the damping of the poles, and is a function of the pole-pole spacing. The zeroes are the high gain limit of the poles in a root locus sense. In order to tailor the high gain characteristics of the system response with increased damping, only those modes that will influence the damping of the zeroes need be treated.

The previous two definitions of zeroes focused on a system response description. The next two definitions are characterized by the operational description of zeroes.

Using the interpretation of a zero as a frequency at which a signal is absorbed, a zero can be defined which expresses this transmission blocking phenomenon directly.

Transmission Blocking Definition 1 *A plant has a zero at a frequency z_k if there exists an ξ_k belonging to R^n, and a u_k a scalar, not both zero, so that for the system*

$$\begin{aligned} \dot{x} &= Ax + bu_k e^{z_k t} \qquad x(0) = \xi_k \\ y &= cx \end{aligned} \tag{2.5}$$

$y(t)$, a scalar, is zero for all $t \geq 0$. This corresponds to the solution of a generalized eigenvalue problem which is square:

$$\begin{bmatrix} z_k I - A & -b \\ -c & 0 \end{bmatrix} \begin{bmatrix} \xi_k \\ u_k \end{bmatrix} = 0 \quad or \quad \begin{bmatrix} \eta_k^T & \gamma_k \end{bmatrix} \begin{bmatrix} z_k I - A & -b \\ -c & 0 \end{bmatrix} = 0 \tag{2.6}$$

where the right and left eigenvectors of this generalized eigenvalue problem are the right and left zero directions respectively. The left zero direction corresponds to the initial conditions and input of the adjoint system, (A^T, c^T, b^T).

The zeroes of this definition are numerically equivalent to the zeroes defined via the two previous definitions [19]. This definition allows the calculation of the transmission zeroes and the limiting case of the pole cancellation zeroes explicitly, as well as a direction for each zero. Information regarding the loss of observability or controllability in the instance of a pole-zero cancellation is available and can be found from the zero direction. If there is a loss of observability of mode i, then $cv_i = 0$. The right zero direction is then given by $[v_i 0]^T$. The null portion of the zero direction is included for the instance of a non-zero direct feedthrough term from the input to the output. Similarly a loss of controllability is signified by $w_i^T b = 0$. This ensures a left zero direction $[w_i{}^T 0]$. From the definitions presented thus far, only this transmission zero definition allows for the solution of a zero direction.

This zero definition is a direct statement of the fact that the zero is an input frequency at which the output is constrained to be zero for all time. This definition, unlike any of the others, includes the initial conditions in addition to the zero state

response. This transmission zero definition has the advantage of yielding both the transmission zeroes and the pole cancellation zeroes and the zero direction explicitly. As an eigenvalue problem, this definition is in a desirable form for performing other zero analysis work. In Section 2.3 a sensitivity analysis of the zeroes to parameter variations is performed using this definition.

One final definition of a zero uses the effect of feedback on a system. The zero can be expressed as the finite termination points of a root locus.

Root Locus Definition 1 *A SISO system as described above has the scalar transfer function* $g(s) = c(sI - A)^{-1}b$. *The finite zeroes of this system are the finite zeroes of the return difference* $1 + \frac{1}{\rho}g(s)$ *in the limit as* $\rho \to 0$.

In the case of an optimally posed full state feedback or output feedback problem, the finite zeroes are the finite asymptotic locations of the roots of the root square locus. This locus is defined by the roots of $1 + \frac{1}{\rho}g(-s)g(s) = 0$ *and hence is symmetric about the imaginary axis, so the zeroes occur in mirror image pairs. The locus of roots can be defined equivalently by the eigenvalues of the Hamiltonian system as* $\rho \to 0$.

$$Z = \begin{bmatrix} A & \frac{1}{\rho}b^T b \\ -c^T c & -A^T \end{bmatrix} \tag{2.7}$$

The root square loci will terminate in the limit as $\rho \to 0$ *at the location of the zeroes. If* $g(s)$ *has a non-minimum phase zero, then* $g(-s)$ *has a corresponding LHP zero.*

The zeroes found from this root locus perspective, specifically the zeroes of $g(s)$, not $g(-s)$, are the same zeroes as may be found by the other definitions [19]. Pole-zero cancellations can be found via this approach. To determine whether the pole-zero cancellation implies a loss of observability or controllability or both, a separate calculation of $w_i^T b$ and cv_i must be performed. As in the transfer function definition the modal controllability and observability must be found separately. The zero direction, thus far only calculable from the transmission zero definition, has a physical interpre-

tation in this root locus definition, explained next. The zero direction however, must be calculated separately.

The physical interpretation of the root locus definition of a zero is as the closed loop pole of an associated system with infinite gain. If a displacement on a structure were being regulated, the zero of the system would correspond to the pole of the same system with that specific displacement measurement location fixed. This is shown to be the case in Chapter 3. The zero direction corresponds to the closed loop mode shape as well as the reaction forces necessary at the fixed measurement locations to keep the closed loop mode stationary at these measurement points. The closed loop mode shape is effectively contructed of open loop modes with an appropriate set of initial conditions.

Four alternatives to describing and calculating zeroes for SISO systems have been presented. While each of the above definitions implies a different solution approach, the two types of zeroes, the interference zeroes, or transmission zeroes, and the pole cancellation zeroes that are calculated from the individual methods are all numerically equivalent. A comparison of the zero definitions was made based on their ability to capture the pole cancellation zeroes, discriminate between loss of observability or controllability, and to produce a zero direction as one particular measure of observability and controllability. All of the definitions predict pole cancellation zeroes, although as in the residue expansion definition, it is possible to miss the pole-zero cancellation if the expansion is evaluated on a frequency by frequency basis. Only the residue expansion and the transmission blocking definitions provide direct modal controllability and observability measures without further calculation. While the root locus definition yields a different physical interpretation of the zero direction, it must be found separately, and hence only the transmission blocking definition provides the zero direction as a controllability and observability measure. It is at least clear from the various methods, in particular the residue expansion and transmission blocking definitions that the zeroes are closely linked to the controllability and observability

measures.

Each of the zero definitions has its merits and all of the methods can easily be extended to the case of infinite order systems. In the next section, a presentation is made extending these SISO definitions to the MIMO case.

2.2 Extension of the Zero Definitions to the MIMO Case

The definitions of the zeroes in SISO systems can easily be extended to the MIMO case. Just as for the SISO scenario, it is desired to compare the information about zero predictions and related topics such as controllability and observability and zero directions for the various MIMO definitions. This discussion of the MIMO case is also motivated by a need to highlight the effects of extending the zero definitions to the MIMO case.

One important new aspect of the MIMO zero definitions is the possibility of having an unequal number of inputs and outputs. The result of such a non-square system is the appearance of a new type of zero, different from the zeroes of a pole-zero cancellation and different as well from the interference or transmission zeroes. This new type of zero has been called a compromise zero [20]. These MIMO compromise zeroes are distinctly unrelated to the other types of MIMO zeroes which as in the SISO case are generally called transmission zeroes and pole cancellation zeroes. The non-square case will be treated whenever possible in the various definitions.

In the following definitions a state representation of the following form is assumed:

$$\begin{aligned} \dot{x} &= Ax + Bu \\ y &= Cx \end{aligned} \tag{2.8}$$

where $x \in R^n, u \in R^{n_i}$, and $y \in R^{n_o}$. The number of inputs and outputs respectively are given by n_i and n_o. The transfer function matrix (TFM)

$$G(s) = C(sI - A)^{-1}B \tag{2.9}$$

If the system is not square, then all three types of zeroes, the transmission zeroes, the pole cancellation zeroes, and the compromise zeroes, are the LHP zeroes of

$$\phi(s)\phi(-s)det[G(-s)^T G(s)] = 0. \tag{2.12}$$

Just as in the SISO case, all zero types, now three, may be found via this transfer function definition. Similar to the SISO case, information regarding observability and controllability is not available from this definition. The zero direction is also not available from this system description, just as in the SISO case.

This definition implies that there exists certain input signals at the inputs, which enter the system at each input in an appropriate ratio to the other inputs, and which produce no response at any of the outputs. The determinant is taken to determine the frequencies at which this occurs.

It is possible through special matrix multiplications to transform the TFM $G(s)$ into a diagonal form with rational polynomials on the diagonal. The poles and zeroes of these individual transfer functions form the set of poles and zeroes of the system, not of the individual TFM elements. This is known as the Smith McMillan form. That there is this bridge between the TFM and the system zeroes is interesting, but the Smith McMillan form is not used often because of computational difficulties [20].

The next system response description is the residue expansion which is extended to the MIMO case. Generalizing the SISO residue expansion to the MIMO case entails expressing the system TFM as a residue expansion.

Residue Expansion Definition 2

$$G(s) = \sum_{i=1}^{n} \frac{R_i}{(s-\lambda_i)} = \sum_{i=1}^{n} \frac{Cv_i w_i^T B}{(s-\lambda_i)} \tag{2.13}$$

where R_i is the residue matrix of the i^{th} pole. If the i_{th} MIMO pole at $s = \lambda_i$ is cancelled by a MIMO transmission zero then $R_i = 0$. When $G(s)$ is square, the transmission zeroes are the frequencies at which the modal responses at each output sums to zero.

The author has not seen a this definition expressed for the non-square case, that is how the transmission zeroes are distinguished from the compromise zeroes. For the square case, the transmission zeroes and the pole cancellation zeroes from a residue expansion are equivalent to those predicted from the previous transfer function description. This definition captures the pole cancellation zeroes by means of a test on R_i. Just as in the SISO case, the pole cancellation zeroes are found explicitly only when the residue expansion is is written out in expanded form so that the residues may be tested. If $G(s)$ is evaluated on a frequency by frequency basis, the pole cancellation zeroes can not be seen unless it is known that a single mode response is not visible in any of the ouputs. The zeroes of individual TFM elements are identical to the zeroes of a SISO plant with the appropriate input and output corresponding to that element. As in the SISO scenario, this definition provides the modal observabilities and controllabilities directly, however a zero direction is not available from this definition.

For square systems the MIMO zeroes' transmission blocking property extends exactly. For an appropriate initial condition and input which is now a vector, the zero is at a frequency such that all outputs are zero for all time.

Transmission Blocking Definition 2 *For square systems, the generalized eigenvalue problem for describing the transmission blocking property in the MIMO sense is conveyed by*

$$\begin{bmatrix} z_k I - A & -B \\ -C & 0 \end{bmatrix} \begin{bmatrix} \xi_k \\ u_k \end{bmatrix} = 0 \tag{2.14}$$

An appropriate left eigenvector can similarly be found.

For non-square systems, to find both the transmission zeroes and the compromise zeroes, the system $G(-s)^T G(s)$ is constructed as in the transfer function definition

[20]. The system $G(-s)^T G(s)$ can be recast as

$$\hat{A} = \begin{bmatrix} A & 0 \\ C^T C & -A^T \end{bmatrix} \quad \hat{B} = \begin{bmatrix} B \\ 0 \end{bmatrix} \quad \hat{C} = \begin{bmatrix} 0 & -B^T \end{bmatrix} \tag{2.15}$$

and the generalized eigenvalue problem with this new system to find the transmission zeroes and the compromise zeroes is constructed and only the appropriate LHP zeroes are the transmission, pole cancellation and compromise zeroes of the system.

$$\begin{bmatrix} z_k I - \hat{A} & -\hat{B} \\ -\hat{C} & 0 \end{bmatrix} \begin{bmatrix} \xi_k \\ u_k \end{bmatrix} = 0 \tag{2.16}$$

As in the SISO case, the transmission blocking perspective produces numerically equivalent zeroes to the root locus definition [19,20]. By the nature of the root locus definition, the zeroes found from the transfer function description are equivalent to those of the root locus description [19]. The pole cancellation zeroes can be found via this definition. Controllability and observability tests can be found in the zero directions for the square case. Unfortunately, for the non-square case there do not exist any eigenvectors for the generalized eigenvalue problem.

This transmission blocking zero definition for the square case has a distinct physical interpretation. For an appropriate initial condition and input which is now a vector, the zero is at a frequency such that all outputs are zero for all time.

The final MIMO zero definition is via a root locus perspective. For the MIMO case, in an optimal control problem, the finite zeroes are the asymptotic locations of the poles as the feedback gains are made arbitrarily large.

Root Locus Definition 2 *The MIMO root square locus ends at the finite zeroes of* $I + \frac{1}{\rho} G(-s)^T G(s)$ *as* $\rho \to 0$.

These zeroes are numerically equivalent to those defined from the transfer funciton definition and the transmission zero definition. The same form exists for the posing of the zero definition. Pole cancellation zeroes can be found from this definition. Like the

SISO case, posing the root locus problem does not allow for solution of controllability and observability tests. The zero directions still have physical significance as high gain closed loop mode shapes along with appropriate reaction forces for the collocated case or internal stress resultants for the non-collocated case. These zero directions must be calculated separately.

As in the SISO case, this root locus definition of the zeroes is as a high gain solution to an associated problem.

For the MIMO case, all of the four definitions yield numerically equivalent zeroes for the square case. Excluding the residue expansion zero definition, they all yield equivalent zeroes for the non-square case as well. Solution of the non-square case is executed by a construction of the system $G(-s)^T G(s)$. All of the definitions allow for the solution of the pole cancellation zeroes although for the residue expansion definition these zeroes must be found by a test of the individual modal residues and not by evaluating the summation expansion on a frequency by frequency basis. The notion of controllability and observability of the zeroes is preserved in the MIMO case although only for the pole cancellation zeroes and the transmission zeroes. It is unclear what physical significance the compromise zeroes have. The zero directions can only be found for the square case, and are only directly available by the transmission blocking definition. The zero directions may be calculated separately for the root locus definition. The MIMO zeroes do not correspond to zeroes of individual single input single output relations but to the input output relations of the system as a whole.

The zero definitions provide a variety of perspectives on the physical meaning of zeroes as well as the difficulties that may arise in calculating or predicting them from a model. A preliminary sensitivity analysis based on the transmission zero definition is presented in the last section.

2.3 Zero Sensitivity Analysis

It is always prudent to do a first order perturbation on any design method to determine to what degree small variations in parameters influence results. A first order perturbation analysis is done for the zeroes from the generalized eigenvalue problem of the transmission zero definition since it conveniently expresses the solution of the zero explicitly. This first order perturbation corresponds to the first derivative of the zero location to small variations ϵ in the physical parameters such as the location of the sensor and actuator or the effective stiffness of the actuator relative to the structure, or the structure proper.

To perform the sensitivity analysis, the system must be square, i.e., the number of sensors and actuators must be equal, resulting in a generalized eigenvalue problem of order N as in Equation 2.14 which is cast as $\mathcal{A}\tilde{v} = z\mathcal{B}\tilde{v}$ where

$$\mathcal{A} = \begin{bmatrix} A & B \\ C & D \end{bmatrix} \quad \mathcal{B} = \begin{bmatrix} I & 0 \\ 0 & 0 \end{bmatrix} \tag{2.17}$$

and $\tilde{v}$ is the right zero direction. This perturbation analysis allows for the possibility that the eigenvalue problem is non-self-adjoint. This occurs whenever $\mathcal{A}$ or $\mathcal{B}$ is not symmetric. Both collocated and non-collocated cases may be considered. The non-self-adjoint nature of the problem implies that the right and left eigenvectors of this eigenvalue problem satisfy the biorthogonality condition $\tilde{w}_k^T \mathcal{B} \tilde{v}_k = 0$ where $\tilde{v}_k$ is the right and $\tilde{w}_k^T$ the left eigenvector.

Perturbations are described as a Taylor series expansion in a perturbation parameter γ,

$$\mathcal{A} = \mathcal{A}^{(0)} + \gamma\mathcal{A}^{(1)} + \gamma^2\mathcal{A}^{(2)} + \cdots \tag{2.18}$$

where the superscript $^{(0)}$ implies the nominal case. $\mathcal{B}$ is not perturbed since it is set by definition. The eigenvalues and eigenvectors of the generalized eigenvalue problem, namely the zeroes and corresponding zero directions, may also be represented as a

Taylor series in γ.

$$\begin{aligned} z_k &= z_k^{(0)} + \gamma z_k^{(1)} + \gamma^2 z_k^{(2)} + \cdots \\ \tilde{v}_k &= \tilde{v}_k^{(0)} + \gamma \sum_{\substack{l=0 \\ l \neq k}}^{N-1} a_{lk} \tilde{v}_l^{(0)} + \cdots \end{aligned} \tag{2.19}$$

The first order perturbation in the right zero direction is represented to lie only in the subspace of the remaining zero directions. Substituting back into the original eigenvalue statement, and collecting like terms in γ yields the first order changes in the k^{th} zero:

$$z_k^{(1)} = \frac{\left[\tilde{w}_k^T\right]^{(0)} \mathcal{A}^{(1)} \tilde{v}_k^{(0)}}{\left[\tilde{w}_k^T\right]^{(0)} \mathcal{B} \tilde{v}_k^{(0)}} \tag{2.20}$$

For the eigenvectors of this eigenvalue problem, the zero directions, the first order perturbation is expressed by the terms that couple the other zero directions to those of the k^{th} zero direction, $\tilde{v}_k$.

$$a_{pk} = \frac{\left[\tilde{w}_p^T\right]^{(0)} \mathcal{A}^{(1)} \tilde{v}_k^{(0)}}{\left(z_k^{(0)} - z_p^{(0)}\right) \left[\tilde{w}_p^T\right]^{(0)} \mathcal{B}^{(0)} \tilde{v}_p^{(0)}} \tag{2.21}$$

From this perturbation analysis, the effect on the k^{th} zero, location and direction, of changes in structural parameters, (A), sensor or actuator type or placement, (C or B), can be quickly determined to first order. The importance of the zero direction is also clear.

As an example, consider the case where there is a pole-zero cancellation due to an uncontrollable and unobservable mode. This would occur if a collocated and dual sensor and actuator pair existed. In this instance, $\tilde{v}_k = [v_k 0]^T$ amd $\tilde{w}_k^T = [w_k^T 0]$. If the B and C matrices were modified slightly to infer a small change in the collocated and dual sensor and actuator pair location, then $\mathcal{A}^{(1)}$ would have the form

$$\mathcal{A}^{(1)} = \begin{bmatrix} 0 & B^{(1)} \\ C^{(1)} & 0 \end{bmatrix} \tag{2.22}$$

where $B^{(1)}$ and $C^{(1)}$ contain both the structure and magnitude of the perturbation in the control influence matrix $B^{(0)}$, and the measurement influence matrix, $C^{(0)}$.

The left and right zero directions for the collocated and dual case are of the form $\tilde{v}_k = [v_k 0]^T$ amd $\tilde{w}_k^T = [w_k^T 0]$ when a simultaneous loss of observability and controllablity result. Hence, no effect on the k^{th} zero, $z_k^{(1)} = 0$ is perceived. This can be advantageous if it is specifically desired to try a pole-zero cancellation. This is validated for a particular case in a sensitivity analysis performed in chapter 3.

If however, the sensor and actuator pair are not collocated, the first order perturbation of the zero is no longer zero. A pole-zero cancellation is attributed to either a loss of observability or a loss of controllability but not both. Hence only the right or the left zero direction has the special form with a null portion to the vector. Consider the case of a loss of observability. The right zero direction would have the form $\tilde{v}_k = [v_k 0]^T$. If the sensor and actuator locations were then perturbed slightly with the structure of Equation 2.22, the first order perturbation in the zero would no longer be zero because the left zero direction would not have the same form as the right zero direction, namely, a null portion corresponding to the input direction.

Finally, the coupling of the zero directions is very sensitive when the zeroes are closely spaced. It would be difficult to capture the right zero direction information in a model of such a system. It is important to be reminded that the test for a loss of controllability or observability is sensitive in such a manner.

From this discussion of the various definitions of zeroes certain implications for modelling and design have become apparent. The definitions presented all yield numerically equivalent zeroes for the SISO and the MIMO cases. This allows for the abstraction of zero results based on one definition to zeroes in general as well as the results from the SISO case to be abstracted to the MIMO case. The zeroes inherently contain controllability and observability information about the corresponding mode. The type as well as the location of the sensors and actuators contribute to the location of the zeroes in the s-plane. Closely spaced zeroes imply more difficulty in adequately modelling the system and determining loss of observability and controllability, or performing model reduction techniques based on these measures. In the rest of this

work it is hoped to explore these implications in more detail to better anticipate the location of zeroes and to model them effectively.

Chapter 3

Zero Frequencies and Their Dependence on Choice and Placement of Sensor and Actuator

In the last chapter the zeroes were highlighted as a combined measure of modal controllability and observability in both the SISO and MIMO case. In general, the zeroes are a manifestation of the input to output characteristic of a system. In examining the behavior of zeroes, the influence of the sensors and actuators must be considered in pairs. The general characteristics of actuators and their sensors will therefore be reviewed.

The degree of controllability of a system via an actuator is a function of its type, impedance, and location. The actuator type can be described by the direction, the spatial distribution, and the reaction characteristics of the actuator. The directional characteristic of the actuator describes the axis along or about which the actuator acts. The spatial distribution of the actuator describes the nature of the actuation as either localized or distributed, and if distributed, how so. The reaction characteristics classify an actuator as being either a relative actuator which reacts against another part of the structure, or an inertial actuator which reacts against an external inertial mass or platform. Actuator impedance refers to the relative stiffness of actuator to the structure. At one extreme, an actuator can be considered a generalized force actuator only when it is known that the actuator stiffness or impedance is infinitessimally small relative to the structure. Conversely, at the other extreme, an actuator can act as a generalized displacement actuator only when its stiffness is very large relative to

the structure and hence has the authority to command displacement. The location of an actuator refers to the point or area of the structure, in the case of localized and distributed actuators respectively, on which the actuator acts.

Likewise, the degree of observability of a system via a sensor is a function of its type, impedance, and location. Just as for the actuator, a sensor type is characterized by its direction, its spatial distribution, and the nature of the sensor as a relative or inertially based form of measurement. Sensor impedance in this instance refers to the content of the measurement as some weighting of generalized force and displacement. A high stiffness sensor in the load path of the structure can be used to measure the force transmitted through that point. A low stiffness sensor out of the load path can be used to measure the local motion of the structure. Finally, the location of a sensor refers to the point or area of the structure over which a measurement is made.

The zeroes depend on the combination of type, impedance, and location of the sensors and actuators. Actuator/sensor pairs of the same *type* are referred to as *dual.* In other work, the term dual is sometimes used to describe sensors and actuators which are both of the same type and at the same location [21]. The meaning of dual here is of sensors and actuators only of the same type. An example of a dual S/A pair is a transverse force actuator and a transverse displacement or rate sensor. Actuators and sensors of the same relative *impedance* to the structure are referred to as *complementary.* Complementary sensors and actuators have a complementary mixture of generalized force and displacement for the actuation and measurement. A pure generalized force actuator and a pure generalized displacement sensor or a pure displacement actuator and force sensor are referred to as *complementary extremes.* The *positive complement* sensor to a given actuator is that in which the measurement is a complementary mixture of generalized force plus displacement measurement. A *negative complement* sensor allows the measurement to be a complementary combination of positive displacement minus applied force. Actuators and sensors at the same *location* are referred to as *collocated.* Collocated sensors and actuators act at

is square if the number of inputs and outputs are equal but may be non-square if $n_i \neq n_o$.

For a square system, the calculation of the transmission zeroes and the pole cancellation zeroes is an eigenvalue problem. There is some combination of inputs all at the same frequency which results in a zero reponse at all of the outputs. Hence the determinant of $G(s)$ is often taken in the MIMO zero definitions. If however the system is not square, the system is made square by constructing the system

$$G(-s)^T G(s) \tag{2.10}$$

. This new system appears repeatedly in the definitions for the non-square case.

The elements of the transfer function matrix each contain a description of the characteristics from the associated input and output. If the elements are expressed in a transfer function form, then each element is a ratio of a product of SISO zeroes to a product of SISO poles. These SISO zeroes of the individual TFM elements do not correspond in general to the MIMO transmission zeroes from all of the inputs to all of the outputs. This is one of the main distinctions between the SISO and the MIMO case.

The zero definitions for the MIMO case are presented as in the SISO case beginning first with the definitions using the product and summation expansion description of the system response and then, the definitions relying on the operational definitions of the zeroes. The transfer function definition is presented first.

Transfer Function Definition 2 *If the system is square, $n_i = n_o$, then the determinant of the transfer function matrix $G(s) = C(sI - A)^{-1}B$ can be taken*

$$det[G(s)] = \frac{\psi(s)}{\phi(s)} \tag{2.11}$$

where $\phi(s) = det(sI - A)$ as in the SISO case and the transmission zeroes and the pole cancellation zeroes are the roots of $\psi(s)$ [19].

the same point or over the same area. An example of a collocated sensor and actuator pair are a torque motor and an angular joint measurement at a common location.

The product of the actuator influence and sensor measurement corresponds to real work or power when the sensor/actuator pair is dual, a complementary extreme pair, and collocated. This special combination of sensor and actuator produces a particular pole-zero pattern that has alternating poles and zeroes. This was proven by Gevarter [2] for the SISO case using the residue expansion description of the system response given by Equation 2.4. This alternating pole-zero pattern occurs when all of the modal residues are positive or zero. This can be understood by considering the response of the sum of two undamped second order modes with positive residues. At some intermediate frequency between the poles, the two responses sum to zero since the contribution to the transfer function of the lower mode has a positive residual and phase of 180 degrees and the contribution of the upper mode has a positive residual and a phase of 0 degrees.

These dual S/A pairs, which are also complementary extremes, and collocated, yield an alternating pole-zero pattern and provide a degree of robustness to the control problem. This robustness is a system property known as hyperstability [6]. The sufficient conditions for hyperstability of structures are that S/A pairs which are a measure of power be chosen for the input and output variables. S/A pairs that are a measure of work, as opposed to power, are also allowed. Hence dual, collocated, and positive complementary or non-complementary sensors and actuator pairs ensure a hyperstable system. A hyperstable system has certain properties which describe the nature of the robustness of the system of alternating poles and zeroes. These properties are prescribed by Stieber and are summarized here [6]. A hyperstable system must have equal number of inputs and outputs. Any hyperstable system is bounded-input-bounded-output (BIBO) stable. This implies that the open loop system with dual, collocated, and positive complementary or non-complementary sensors and actuators is always BIBO stable. Hyperstability also ensures that the

closed loop system is hyperstable if the feedback form around the hyperstable system is hyperstable. Constant gain feedback with such actuation and measurement qualifies as a hyperstable system since its input output relation will be a measure of power. Linear hyperstable systems have only left half plane or purely imaginary zeroes. Such robustness properties guaranteed by dual, complementary extremes, and collocated S/A pairs are desirable.

The purpose of this chapter is to study the effects on zeroes of the design parameters of sensors and actuators, namely their type, impedance, and location. The effects on the zeroes are characterized by the s-plane pole-zero patterns. These are the open loop locations of the poles and zeroes of the plant for which the sensors and actuators have been chosen. These patterns may be described by certain criteria. It is an objective of this chapter to determine the design decisions which affect the relative spacing of the poles and zeroes in an alternating pattern, and those design decisions which destroy the alternating patterns, and hence the associated stability guarantees. It would be useful as well to understand which design decisions affect all the zeroes in a similar fashion, such as shift them all upwards in frequency. Other design choices, in contrast to affecting the relative spacing of the poles and zeroes of all modes, affect the zeroes of modes on an individual basis. Some design choices may destroy the alternating pole-zero pattern in such a way as to produce a missing zero. This may be used to produce a forward loop transfer function with enough gain margin to roll off a controller.

It is desired to study these parameters of sensor and actuator choice and placement and to determine how the zeroes are affected relative to the poles when the S/A pairs are no longer dual or complementary or collocated. Three basic studies are performed, where only one descriptor (type, impedance, or location) is explored at a time, leaving the other descriptors of the problem fixed. The first study is the effect of sensor and actuator type. For this first study, the sensor and actuator are complementary extremes (either exclusively generalized forces or generalized displacements)

and collocated. Sensors and actuators are evaluated as pairs. Dual sensor and actuator pairs are discussed as well as S/A pairs which act as dual on certain structures. The second study focuses on the impedance of the actuator and sensor relative to the structure and the use of mixed measurements. In this study the S/A pair are assumed to be collocated and dual. The zeroes are analyzed as the impedance of the actuator and the impedance of the sensor, relative to the structure, are varied parametrically. Finally, the effect on the zeroes of location on the structure of a collocated and dual S/A pair is explored parametrically. The non-collocated scenario is parametrically studied as well, viewing the non-collocation first as a perturbation on the collocated case and then as the non-collocation becomes more pronounced.

3.1 Duality of Sensor and Actuator Pairs

The zeroes are a reflection of the characteristic of a system from input to output. Sensors and actuators must be considered as pairs, of the same or different *type*. As an example of the importance of choice of type of an actuator or sensor, consider the case of a moment actuator and a transverse displacement sensor at the center of a free-free beam. These are a collocated and complementary extreme, but non-dual, pair. The actuator excites the asymmetric modes but does not excite symmetric ones. The sensor at the same center location detects the symmetric modes but does not detect any motion of the asymmetric modes of the structure. The result, from input to output, is pole-zero cancellation of every mode. The actuator produces only half of the pole-zero cancellations and the sensor produces the other half. The input-output behavior of the system is clearly a function of the type of both the sensor and actuator which must be considered as a pair.

For the purposes of exploring in this section the effects of sensor and actuator type, the actuator and sensor are assumed to be collocated, and at a fixed location. It is also assumed that the actuator and sensor are complementary extremes, that is, that the actuator is a pure generalized force and the sensor a pure displacement or

rate type.

Figure 3.1 shows schematically some common examples of S/A pairs which are dual, i.e., of the same type. Note that each dual S/A pair has the sensor and actuator acting in the same direction, over the same local area, and in the same inertial or relative sense. These localized dual pairs are rather common. An axial or in plane force and displacement pair can be used to control extension of one dimensional structures or to control in plane stretching of two dimensional structures. Out of plane control via this S/A pair is also possible with a non-isotropic structure [22]. Transverse force and displacement as well as moment and local angle can be used to control out of plane motion. Torque actuators and angular measurements are common in manipulator applications or attitude control. In addition to inertial S/A pairs there are S/A pairs that react relative to another part of the structure as in Figure 3.1(c) or (e). Examples are relative in-plane force and strain, or moment doublet and curvature. Note that a moment doublet can be created either by a pair of external moments or a pair of relative in-plane forces. While these S/A pairs by nature do not act on a single point, the actuators and sensors can be considered localized if they act over a length much smaller than the wavelength of modes under consideration. Relative sensors such as strain gages can, in the limit, measure strain at a localized location. However, as a dual measurement to a relative actuator, the strain sensor must measure the average strain over the area of influence of the relative actuator. These relative actuators are often realized with active materials such as piezoceramics, electrostrictors, or shape memory alloys [23, 12, 24, 25]. They can be embedded or surface mounted to a structure [12] or incorporated into active truss elements [13, 26].

When the S/A pairs are dual, collocated, and complementary extremes, positive residues result for all modes. In this specialized case, these residues are a measure of the actual work done by the actuator on a mode of the structure. The residue for the

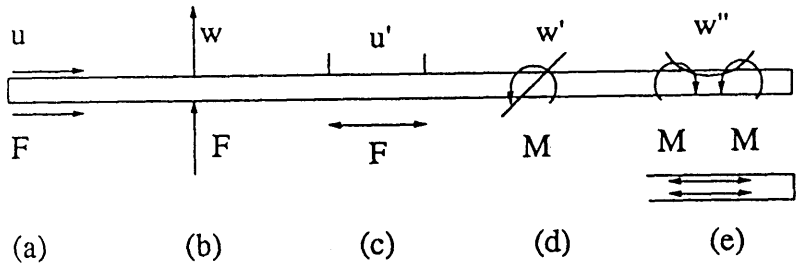

Figure 3.1: Some common examples of localized dual sensor and actuator pairs. Each dual S/A pair has the sensor and actuator acting in the same direction, over the same local area, and in the same relative sense

SISO case

$$r_i = (cv_i)(w_i^T b) \tag{3.1}$$

is composed of the inner product of the amount of generalized force an actuator exerts on a mode and the amount of generalized motion the sensor measures of that mode. Modal controllability and observability as a function of location must be computed by using the mode shape or its spatial derivative corresponding to the actuation variable type and sensing variable type. For example, modal observability of angle and as a function of location must be made with the first spatial derivative of the mode shape (i.e. the local slope). For dual sensor/actuator pairs which act along or about the same axis, the modes and their spatial derivatives representative of modal observability and modal controllability as a function of location are the same. This guarantees that dual and collocated S/A pairs always have positive residues for each mode, irrespective of the structure to which they are coupled.

It is possible for S/A pairs which are collocated and complementary extremes but are not dual to be coupled to a *particular* structure in such a way as to ensure all positive or all negative modal residues and thereby still maintain the robust properties of alternating pole-zero patterns. Negative modal residues may be allowed in the instance of no rigid body control, so that the sign of the feedback gain may be

Table 3.1: Dual and pseudo-dual sensor/actuator pairs for structures represented by spatial sinusoids

	u, w	$u\prime$, $w\prime$	$w\prime\prime$
force	DUAL		(-) PSEUDO-DUAL
force couple/moment		DUAL	
moment couple	(-) PSEUDO-DUAL		DUAL

appropriately altered. Such S/A pairs will be referred to as *pseudo-dual.*

The vibrational motion of a general uniform structure can be described by two characteristic functions, *sinusoidal* and *exponential.* For example, low order structures such as one dimensional uniform rods are governed completely by sinusoidal functions. One dimensional beams are governed by both sinusoidal and exponential functions, depending on the boundary conditions. Pseudo-duals can be discussed with reference to two pure classes of structures, those governed completely by pure sinosoidal functions, and those governed by pure exponential functions. The effects of a structure governed by a combination of functions can then be considered.

Table 3.1 portrays a variety of combinations of collocated actuators and sensors which can be considered localized. Displacement and its first and second derivative are considered as sensors. Any of these sensors can be replaced by their corresponding rates. Axial displacement is represented by u, axial strain by its first derivative, $u\prime$, as in Figure 3.1 (a and c). Similarly, transverse displacement is represented by w, transverse slope by $w\prime$, and curvature as $w\prime\prime$ as in Figure 3.1 (b,d, and e). A force, force couple or moment, and moment couple are considered as actuators. A force actuator represents either an axial force or a transverse force. A force couple describes either a relative force actuator when in the axial direction as in Figure 3.1(c) or a pure moment when in the transverse direction as in Figure 3.1(d). A moment couple may be realized by either two closely spaced torque actuators or more likely by a pair of

force couples both in the axial direction but off the neutral axis. For one dimensional axial motion only the top left two by two section of Table 3.1 is applicable.

The dual S/A pairs in Table 3.1 are along the diagonal. Dual S/A pairs always have a positive inner product because the mode shape or its spatial derivative used to calculate the controllability and observability are always equal. Now consider a S/A pair off the diagonal such as the case of a transverse force actuator and a curvature sensor. If the motion of the structure is sinusoidal, as is the case assumed for this table, then the modal representation which corresponds to a transverse force is the zeroth derivative, and the modal representation which corresponds to a curvature sensor is the second derivative, and hence is spatially 180 degrees out of phase. For every mode, and for any collocated location of such a pair on such a sinusoidal structure, the modal residue is always negative yielding alternating pole-zero patterns. Similarly, if a moment couple and transverse displacement are considered, the modal representation corresponding to the observability and controllability are also 180 degrees out of phase. These two S/A combinations are called pseudo-dual. It should be emphasized that for structures governed by spatial sinusoids, these pseudo-duals are consistently out of phase with each other for each mode. The other combinations of sensor and actuator pairs may not be considered pseudo-dual. Consider a force actuator and a slope sensor. Then if the modal representation which corresponds to that force is sinusoidal, then the modal representation of the slope or angular measurement is cosinusoidal. These functions will not be consistently of the same sign for all modes for any given location. This is true of any sensor and actuator pair on a structure governed by spatial sinusoids where the sensor and actuator operate on modes separated by only one spatial derivative. Thus the only pseudo-duals are those indicated in Table 3.1.

A similar discussion is used to produce Table 3.2 for structures described by purely exponential functions. The second derivative of an exponential yields another exponential, scaled but of the same sign, as opposed to the sinusoidal case where a minus

Table 3.2: Dual and pseudo-dual sensor/actuator pairs for structures represented by spatial exponentials

	u,w	*u'*, *w'*	*w''*
force	DUAL		PSEUDO-DUAL
force couple /moment		DUAL	
moment couple	PSEUDO-DUAL		DUAL

sign is present. The pseudo-duals are the same pairs as in the sinusoidal case but a 180 phase shift no longer exists. For the other sensor and actuator combinations where the modal representation of the controllability and observability are distinct from each other by one spatial derivative, the derivative of an exponentially decreasing mode shape with the positive spatial coordinate has one sign, while that of an exponentially increasing mode shape with a positive spatial coordinate has another. Hence, it is not possible to ensure all positive or all negative residues for such sensor and actuator pairs unless it can be determined that the sensor and actuator are located at a position governed exclusively by exponentially increasing or exponentially decreasing mode shapes for all modes. One example of such a case is a clamped-free beam with transverse force actuator and slope sensor at the free end.

It may be desirable to use such pseudo-duals in place of duals for a particular objective. As an example, deLuis [12] proved that for highly distributed induced strain actuators which act as distributed moment couples, the optimal measurements to yield the most banded fixed gain controllers are transverse velocity and a curvature measurement. The relation between transverse velocity and moment couple is pseudo-dual.

For most general structures, the open loop mode shapes are not purely sinusoidal or purely exponential, but are a mixture of such contributions so as to satisfy the boundary conditions. For these S/A pairs to act as pseudo-duals, the mode shapes

of the structure must be dominated by sinusoidal or by exponential modes in the vicinity of the collocated S/A pair for every mode in order to ensure a consistent sign on the residue. A simple test for the sign of the modal residue of each mode, at a collocated location may be found. This test may be performed to determine the dominating spatial function (sinusoidal or exponential) in a region of a structure. If a mode shape is dominated by spatial sinusoids, then the displacement and curvature should be consistently out of phase, or

$$\phi(x)\phi''(x) < 0 \tag{3.2}$$

Similarly, if a mode shape is dominated by spatial exponentials, the displacement and curvature mode shape should be in phase, as discussed in Tables 3.1 and 3.2. Hence,

$$\phi(x)\phi''(x) > 0 \tag{3.3}$$

implies exponential dominance.

The transition point from a region of exponential dominance to sinusoidal dominance may also be found. A necessary condition for the transition point is given by

$$\phi(x)\phi''(x) = 0. \tag{3.4}$$

Equation 3.4 is zero when either the displacement mode shape or the curvature mode shape is zero. However Equation 3.4 is not sufficient to declare a point a transition point from sinusoidal to exponential dominance of the mode shape because every node of a sinusoidal function satisfies this criterion. The additional test for transition is simply that the points satisfying Equation 3.4 must not be local maxima, but that

$$\frac{d}{dx}[\phi(x)\phi''(x)] \neq 0. \tag{3.5}$$

This ensures that $\phi(x)\phi''(x)$ transitions from a negative to a positive product. Hence, if $\phi(x)\phi''(x)$ is tested to be always positive or always negative in a region then the S/A pairs as outlined in Tables 3.1 and 3.2 are pseudo-dual for all modes and can be used as a dual pair, producing alternating pole-zero patterns.

These criteria for the transition point, Equations 3.4 and 3.5 have not assumed any specific form of structure on which the S/A pair act. The test is a general test to determine the sign of the modal residues for all modes as a function of the collocated location of the sensor and actuator. If the mode shapes consist of sinusoidal and exponential functions, then the test yileds information regarding the dominating function in a region. Because of the nature of the mode shapes for different uniform beam structures, a set of general criteria for determining the suitability of such structures for pseudo-dual S/A pairs may be found. For all $\phi(x)$ governed by a mixture of sinusoidal and exponential functions, the displacement mode shapes take the form

$$\phi(x) = cosh(\frac{\lambda_i x}{l}) - \sigma_i sinh(\frac{\lambda_i x}{l}) + \begin{cases} cos(\frac{\lambda_i x}{l}) - \sigma_i sin(\frac{\lambda_i x}{l}) & (a) \\ -cos(\frac{\lambda_i x}{l}) + \sigma_i sin(\frac{\lambda_i x}{l}) & (b) \end{cases} \tag{3.6}$$

The curvature mode shapes have the same form except that (a) and (b) are reversed. Therefore the product of $\phi(x)\phi''(x)$ has a constant form for all possible combinations of boundary conditions for uniform beams. This product is only zero when either the diplacement or the curvature mode shape has a node location. Hence, the displacement and curvature mode shapes can show immediately whether such a transition point between sinusoidal and exponential functions may exist. The slope of the product is then examined to determine which of these is actually the boundary between the sinusoidally and exponentially dominated regions.

The test for sinusoidal or exponential behavior of a structure in a particular region, as well as the transition point from one region to another are illustrated by means of two examples. Figure 3.2 shows the product $\phi(x)\phi''(x)$ for the first and second modes of a free-free beam where $\phi(x)$ is given by Equation 3.6(a). The middle region is governed by sinusoidal functions since the product is negative while the outer region is dominated by exponential functions since the product is positive. The criteria of Equations 3.4 and 3.5 are both met at the transition points. With increasing mode number the exponential regions become smaller. In this free-free beam instance, the displacement/moment couple S/A pair should be placed between the nodes of the first

mode to assure negative pseudo-dual behavior for all modes. This S/A pair could also be placed at the very tips of the free-free beam to ensure positive pseudo-dual behavior for all modes. However, at the tips, the modal observability or controllability would be zero for every mode.

Figure 3.3 displays the product $\phi(x)\phi''(x)$ for the first two modes of a clamped-free beam where $\phi(x)$ is given by Equation 3.6(b). The first mode of a clamped-free beam is purely exponentially dominated since the product is positive everywhere. In order for a pseudo-dual to produce alternating pole-zero patterns, the structure must be governed exclusively by either a sinusoidal or an exponential function for every mode. This is necessary because the residues of pseudo-duals on sinusoidal structures are negative while those on exponential structures are positive. Hence, for the clamped-free case, a pseudo-dual S/A pair such as a moment couple and transverse displacement sensor may not be be used. Only at the boundaries of the structure, exponential behavior is assured for each mode. At the boundaries of the clamped-free beam however, the moment couple actuator or the transverse displacement sensor will lose authority.

If it is assumed that the exponential contribution to the mode shapes occurs exclusively near the boundaries, then the first node locations of the displacement and curvature mode shape determine the transition point from exponential to sinusoidal dominance. The first zero of the criterion given in Equations 3.4 is synonymous with the location of the first node, which can be approximated for a uniform beam by a Taylor series of the mode shape about the end of the beam. Using the mode shape described by Equation 3.6(a)

$$\begin{aligned} \phi(0) = 1 + \frac{\frac{\lambda x}{l}^2}{2!} + \frac{\frac{\lambda x}{l}^4}{4!} + \cdots \\ -\sigma(\frac{\lambda x}{l} + \frac{\frac{\lambda x}{l}^3}{3!} + \frac{\frac{\lambda x}{l}^5}{5!} + \cdots) \\ +1 - \frac{\frac{\lambda x}{l}^2}{2!} + \frac{\frac{\lambda x}{l}^4}{4!} + \cdots \end{aligned} \tag{3.7}$$

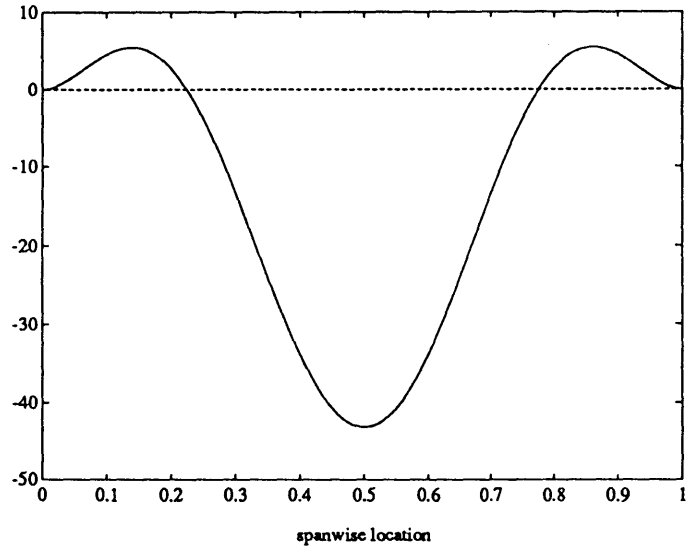

(a)

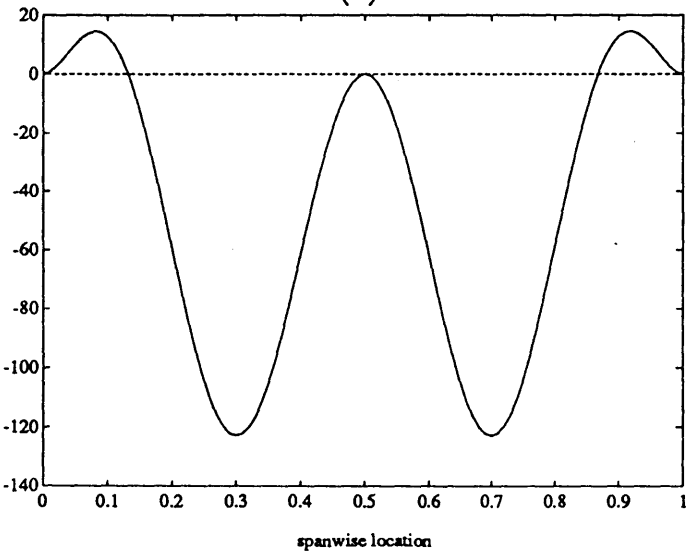

(b)

Figure 3.2: $\phi(x)\phi''(x)$ for the first (a) and second (b) modes of a free-free beam as a function of the span. Positive values for $\phi(x)\phi''(x)$ imply exponential function dominance of the mode shape in that region. Negative values for $\phi(x)\phi''(x)$ imply sinusoidal dominance.

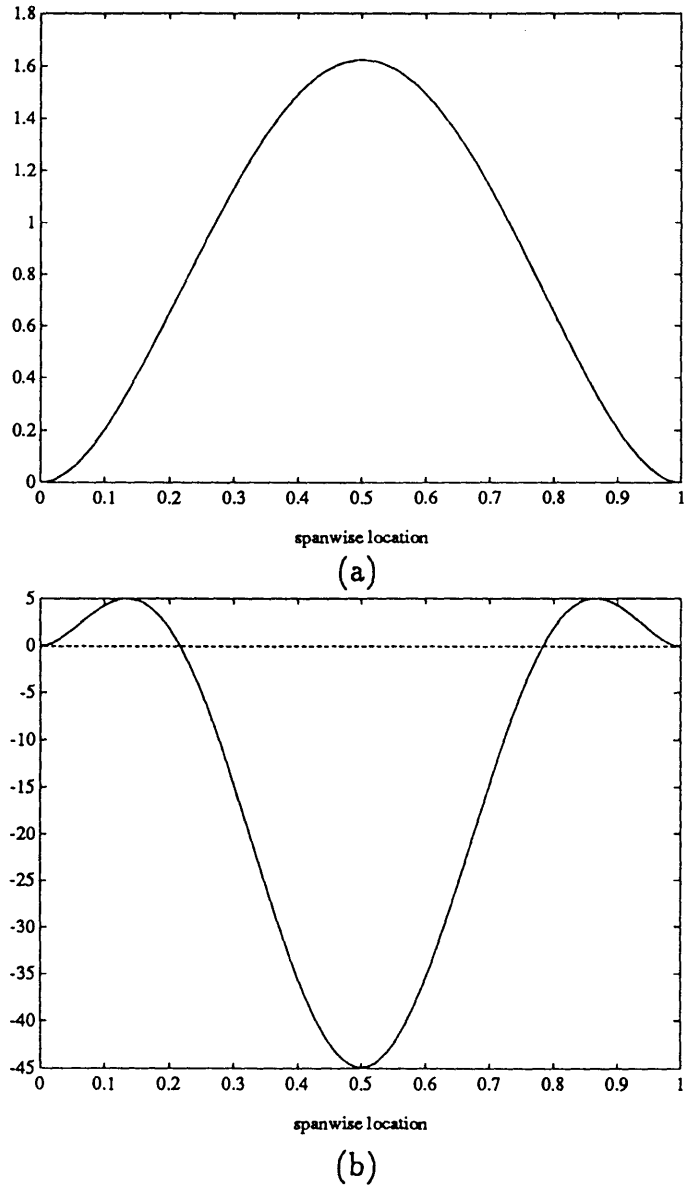

Figure 3.3: $\phi(x)\phi''(x)$ for the first mode (a) and second mode (b) of a clamped-free beam as a function of the span. The first mode is dominated purely by exponential functions since $\phi(x)\phi''(x)$ is positive along the span.

$$-\sigma(\frac{\lambda x}{l} - \frac{\frac{\lambda x}{l}^3}{3!} + \frac{\frac{\lambda x}{l}^5}{5!} + \cdots)$$

the location of the node of the first mode shape can be found by setting $\phi(x) = 0$. This yields an estimate for the first node of a mode shape, and hence the location of the transition point from exponential to sinusoidal dominance of

$$x_{tr} = \frac{l}{\sigma\lambda} \tag{3.8}$$

This would in fact predict the node location of a free-free beam at $x_{tr} = \frac{1}{4.73004(0.98250)} =$ 21.5%. The true node location is at 22.5%. This is an adequate approximation. In fact, it is valid to fourth order in $\frac{\lambda x}{l}$. Equation 3.8 can be used to quickly estimate the boundaries for placing a pseudo-dual pair.

If the structure is governed by exponential functions in a region for all modes then a pseudo-dual S/A pair will guarantee alternating pole-zero patterns. Similarly, a structure dominated by spatially sinusoidal mode shapes will guarantee alternating pole-zero patterns for the pseudo-dual S/A pairs. The transition point may be estimated using Equation 3.8.

While the robustness property for any structure of dual S/A pairs is often desirable, there may be occasion when a pseudo-dual, collocated and complementary extreme, S/A pair choice is desired. deLuis [12] showed that for structures with highly distributed induced strain actuators configured for bending, as in the actuator of Figure 3.1(e), the sensors which yielded the most banded constant gain controller are curvature, the dual measurement, and transverse velocity, a pseudo-dual measurement. In his analysis deLuis assumed an infinitely long structure and hence the analysis was implicitly limited to the case of structures governed by purely sinusoidal mode shapes.

The behavior of a pseudo-dual pair was experimentally documented for a free-free beam, built by deLuis. The S/A pair used by deLuis for his free-free beam, transverse velocity and a moment couple, is typified by Figure 3.4(d). The S/A pair was placed

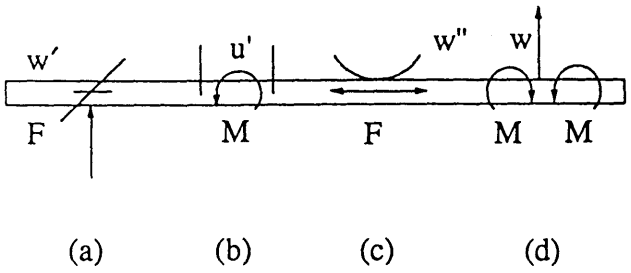

Figure 3.4: A sample of collocated but non-dual sensor and actuator pairs. A pseudo-dual pair is shown in (d) as a moment couple actuator and transverse displacement sensor

on the beam at a point which does not guarantee consistently sinusoidally dominated or consistently exponentially dominated mode shapes.

Figure 3.5 shows an experimental test configuration for the free-free beam with the piezoceramic moment couple actuator/ velocity measurement pair at 9.375% along the span. This corresponds in the figure to the first S/A pair from the left, which is well outside the node of the first mode shape of a free-free beam at 22.5% and therefore initially in a region of exponential dominance. The resulting transfer function is shown in Figure 3.6. The poles are visible at 34 Hz, 59 Hz, and 99 Hz. At each pole pair, the phase drops by roughly 180 degrees. A zero pair may be seen by the phase rising by approximately 180 degrees. Zeroes are visible at 57 Hz and 101 Hz. The pole-zero pattern is therefore pole at 34 Hz, zero at 57 Hz, pole at 59 Hz, pole at 99 Hz, zero at 101 Hz. There is no zero between the second and third modes at 57 Hz and 98 Hz. The alternating pole-zero pattern is destroyed between the second and third poles. This is shown schematically in Figure 3.7.

The mode at which the alternating pattern is destroyed may be estimated using Equation 3.8. The results are shown in Table 3.3. The transition point is correctly predicted to occur between the second and third mode. For the first and second mode, a moment doublet actuator, and transverse velocity sensor are in the exponentially

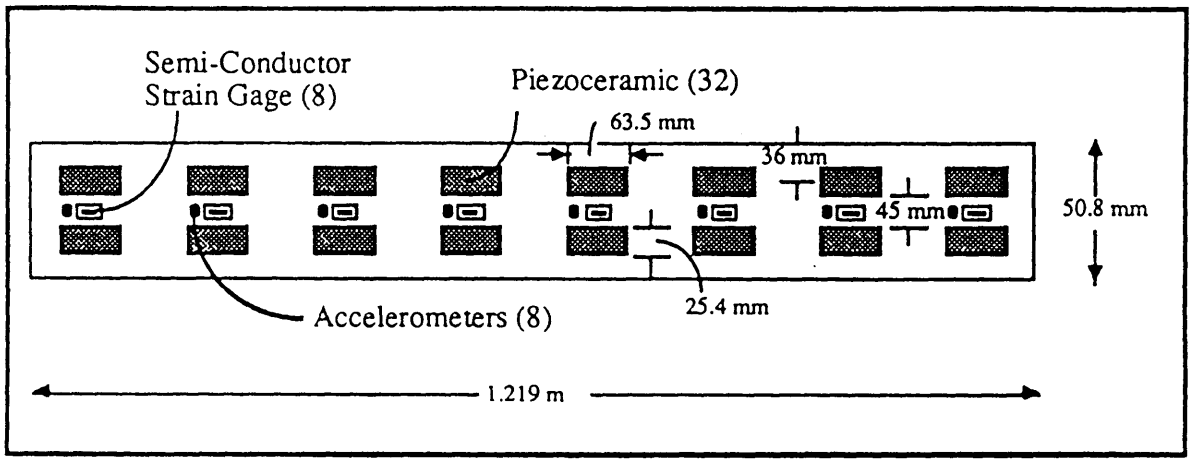

Figure 3.5: Experimental configuration of free-free beam with embedded piezoceramic actuators and collocated accelerometer sensors. A transfer function is taken from the voltage to the leftmost actuator, producing a moment couple, to the collocated acceleration sensor, integrated to velocity. The center of this S/A pair is located at 9.375% along the span, outside of the node of the first mode shape and hence initially in a region dominated by exponential behavior.

dominated region, and pseudo-dual. For the third and higher they are in a sinusoidally dominated, and negative pseudo-dual. This sign change in the residues causes the missing zero apparent in the transfer function.

Dual, collocated, and complementary extreme S/A pairs provide a measure of real power or work. Dual, collocated, and complementary extreme S/A pairs ensure that the alternating pole-zero pattern is present irrespective of the structure on which they act. There are instances where the dual requirement on S/A pair may be relaxed and the alternating pole-zero pattern is still assured. This occurs only for certain structures which have S/A pairs referred to as pseudo-dual. These structures are dominated by exponential or sinusoidal functions in the region of the S/A pair for all modes. Collocated and dual sensors and actuators which operate on modes separated by two spatial derivatives will produce alternating pole-zero patterns on both

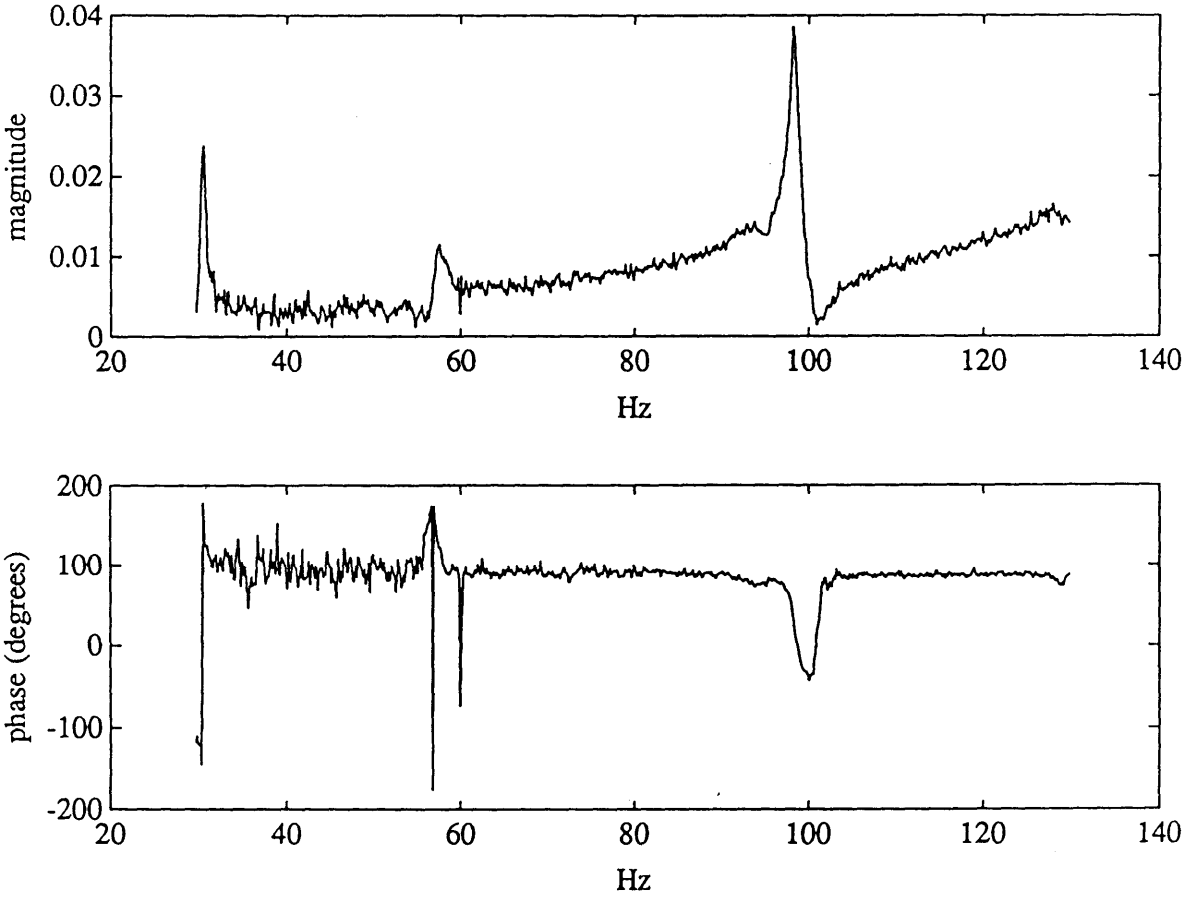

Figure 3.6: Transfer function from voltage to collocated velocity of S/A pair described in Figure 3.6. Poles occur at 34, 59, and 99 Hz, zeroes at 57 and 101 Hz

Table 3.3: Estimate of transition point, x_{tr} from exponentially dominated to sinusoidally dominated mode shape for a free-free beam

mode number	λ_i	σ_i	x_{tr}
1	4.73004	0.98250	21.5%
2	7.85320	1.00078	12.7%
3	10.9956	0.99997	9.1%

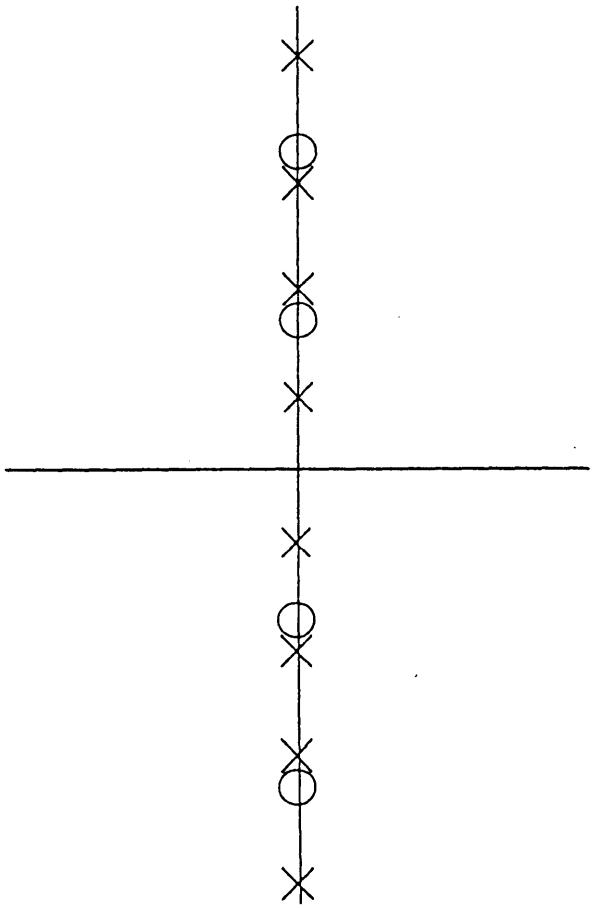

Figure 3.7: Effect on the pole-zero pattern of a pseudo-dual S/A pair when the mode shape behavior transitions from spatial sinusoidally to exponentially dominated functions. The alternating pole-zero pattern is destroyed at the mode where transition occurs, here between the second and third modes, resulting in a missing zero.

purely sinusoidal and purely exponential structures. Collocated and dual sensor and actuator pairs which operate on modes separated by one spatial derivative can never produce alternating pole-zero patterns on structures governed by purely sinusoidal mode shapes, although may produce alternating pole-zero patterns on structures governed by exponential mode shapes, if the exponential behavior is always consistently increasing or decreasing. Hence a free-free beam with a moment couple actuator and transverse velocity sensor were shown to have an alternating pole-zero pattern if the collocated S/A pair were placed within the nodes of the first mode. A clamped-free beam was shown not to be able to produce alternating pole-zero patterns with such a S/A pair. If the exponential or sinusoidal behavior is not maintained for all modes for the pseudo-duals, then a zero in the alternating pole-zero pattern is missed at the frequency at which the transition point passes through the collocated S/A pair. This effect on the pole-zero pattern may be used to control when a zero is missed if this is desired for a particular control scheme [27]. Most often however, violating duality while still maintaining a collocated S/A pair results in destruction of the alternating pole-zero pattern and in fact, there is no guarantee that the system has imaginary zeroes.

In addition to the design decision of type of sensor and actuator pair which is a discrete set of possible combinations, the choice of sensor and actuator impedance relative to the structure influences the pole-zero pattern, but the design choice is given by a continuous spectrum of possibilities. This effect of impedance is explored next.

3.2 Impedance of Sensor and Actuator Pairs

The relative stiffness or mechanical impedance of the actuator to the structure determines whether the actuator acts as a generalized force or a generalized displacement (or velocity) along a certain axis. For example, consider the case of a relative actuator, one that reacts against another part of the structure, such as an embedded active

material. If the actuator is very stiff relative to the structure locally, the actuator acts like a displacement (or velocity) source, the structure being compliant. Conversely, if the structure is very stiff locally relative to the actuator, the actuator acts like a force source.

Similarly a sensor may be considered to have a certain impedance relative to the structure. A load cell, a generalized force sensor, tends to be comprised of a very stiff spring. A generalized displacement (or velocity) sensor is characterized by a very compliant spring relative to the structural stiffness such as a strain gage, or a devise with no stiffness at all such as an optical metrology path. In such cases the sensor tends not to disturb the motion of the original structure.

When an actuator and sensor have the same relative mechanical impedance to the structure, they are referred to as complementary. Hence a generalized force actuator which has a very low relative mechanical impedance to the structure (i.e. a force source) is a complement to a displacement (or velocity) sensor. If the relative mechanical impedance of the actuator is varied parametrically, a spectrum of actuation results, continuously varying from a pure generalized force to a pure generalized displacement as shown in Figure 3.8. The relative impedance of the sensor to the structure can similarly be varied to produce the sensing spectrum as in Figure 3.8. The ends of the spectrum corresponding to sensors and actuators with very low impedance or very high impedance are referred to as complementary extremes. A low impedance sensor measures generalized displacement, a high impedance sensor force. The spectra are drawn such that at any given distance along the actuator spectrum, the positive complementary measurement is the corresponding point on the spectrum just below. The pure force actuator and pure displacement sensor form a dual and positive complementary pair, as do the pure displacement actuator and pure force sensor. A complementary S/A pair has matched relative impedance. In addition to the positive complements where the measurement is the sum of displacement and applied force at a given location, there may be a negative complement which

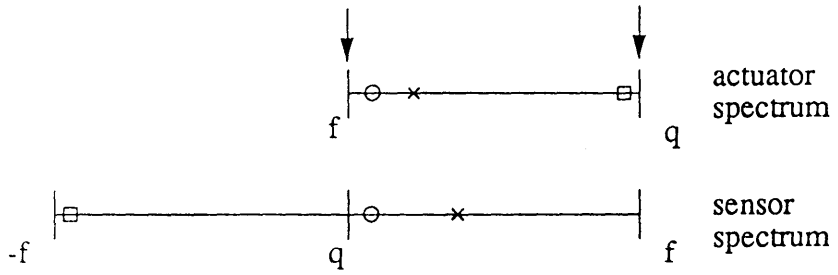

Figure 3.8: Spectra of sensor and actuator from pure generalized force to pure generalized displacement (or velocity). Complementary extremes are denoted by arrows, positive complements by circles, negative complements by squares and positive non-complements by x.

corresponds to a measurement of displacement minus applied force. This negative part of the spectrum is also visible in Figure 3.8.

It is desired to show in this section how the pole-zero distributions are altered parametrically as a function of the mechanical impedance of the actuator and the impedance of the sensor relative to the structure when the S/A pair are dual, positive complementary, and collocated. The effect on the pole-zero pattern of negative complements is also explored. The effect due to a mismatch in the relative impedance of the sensor to the structure with respect to the relative mechanical impedance of the actuator is also presented.

A study is performed to focus on the pole-zero patterns of various complementary S/A pairs. The study is based on an appropriate simple model which attempts to capture all of the relevant behavior. This model is shown in Figure 3.9(c). For the purposes of this model the sensor and actuator variables are dual, i.e. linear force and displacement, and collocated. The unactuated structural model is shown in Figure 3.9(a). The parameter γ is used to modify the relative structural stiffness of the non-actuated part of the structure to the actuated part. The actuator model is displayed in Figure 3.9(b). It is assumed that the actuator acts statically. Hence, no conclusions regarding the behavior of an actuator with internal dynamics may be

made. The actuator model allows for the actuator stiffness k_a to be varied parametrically relative to k_s by setting $k_a = \alpha k_s$. Hence the actuator can be transformed uniformly from a pure force actuator, with low relative stiffness α, to a pure displacement actuator with high relative stiffness α. The resulting force applied on the first structural mass, f_{app}, by the actuator is

$$f_{app} = f_{comm} - k_a q_1 = f_{comm} - \alpha k_s q_1 \tag{3.9}$$

where f_{comm} is the commanded force. As α is increased f_{app} decreases until ultimately the stiffness of the actuator dominates that of the structure and the commanded force in effect imposes a commanded displacement on the structural mass.

The impedance of the sensor needs to be modelled as well. As the relative impedance of the sensor decreases from being infinitely stiff to being compliant, the sensor measurement is also caused to vary from a pure generalized applied force to a mixed measurement of f_{app}, normalized by the structural stiffness, and the displacement of the structural mass, q_1.

$$y = q_1 + c\frac{f_{app}}{k_s} \tag{3.10}$$

The equations of motion for this model are given by:

$$\begin{bmatrix} m & 0 \\ 0 & m \end{bmatrix} \begin{bmatrix} \ddot{q}_1 \\ \ddot{q}_2 \end{bmatrix} + \begin{bmatrix} k_s + \alpha k_s + \gamma k_s & -\gamma k_s \\ -\gamma k_s & \gamma k_s \end{bmatrix} \begin{bmatrix} q_1 \\ q_2 \end{bmatrix} = \begin{bmatrix} 1 \\ 0 \end{bmatrix} f_{comm} \tag{3.11}$$

Dividing through by k_s and letting $\frac{m}{k_s} = 1$ yields

$$\begin{bmatrix} 1 & 0 \\ 0 & 1 \end{bmatrix} \begin{bmatrix} \ddot{q}_1 \\ \ddot{q}_2 \end{bmatrix} + \begin{bmatrix} 1 + \alpha + \gamma & -\gamma \\ -\gamma & \gamma \end{bmatrix} \begin{bmatrix} q_1 \\ q_2 \end{bmatrix} = \begin{bmatrix} \frac{1}{k_s} \\ 0 \end{bmatrix} f_{comm} \tag{3.12}$$

Equal α and c imply a positive complementary S/A pair. These equations of motion produce a transfer function from $\frac{f_{comm}}{k_s}$ to y of

$$\frac{y}{\frac{f_{comm}}{k_s}} = \frac{c(s^4 + (\frac{1}{c} + 2\gamma + 1)s^2 + \gamma(\frac{1}{c} + 1))}{s^4 + (\alpha + 2\gamma + 1)s^2 + \gamma(\alpha + 1)} \tag{3.13}$$

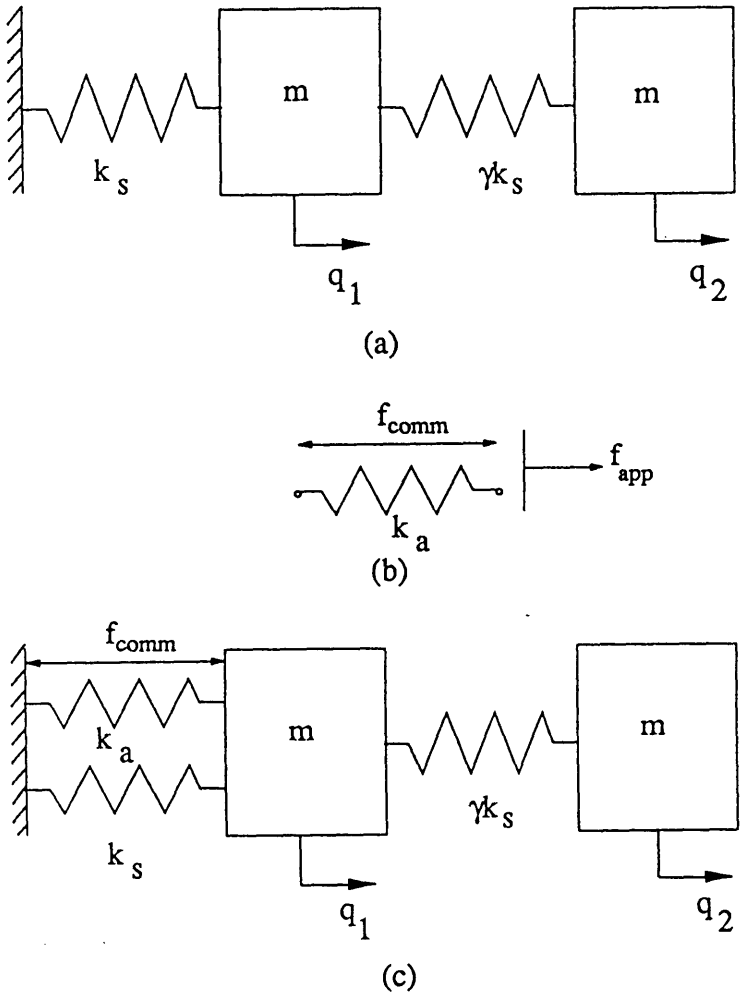

Figure 3.9: Model used to study actuator and sensor impedance relative to the structure. The unactuated structural model is given by (a) consisting of two modes. The actuator model is depicted in (b). The applied force is a function of the actuator stiffness as given by Equation 3.14. The complete system is given in (c).

It should be noted that in this model, the zeroes are functions only of c, the measurement weighting parameter, and γ, and the poles are a function solely of the actuator stiffness, α, and γ. The leftmost pair of the spectrum of Figure 3.8 is found by setting $c = \alpha = 0$ which represents a complementary sensor and actuator pair where both the sensor and actuator have a low impedance relative to the structure. As the spectrum is traversed both α and c increase.

The spectrum of Figure 3.8 may be normalized so that the actuator spectrum maps from $b = 0$ to $b = 1$ and similarly the sensor spectrum maps from $d = 0$ to $d = 1$. This is done by rewriting Equations 3.9 and 3.10 as

$$f_{app} = f_{comm} - \frac{b}{1-b} k_s q_1 \tag{3.14}$$

and

$$y = (1-d)q_1 + d\frac{f_{app}}{k_s} \tag{3.15}$$

respectively. A pure force actuator and a pure displacement sensor correspond to $b = 0$ and $d = 0$, and a pure displacement actuator and force sensor correspond to $b = 1$ and $d = 1$. These two cases correspond to complementary extremes.

The transfer function from $\frac{f_{comm}}{k_s}$ to y can be rewritten in terms of b and d as

$$\frac{y}{\frac{f_{comm}}{k_s}} = \frac{d(s^4 + (\frac{1}{d} + 2\gamma)s^2 + \frac{\gamma}{d})}{s^4 + (\frac{1}{1-b} + 2\gamma)s^2 + \frac{\gamma}{1-b}} \tag{3.16}$$

It is interesting to note that in the extremes of $d = 0$ and $d = 1$, the measurement (Equation 3.15) yields a quantity whose variation, if premultiplied by f_{comm} is a measure of the true work done on the system. In the case of $d = 0$, it is clear that

$$\delta y = \delta q_1 \tag{3.17}$$

In the limiting case of $d = 1$ and $b = 1$, (i.e. infinite k_a), then examining the first of equations 3.11 indicates that q_1 responds quasistatically to f_{comm}

$$f_{comm} = m\ddot{q_1} + (k_s + \gamma k_s + k_a)q_1 \tag{3.18}$$

$$\cong (k_s(1+\gamma) + k_a)q_1 \tag{3.19}$$

so that the applied force f_{app} is given

$$f_{app} = f_{comm} - k_a q_1 \cong k_s(1+\gamma)q_1 \tag{3.20}$$

Substituting into Equation 3.15 gives

$$\delta y = \frac{\delta f_{app}}{k_s} \cong (1+\gamma)\delta q_1. \tag{3.21}$$

In the intermediate cases between the extremes, the relationship between y and a true displacement variable is dynamic. Rewriting the first of Equations 3.11 again as

$$f_{comm} = f_{app} + k_a q_1 = m\ddot{q_1} + (k_s + \gamma k_s + k_a)q_1 \tag{3.22}$$

then the relationship between f_{app} and q_1 is given by the driving point dynamic stiffness of the structure in the absence of the actuator stiffness

$$f_{app} = m\ddot{q_1} + (k_s + \gamma k_s)q_1 = Z_s q_1 \tag{3.23}$$

so that if Equation 3.15 were rewritten as

$$y = (1-d)q_1 + d\frac{f_{app}}{Z_s} \tag{3.24}$$

The variation of the measurement, multiplied by the commanded force, would produce a true measure of work. However since this produces a complex frequency dependent measurement equation, the static stiffness of the structure as seen by the actuator is appropriate to substitute for the complex impedance. Substituting the static stiffness of the structure will no longer ensure a measure of the work for the S/A pair, however the pole-zero patterns appear to alternate.

From the transfer function of Equation 3.16 the nature of the pole-zero behavior is apparent. Pole-zero cancellation occurs when $d = 1 - b$ which can occur for an infinite number of combinations of b and d, and for positive complements when $d = b = 0.5$. The zeroes at $d = 0$ are identical to the poles at $b = 1$. The zeroes when the measurement is pure displacement correspond to the poles when the actuator is infinitely stiff. Similarly, the zeroes when $d = 1$ are identical to the poles when $b = 0$.

The zeroes when the measurement is a pure force, or a stiff sensor, correspond to the poles when the actuator is very compliant.

Figure 3.10 shows the imaginary poles and zeroes predicted by this model as a function of both b and d. The first pole is given by a dashed line, the second by a solid line. The zeroes are represented by o's. A value of $\gamma = 1$ is used in Figure 3.10(a), and $\gamma = 0.1$ is used in Figure 3.10(b). Decreasing γ is seen to shift the poles and zeroes down and decrease the sensitivity of the poles to b but not to change any trends.

In Figure 3.10, since the zeroes are not a function of b, each horizontal row of o's represents a different value of d. For positive complements, namely positive values of d, the zeroes are always imaginary. Zeroes are shown for values of d of $0.1, 0.3, 0.5$, and 0.9 where increasing d produces zeroes of lower frequency. The pole-zero pattern is alternating for both complementary sensor and actuator, given by equal b and d, and for non-equal values of b and d as well, except for pole-zero cancellations visible for all cases of $d = 1 - b$. Hence a collocated and dual but positive non-complementary S/A pair is shown to preserve the alternating pole-zero pattern, save pole-zero cancellation. For positive complementary S/A pairs, Figure 3.10 shows that the zero frequencies may be either consistently above or below the pole frequencies. This is determined by which end of the spectrum the S/A pair is located. A complementary S/A pair at the far left end of the spectrum, namely, a force actuator and displacement sensor, have a pole first and then a zero. A complementary S/A pair at the other end of the spectrum, a displacement actuator and force sensor have a zero first in frequency, then a pole. For $\gamma = 1$, the poles may vary from 0.618 to 1 and from 1.618 to ∞. The zeroes may vary from 1 to 0.618 and from ∞ to 1.618. The simple model also shows that irrespective of the type of actuator, a pure displacement sensor produces zeroes consistently at or above the poles and a pure force sensor produces zeroes consistently at or below the poles.

The pole-zero spacing is a function of the location of the actuation and sensing mechanisms along the spectrum. The pole-zero spacing is largest when the sensor and

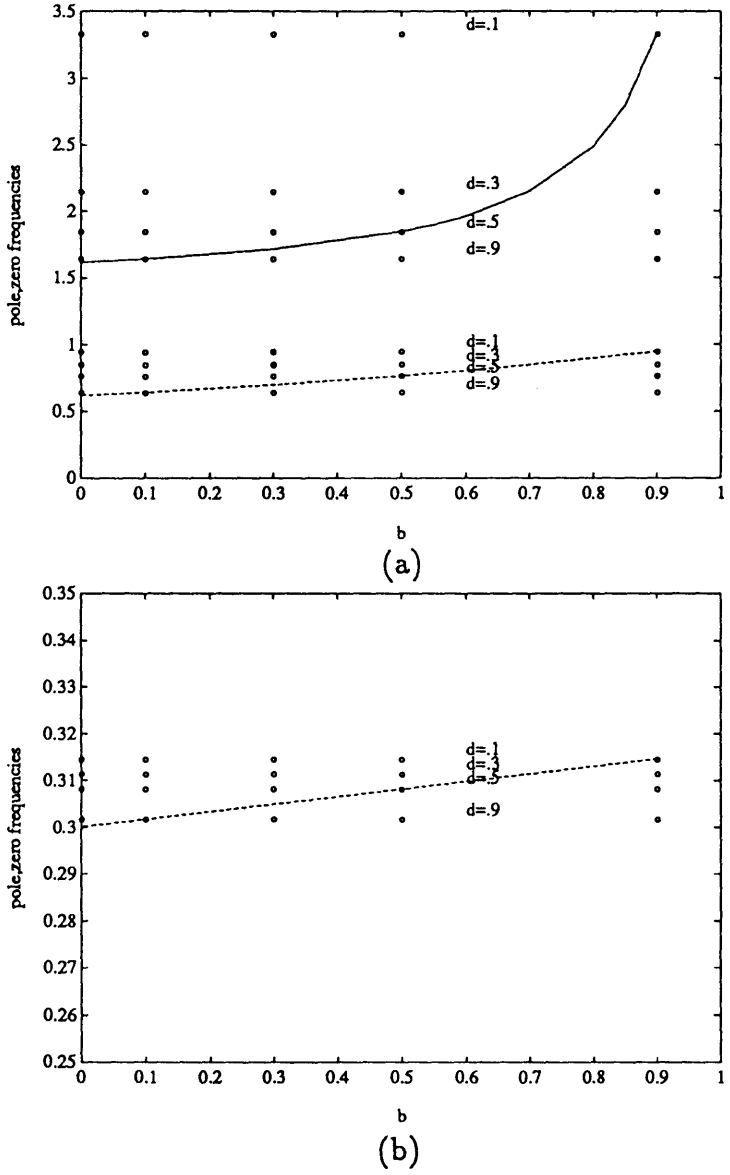

Figure 3.10: Poles and zeroes of simple model as a function of b and d for positive complements and non-complements. Poles are represented as the dashed and solid lines. The zeroes are represented as circles. Solutions of $\gamma = 1$ (a) and $\gamma = 0.1$ (b) are shown. The pole-zero pattern is alternating for any values of b and d. Pole-zero spacing is largest at the complementary extremes.

actuator are complementary extremes. As the impedance of the complementary S/A pair is increased from the force actuator/displacement sensor the pole-zero spacing decreases, with the pole first in frequency, until the center of the spectrum is reached. As the impedance is increased further, the pole-zero spacing increases again, this time with the zero first in frequency. The effect of traversing the the spectrum from low to high relative impedance for complementary S/A pairs is to shift all the zeroes consistently downwards. This is shown schematically in Figure 3.11. This effect on the pole-zero pattern contrasts with that of sensor type selection.

For non-complementary S/A pairs, the relative spacing is still a function of the sensor and actuator location along the spectrum. Consider the case where $b = 0$ and d may vary. The zeroes slowly move closer to the poles, moving downwards as d is increased. Similarly, when $d = 0$ and b is allowed to vary, the zeroes move closer to the poles as b is increased.

The relative pole-zero spacing for systems with only imaginary zeroes affects the average slope of the transfer function. The limiting case of course is pole-zero cancellation of every mode and hence a transfer function of unity which has a slope of zero. If the zeroes were all shifted slightly upwards, a pole would occur first and then a zero. The average slope of the transfer function overall would be slightly negative. If the zeroes were moved further away, the average slope of the transfer function would become more negative. If in the limit the zeroes were to shift upwards until they reached and cancelled the poles just above them, then only the first pole would remain, and the average slope of the transfer function would be -40dB/decade. Compared to the initially flat transfer function, the relative spacing of the poles and zeroes can alter the average slope of the transfer function. For complementary S/A pairs with low relative impedance to the structure, the average slope of the transfer function is negative, while for complementary S/A pairs with high relative impedance to the structure, the average slope of the transfer function is positive.

While α, the relative actuator stiffness must always be positive due to the physics

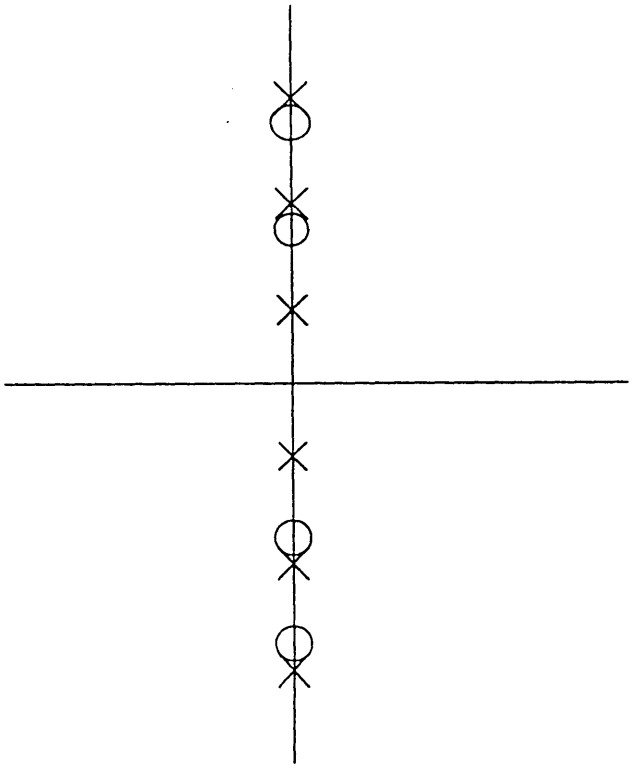

Figure 3.11: Effect of the pole-zero pattern in the s-plane of impedance of actuator and sensor relative to the structure for positive complements or non-complements. Altering the relative impedance of the actuator or the sensor or both effects the relative spacing of the poles and zeroes. As dual, collocated and positive complementary or non-complementary sensors and actuators ensure an alternating pole-zero pattern.

of the problem, the mixture of measurements can be influenced in two ways. The first is by physically changing the mechanical stiffness of the sensor, which will yield only positive complements, and the second is by making two independent measurements, one low impedance and one high, and then algebraically mixing their signals. In the latter case, the signals can be summed to yield positive complements, or differenced to yield negative complements. In the negative complement case, Equation 3.10 is rewritten as

$$y = (1 - d')q_1 - d'\frac{f_{app}}{k_s}. \tag{3.25}$$

This produces a transfer function from f_{comm} to y for the differential case of

$$\frac{y}{\frac{f_{comm}}{k_s}} = \frac{-d'(s^4 + (-\frac{1}{d'} + 2 + 2\gamma)s^2 + \gamma(-\frac{1}{d'} + 2))}{s^4 + (\frac{1}{1-b} + 2\gamma)s^2 + \gamma(\frac{1}{1-b})}. \tag{3.26}$$

The locus of zeroes as a function of d' for this negative complement case are found in Figure 3.12 for $\gamma = 1$. Once again, the poles are included for reference. The imaginary zeroes are denoted by o's. In the case of negative complements there are real zeroes which are at $s = \pm 2.7$ when $d' = 0.1$, and $s = \pm 0.9$ when $d' = 0.3$. The initial effect of a small d' for this negative complement is to make the imaginary zeroes move upwards in frequency as d' is increased. This has the desired property of keeping the zero above the first pole consistently between the first and second pole as b is increased, thus preserving the pole-zero-pole pattern. However, the highest imaginary zero pair is already at $\pm j\infty$ on the imaginary axis. So for small d' this zero pair moves instead to symmetric positions along the real axis. As d' is increased such that $0 < d' < 0.5$, the real zeroes move closer in to the imaginary axis. The real zero pair produces a non-minimum phase zero for negative complements with $0 < d' < 0.5$. Irrespective of γ, there is a transition point at $d' = 0.5$ just as there was in the positive complement. For $0.5 < d' < 1$ both zeroes are again imaginary, and steadily approach the poles from below. Pole-zero cancellation occurs when $b = 0$ and $d' = 1$ for this differential case. For values of d' near 1, or a near negative force measurement, the zeroes relative to the poles are again characterized by a zero first

in frequency, as was the case for the positive complement. For the range of values $0 < d' < 1$, one zero is bounded from below by 1 and above by the second pole. The other zero takes on real values from ∞ to 0, and then imaginary zeroes from 0 to $\sqrt{2}$. Hence, choosing values of d in the range $0 < d < 1$, and d' in the range $0 < d' < 1$ has caused the entire range of possible zero positions to be spanned.

Equation 3.25 shows that this non-minimum phase zero effect is not an artifact of a truncated model. Initially, a small positive f_{app} is applied and the initial output is negative since the mass does not move instantaneously. In the steady state, y becomes positive as the $(1 - d')q_1$ term dominates so long as $0 < d' < 0.5$. For the case of $0.5 < d' < 1$, the static response of y to f_{comm} is negative, implying that positive as opposed to negative feedback will have to be used.

The results of this simple model are consistent with the trends reported in two experiments. Figure 3.13, from [13], shows results from an experiment involving an active piezoceramic element controlling a cantilevered truss structure. This piezoelectric element is substantially stiffer than any of the surrounding truss members. A collocated eddy current displacement sensor and a collocated load cell sensor are available. Because of its high stiffness, the actuator acts almost as a pure displacement source. When the measurement is collocated displacement, near pole-zero cancellation is achieved with zeroes just above the poles as can be seen in Figure 3.13(a). A pole at approximately 8 Hz is encountered before any zeroes. This is as predicted by the simple model for a pure displacement sensor, irrespective of the impedance of the actuator. The phase of such a transfer function with near pole-zero cancellation is practically constant with small excursions at the locations of the pole-zero pairs. The slope of the displacement transfer function is flat. A collocated load cell measurement yields larger pole-zero spacing, with a zero at approximately 6.5 Hz appearing before the first pole at approximately 8 Hz shown in Figure 3.13(b). Both positive and negative complements with a pure force measurement predict the zero first in frequency. The average slope of the force measurement transfer function is

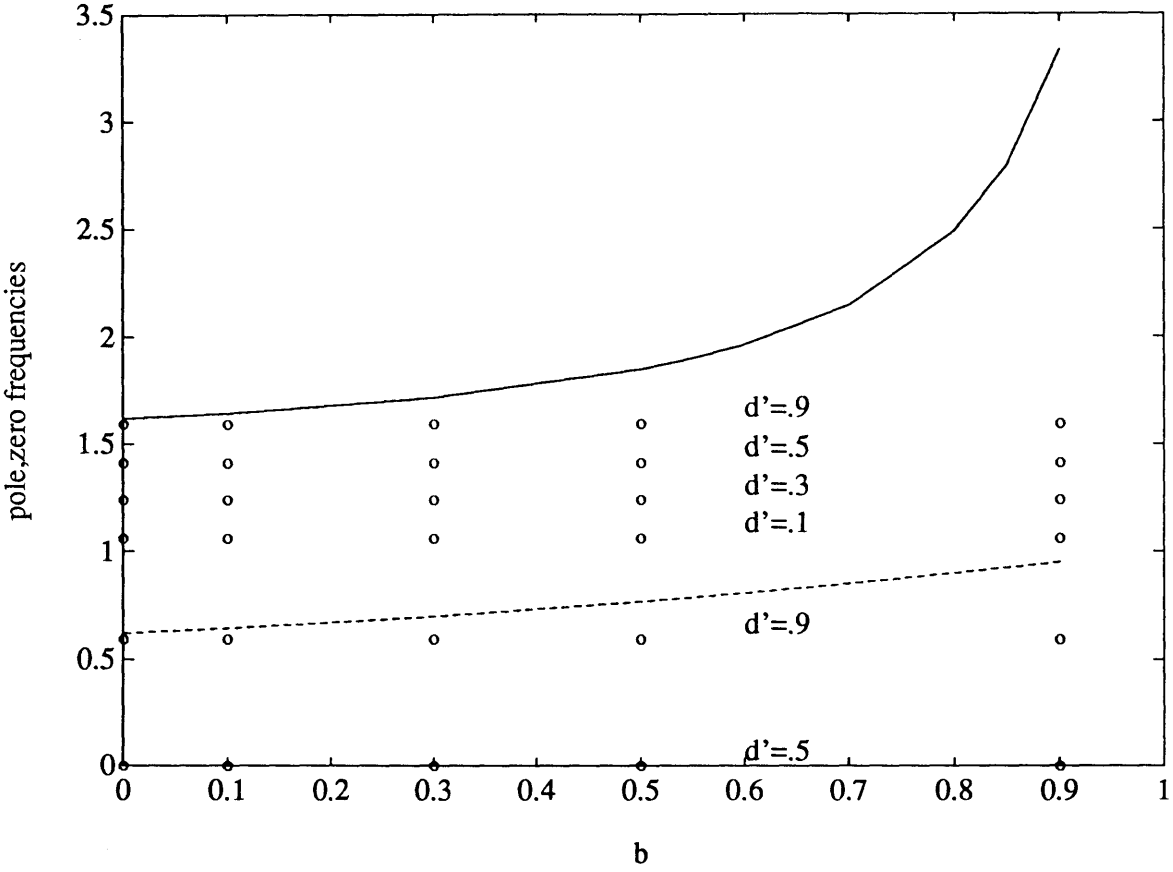

Figure 3.12: Poles and zeroes of simple model as a function of b and d' for negative complements and non-complements. For $0.5 < d' < 1$ the zeroes are purely imaginary and are depicted by circles. For $0 < d' < 0.5$ one zero pair is real and moves closer to the imaginary axis as d' increases. Real zeroes occur at $s = \pm 2.7$ when $d' = 0.1$ and $s = \pm 0.9$ when $d' = 0.3$.

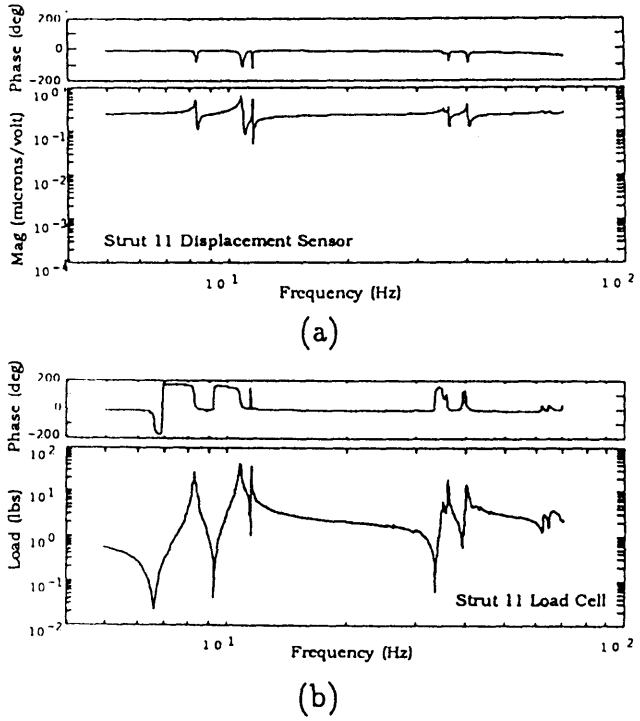

Figure 3.13: Transfer functions from Fanson *et.al.* from voltage applied to an active strut to collocated displacement (a) and load cell (b). Poles and zeroes are very closely spaced with zeroes following poles for the displacement sensor due to the very stiff actuator. Pole-zero spacing is improved for the transfer function with a force measurement.

slowly rising as it should since a zero occurs first in the transfer function with a force measurement. The average slope of the transfer function is modified by the change in relative pole-zero spacing.

Fanson [13] used a different model, shown in Figure 3.14 to explain the reason for the close pole zero spacing and feedthrough nature of the displacement measurement transfer function. The actuator was modelled as acting on a residual input stiffness, β, as opposed to acting directly on the structural mass. For low residual input stiffness, close pole-zero spacing and a feedthrough term were predicted. This low residual input stiffness is akin to claiming a high relative stiffness actuator compared to the local stiffness of the structure.

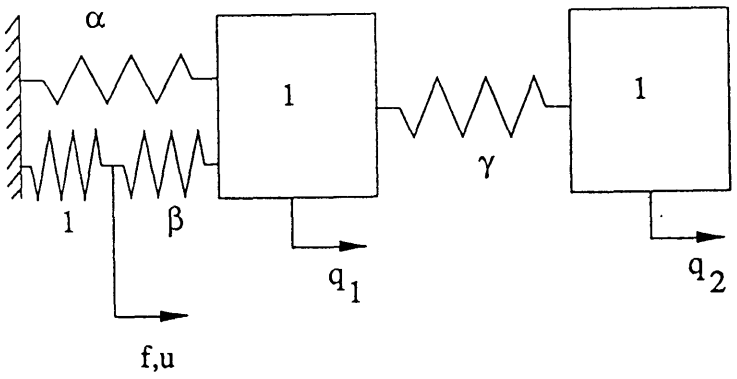

Figure 3.14: Model used by Fanson *et.al.* to predict close pole-zero spacing included a stiffness in series with the actuator. This captures the effect of the actuator impedance relative to the structure. Close pole-zero spacing was correctly predicted.

Another experimental example can be found in Chen, Lurie, and Wada [28]. The objective of the experiment is to incorporate impedance matching of an active strut actuator via feedback of collocated force and/ or velocity to destiffen and add damping to the actuator dynamics, if needed, to match the actuator stiffness to the structural stiffness. The data presented in Figure 3.15 are for a cantilevered truss with the active element in a longeron at the root. This active strut is the same strut used in [13] but the truss structure is not the same. The open loop transfer functions are shown for the displacement measurement, Figure 3.15(a) and sensed force (b) cases. The displacement and force measurement transfer functions have distinctly different pole-zero distributions, the displacement transfer function, nearly flat, showing near pole-zero cancellations due to a stiff actuator. The force measurement transfer function has the first zero at approximately 10.5 Hz, below the first pole at 12.5 Hz. The average slope of the force transfer function slowly rises due to the zero appearing first in frequency and the better pole-zero spacing.

The simple model used here correlates well with the complex experiments presented. The order of the pole-zero pattern is properly predicted as well as the relative

spacing of the poles and zeroes and the average slope of the transfer function.

All dual, and collocated pairs produce alternating pole-zero patterns in the most general sense. Dual, positive complementary, and collocated S/A pairs ensure alternating pole-zero patterns, save pole-zero cancellation at the center of the spectrum. Increasing the impedance of positive complementary, dual, and collocated S/A pairs from low impedance complementary extremes causes all of the zeroes to decrease. The relative pole-zero spacing is largest at the complementary extremes, and is smallest (pole-zero cancellation) when the complements are at the center of the spectrum. For high impedance complementary sensors and actuators, the alternating pole-zero pattern begins with a zero first in frequency, for a restrained structure. For low impedance complementary sensors and actuators the pattern begins first with a pole, for a restrained structure. The average slope of the transfer function may be altered by varying the pair of S/A complements used. Positive non-complementary, dual, and collocated S/A pairs still yield alternating pole-zero patterns, save pole-zero cancellations when the sensor and actuator are at opposite locations of the spectrum, when $b = 1 - d$. The relative pole-zero spacing may be varied by modifying the operating point of the sensor on the spectrum, or of the actuator on the spectrum without sensor and actuator complements. Negative complements and non-complements may produce alternating pole-zero patterns as well. However, for certain combinations of measurement, a non-minimum phase plant may arise. The non-minimum phase zero is furthest away from the imaginary axis when d' is small. Traversing the positive sensor spectrum of a dual S/A pair while leaving the relative impedance of the actuator fixed, or vice versa, produces this same effect of stiffening or destiffening all of the zeroes consistently.

3.3 Location of Sensor and Actuator Pairs

The previous two sections discussed respectively how the type and how the impedance of the sensor and actuator influence the pole-zero patterns. There is a third para-

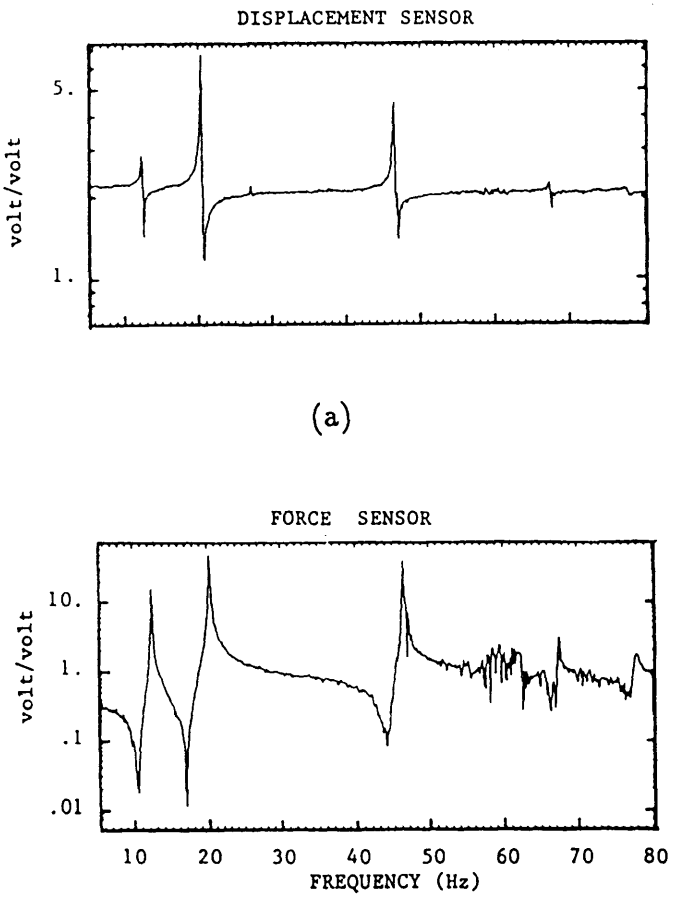

Figure 3.15: Transfer functions from Chen *et.al.* from voltage to active strut to collocated displacement (a) and load cell (b). Although a similar configuration to that of Figure 3.13, the structure was actually different. Results from the simple model correlate well with this data from

metric dependence, one of location of the sensor and actuator. This is explored by explicitly solving for the exact zero frequencies of simple continua, a longitudinal rod and a Bernoulli-Euler beam with various boundary conditions. Initially, a dual, complementary extreme, and collocated S/A pair, displacement and force, is assumed to act. After the effects on the zero frequencies of the collocated and dual S/A pair have been studied, the non-collocated case is then examined, first for small degrees of non-collocation, then for larger non-collocation distances. The behavior of these zero frequencies as a function of location yields interesting information about the character of zeroes and their sensitivity to sensor and actuator location.

Collocated Sensor and Actuator Pairs

The effects on the zeroes as a function of the location of the sensor and actuator are studied first for the collocated case. Exact zeroes are found from infinite dimensional spatially continuous models. The solution method borrows from the root locus definition that the zeroes of an open loop transfer function are equal to the poles of the closed loop system with infinite gain (Section 2.2). Finding the zeroes directly from an infinite order model ensures that no errors in the zero locations are introduced by finite order modelling effects. These finite order modelling effects are the focus of Chapter 4.

To allow for exact solution for the zeroes of a collocated S/A pair, the Bernoulli-Euler beam is assumed uniform along its length. Two sets of beam boundary conditions are examined in the collocated S/A pair case, free-free and clamped-free. These choices of boundary conditions allow the presence or absence of rigid body constraints and plant symmetry to be examined.

Referring to Figure 3.16, the actuator force f is assumed to act on the beam at the location x_a. In this collocated case, the sensor at location x_s is assumed to act at the same point. The structure can be subdivided into two regions corresponding to spanwise locations $x < x_a$, region 1, or $x > x_a$, region 2. The partial differential

equation for each region of a uniform Bernoulli-Euler beam is given by

$$EI\frac{\partial^4 w}{\partial x^4} + \rho A\frac{\partial^2 w}{\partial t^2} = 0. \tag{3.27}$$

The problem is solved by assuming separate solutions in the two regions

$$\begin{aligned} w_1(x) &= a_1 cos(\beta x) + b_1 sin(\beta x) + c_1 cosh(\beta x) + d_1 sinh(\beta x) \\ w_2(x) &= a_2 cos(\beta x) + b_2 sin(\beta x) + c_2 cosh(\beta x) + d_2 sinh(\beta x) \end{aligned} \tag{3.28}$$

with an internal boundary at the location of the actuator, x_a, to ensure compatibility. Displacement and slope compatibility at the boundary yield two equations

$$w_1(x_a) = w_2(x_a) \tag{3.29}$$

$$w_1{}'(x_a) = w_2{}'(x_a). \tag{3.30}$$

At the actuator location there are also two force equilibrium equations.

$$EI\frac{\partial^2 w_1}{\partial x^2}(x_a) - EI\frac{\partial^2 w_2}{\partial x^2}(x_a) = 0 \tag{3.31}$$

$$EI\frac{\partial^3 w_1}{\partial x^3}(x_a) - EI\frac{\partial^3 w_2}{\partial x^3}(x_a) + f(x_a) = 0 \tag{3.32}$$

If the sensor is collocated with the actuator, then

$$f(x_a) = -kw_1(x_s) = -kw_1(x_a) \tag{3.33}$$

is an example of the possible feedback for the collocated case. This physically corresponds to a simple mechanical spring at x_a, as shown in Figure 3.16(b). If the gain is increased to infinity, the limiting location of the poles of the system at high gain will be the zeroes of the open loop transfer function from actuator to sensor. Physically this corresponds to finding the poles of the beam with $k \rightarrow \infty$, i.e., a pin at x_a.

Substituting Equation 3.33 into Equation 3.32 gives

$$EI\frac{\partial^3 w_1}{\partial x^3}(x_a) - EI\frac{\partial^3 w_2}{\partial x^3}(x_a) - kw_1(x_a) = 0. \tag{3.34}$$

Together with the boundary conditions for the free-free case,

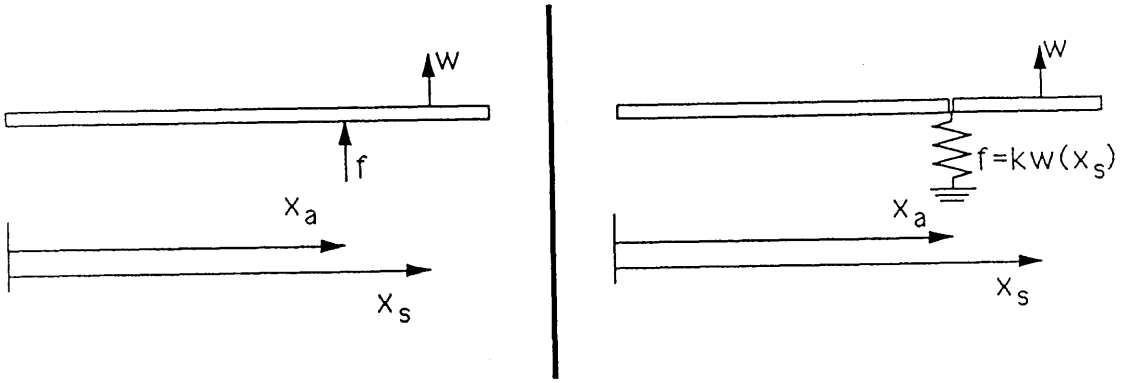

Figure 3.16: Incorporating feedback mechanism at internal boundary. Feedback is implemented via a mechanical spring whose applied force at x_a is proportional to the displacement at the sensor location.

$$EI\frac{\partial^2 w_1}{\partial x^2}(0) = 0 \tag{3.35}$$

$$EI\frac{\partial^3 w_1}{\partial x^3}(0) = 0 \tag{3.36}$$

$$EI\frac{\partial^2 w_2}{\partial x^2}(1) = 0 \tag{3.37}$$

$$EI\frac{\partial^3 w_2}{\partial x^3}(1) = 0 \tag{3.38}$$

this yields a generalized eigenvalue problem for the free-free case

$$\begin{bmatrix} -1 & 0 & 1 & 0 & 0 & 0 & 0 & 0 \\ 0 & -1 & 0 & 1 & 0 & 0 & 0 & 0 \\ c(\mathcal{X}) & s(\mathcal{X}) & ch(\mathcal{X}) & sh(\mathcal{X}) & -c(\mathcal{X}) & -s(\mathcal{X}) & -ch(\mathcal{X}) & -sh(\mathcal{X}) \\ -s(\mathcal{X}) & c(\mathcal{X}) & -sh(\mathcal{X}) & ch(\mathcal{X}) & s(\mathcal{X}) & -c(\mathcal{X}) & -sh(\mathcal{X}) & -ch(\mathcal{X}) \\ -c(\mathcal{X}) & -s(\mathcal{X}) & ch(\mathcal{X}) & sh(\mathcal{X}) & c(\mathcal{X}) & s(\mathcal{X}) & -ch(\mathcal{X}) & -sh(\mathcal{X}) \\ s(\mathcal{X}) & -c(\mathcal{X}) & sh(\mathcal{X}) & ch(\mathcal{X}) & -\kappa c(\mathcal{X}) - s(\mathcal{X}) & -\kappa s(\mathcal{X}) + c(\mathcal{X}) & -\kappa ch(\mathcal{X}) - sh(\mathcal{X}) & -\kappa sh(\mathcal{X}) - ch(\mathcal{X}) \\ 0 & 0 & 0 & 0 & -c(\lambda) & -s(\lambda) & ch(\lambda) & sh(\lambda) \\ 0 & 0 & 0 & 0 & s(\lambda) & -c(\lambda) & sh(\lambda) & ch(\lambda) \end{bmatrix} \begin{bmatrix} a_1 \\ b_1 \\ c_1 \\ d_1 \\ a_2 \\ b_2 \\ c_2 \\ d_2 \end{bmatrix} = \begin{bmatrix} 0 \\ 0 \\ 0 \\ 0 \\ 0 \\ 0 \\ 0 \\ 0 \end{bmatrix} \tag{3.39}$$

where $c(\cdot)$, $s(\cdot)$, $ch(\cdot)$, and $sh(\cdot)$ refer to $cos(\cdot)$, $sin(\cdot)$, $cosh(\cdot)$, and $sinh(\cdot)$ respectively and $\mathcal{X} = \beta x_a$, $\lambda = \beta l$, and $\kappa = \frac{k}{EI\beta^3}$. This generalized eigenvalue problem has order twice as large as the simple structural solution without explicit consideration of the forcing. From this eigenvalue problem a transcendental equation results which is a function of the spring stiffness k. The form of the transcendental equation is

$f_1(\beta, x_a) + \kappa f_2(\beta, x_a) = 0$. The limit as $\frac{k}{EI} \rightarrow \infty$ is then taken. The resulting transcendental equation, $f_2(\beta, x_a) = 0$, yields the roots which are the zeroes of the original open loop system.

This solution technique has been verified to ensure that the rigid body information is properly captured in the case of a free-free beam. With two rigid body modes and only one actuator and sensor pair, one of these rigid body modes is uncontrollable and/or unobservable and remains at the origin. As $\kappa \rightarrow \infty$ the second pair of rigid body poles moves off to infinity on the imaginary axis.

For the collocated scenario and the dual S/A pair examined here, the zeroes are equivalent to the poles of a flexible structure with a pin at the location of the S/A pair. The zero directions, as described in Equation 2.6, are given by an initial conditions vector and an input direction vector, the latter being a scalar for the SISO case. The initial conditions portion of the zero direction is given by the mode shapes of this pinned system. The input direction is given by the reaction force at the pin.

This solution method can also be applied to the collocated but non-dual, and non-collocated cases. For a non-dual but collocated sensor and actuator pair, or a non-collocated sensor and actuator pair, the zero directions can be constructed in the same fashion by finding the closed loop mode shapes and the reaction forces at the actuator location.

The zero frequencies as a function of the location of a collocated S/A pair spanwise location are shown in Figure 3.17 for the free-free beam, and in Figure 3.18 for the clamped-free beam, each for the first four modes.

These zero frequency plots are referred to as zero trajectories. The zero and pole frequencies are expressed as a dimensionless parameter $\lambda = \beta l$ where the true zero or pole frequency of mode i, in radians, is given by

$$\omega_i = \lambda_i^2 \sqrt{\frac{EI}{mL^4}} \tag{3.40}$$

Included with the zero trajectories are the neighboring pole frequencies for reference. The pole frequencies are represented by dashed lines, while the zeroes are represented

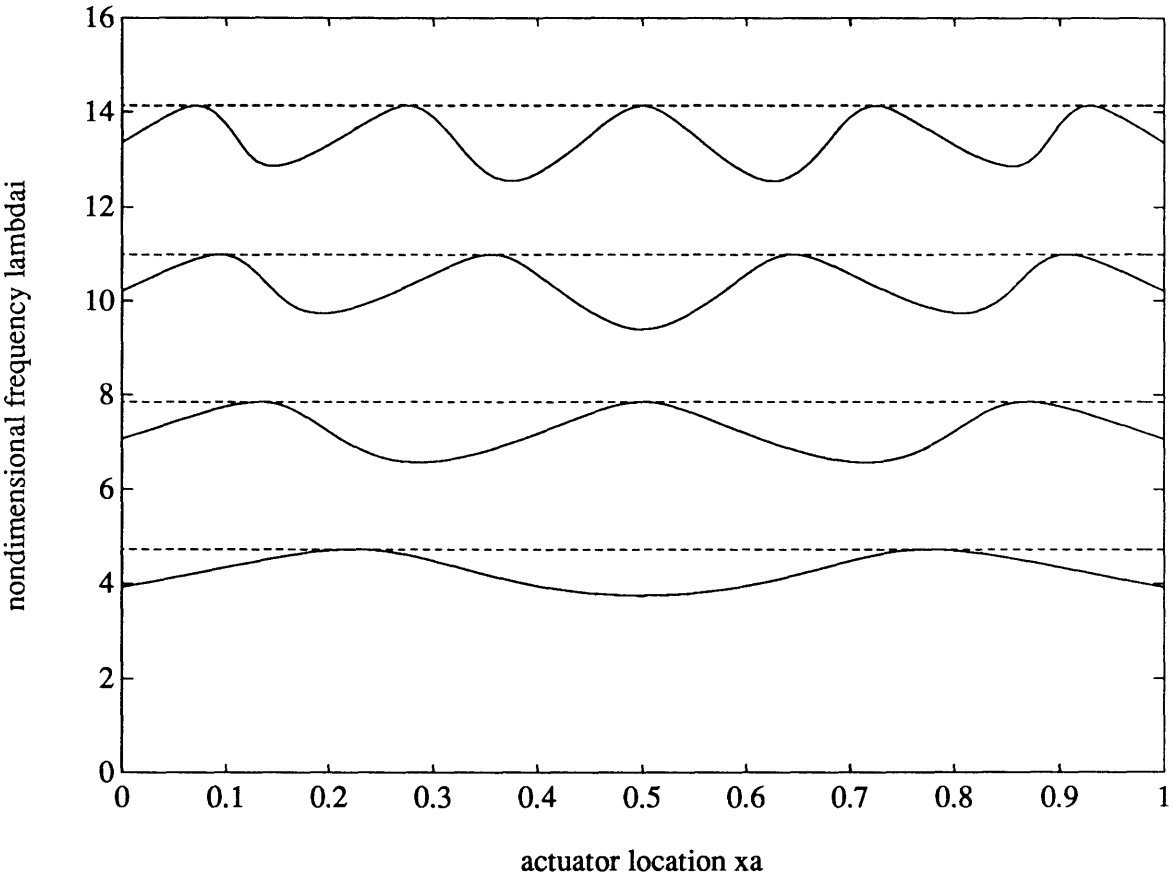

Figure 3.17: Zero trajectories for free-free beam with collocated transverse forcing and displacement measurement, as a function of spanwise location of sensor/ actuator pair. Poles are included for reference as horizontal lines.

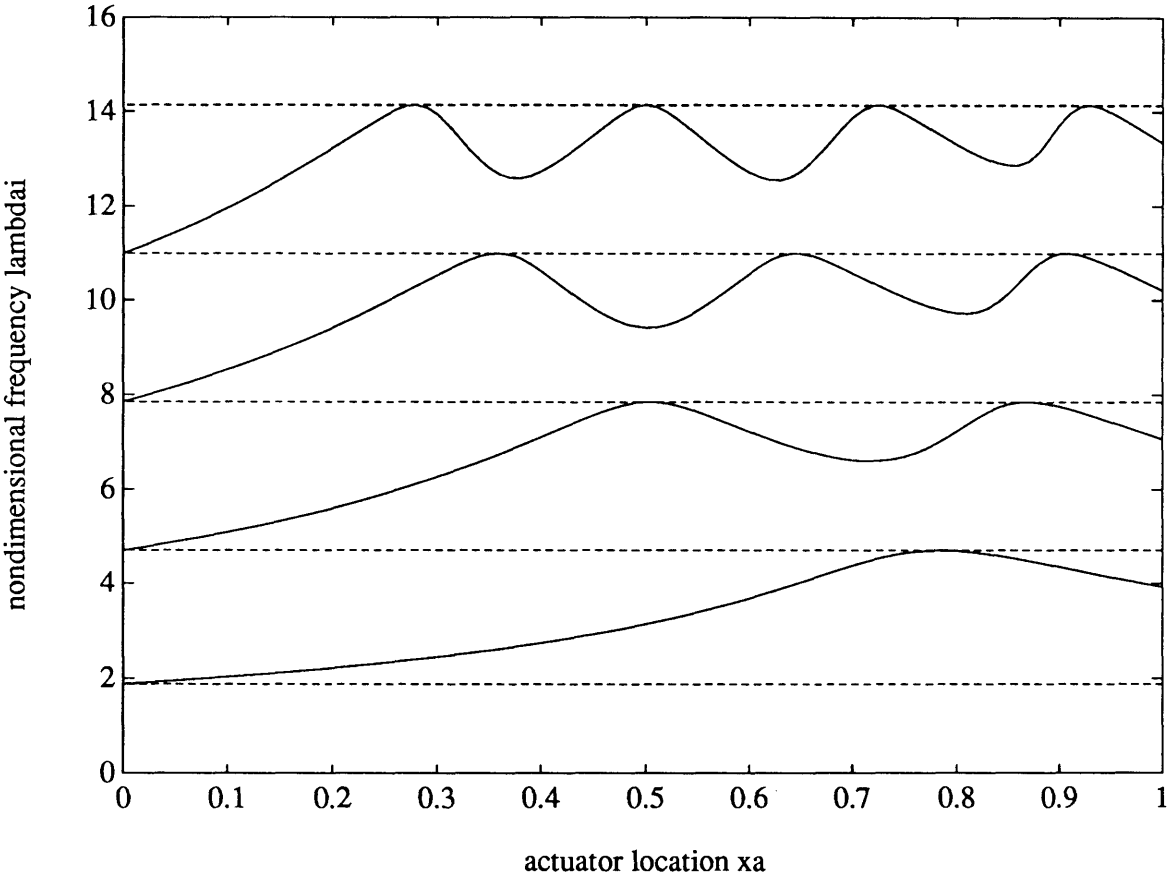

Figure 3.18: Zero trajectories for clamped-free beam with collocated transverse forcing and displacement measurement, as a function of spanwise location of sensor/ actuator pair. Poles are included for reference as horizontal lines.

by solid lines.

These trajectories have many interesting features. The free-free beam results are discussed first and then contrasted with the clamped-free case. For the free-free case, the zero trajectories are symmetric about the midspan due to the symmetry of the structure. The pole-zero cancellations at the node locations of the modes are apparent. There is a loss of both observability and controllability at this pole-zero cancellation. This is due to the sensor and actuator being dual and both being situated at the node of the mode shape.

The local slope of the zero trajectory at the pole-zero cancellation is also zero, consistent with the prediction in the general sensitivity analysis of Chapter 2. Section 2.3 used a transmission zero definition to perform a first order perturbation on the zero frequencies, given by

$$z_k^{(1)} = \frac{\left[\tilde{w}_k^T\right]^{(0)} \mathcal{A}^{(1)} \tilde{v}_k^{(0)}}{[\tilde{w}_k^T]^{(0)} \mathcal{B} \tilde{v}_k^{(0)}} \tag{3.41}$$

A simultaneous loss of observability and controllability produces right and left eigenvectors given by $\tilde{v}_k = [v_k 0]^T$ amd $\tilde{w}_k^T = [w_k^T 0]$. Hence, a slight change in B or C signifying a change in location of the sensor and actuator pair produces no change in the k^{th} zero. This may be shown by examining the numerator of $z_k^{(1)}$ for the case of first order changes in B and C but not in A.

$$z_k^{(1)} = \left[\; [w^T]^{(0)} 0 \; \right] \begin{bmatrix} 0 & B^{(1)} \\ C^{(1)} & 0 \end{bmatrix} \begin{bmatrix} v^{(0)} \\ 0 \end{bmatrix} \tag{3.42}$$

This case clearly gives the first order perturbation in z_k as zero. If however, only observability or controllability were lost and not both, $z_k^{(1)} \neq 0$. This result, general for any structure has two basic implications. Attempting a pole-zero cancellation in a collocated scenario is a viable technique due to the low sensitivity to error in A/S location or actual node location. This was suggested by Juang and Williams [29]. Conversely, in order to effect large changes in the pole-zero spacing, the S/A pair must be moved substantially if it is in the vicinity of a nodal point of a mode of interest.

Aside from the local slope at these node locations, the sensitivity of the zero has another important property. The frequency with which the zero trajectories oscillate grows higher with increasing zero number. The sensitivity of the zero to changes in the S/A pair location therefore generally becomes stronger with increasing frequency. Just as higher frequencies of structures are not predicted with a good deal of certainty, the zero frequencies become more unreliable as a result.

The migration of the zero frequency for each zero in Figures 3.17 and 3.18 is bounded between the poles immediately above and below it. This must hold true to satisfy the alternating pole-zero spacing of collocated and dual systems. Irrespective of the location of a collocated, dual, and complementary extreme S/A pair, or of the structure on which the pair acts, the pole-zero pattern alternates. For the free-free case of Figure 3.17, the zero trajectories never encounter the lower pole as they do the upper for pole-zero cancellation. For the clamped-free case of Figure 3.18, however, the zeroes migrate over the full range between the lower bounding and upper bounding pole. The open loop zeroes, equivalent to the closed loop high gain poles, are the poles of an initially free-free or clamped-free beam to which a pin has been added at the collocated sensor and actuator location. A pin introduced to the free-free beam produces a finite change in the stiffness of the structure which initially had no constraints. Hence the zeroes of the free-free beam do not ever drop so low as to encounter the lower bounding pole. If the open loop system begins completely unconstrained, the zeroes will never approach the open loop poles just below. For the clamped-free case, the introduction of a pin near the already constrained end causes the infinite gain closed loop poles to gradually depart from the open loop poles as the pin is moved away from the fixed end.

The separation between the upper pole and the zero trajectory of Figure 3.17 of a given zero appears to look like the function $\phi^2(x)$, i.e., the square of the transverse displacement mode shape. Recalling the residue expansion definition of a zero of Section 2.1, the pole cancellation zero is the limiting case of a general transmission

zero. The pole cancellation zero is determined by a test of the modal residue

$$r_i = (cv_i)(w_i^T b) \tag{3.43}$$

which is the inner product of the modal observability and controllability. For the point actuators and sensors adopted here, c and b are unit vectors, and r_i takes the form

$$r_i = \phi_i \phi_i^T \tag{3.44}$$

which is seen to vary as the mode shape squared as the collocated S/A pair traverses the span. If the zero were a simple linear function of the residue, then the separation would depend exactly on $\phi\phi^T$. However, the transmission zero is not a linear function of the individual residue of that particular mode. In fact, the other modes contribute an ever stronger influence as the zero moves from a pole cancellation zero, although the zero trajectory maintains a characteristic preference for that particular mode. Hence the zero trajectory and the function $\phi^2(x)$ do not coincide exactly. But this reaffirms the role of the zero as a controllability and observability measure of the flexible modes, at least for the collocated case.

For the clamped-free beam of Figure 3.18, there are similarities and differences to the features of the zero trajectories observed in the free-free case. The zero trajectories are no longer symmetric as the plant symmetry is lost. The pole-zero cancellations are still visible, and occur as the trajectory for a given zero is at a maximum. Hence, again there is a zero local slope when the S/A pair is at the node locations. This is another case exemplifying the sensitivity prediction of Section 2.3. The sensitivity of the zero in general increases with rising zero number as in the free-free beam. When the S/A pair is at the clamped end, the zeroes are equal to the poles of a clamped-free beam. As the S/A pair is moved slightly away from this constrained end, the zeroes increase in frequency. In contrast to the free-free case, the zero migrations of the clamped-free beam are bounded exactly from above and below by the poles.

From these results it is clear that the zeroes are a modal controllability and observability measure. The trajectories appear similar to the mode shape squared which

is a quantity often weighted to produce the modal cost used to truncate models. The migration of the zeroes for collocated and dual S/A pairs is bounded by the poles immediately above and below, irrespective of the rigid body or constrained behavior of the system. The zero migrations for the unconstrained structure are smaller relatively to the pole spacing than those for corresponding constrained systems. The zero trajectories are symmetric as a function of spanwise collocated and dual S/A pair location when the structure is symmetric.

Slightly Non-Collocated Sensor and Actuator Pairs

The effects of non-collocation may be viewed first as a perturbation on the collocated case, as is done in this subsection, and then for the highly non-collocated case discussed in the next subsection. This approach promotes a deeper understanding of non-collocated systems.

The solution method described in the previous subsection is extended to the non-collocated case. The technique of modelling the actuator as a transverse force acting at an internal boundary of the structure is retained. The distinction is that now a non-collocated displacement measurement is fedback. For a uniform beam, the governing equation is given by Equation 3.27, with solutions 3.28 and displacement and slope compatibility at the actuator location x_a given by Equation 3.29 and 3.30. At the actuator location there are still two force equilibrium equations, Equations 3.31 and 3.32, but now the force fedback is proportional to the displacement at the sensor location

$$f(x_a) = -kw(x_s) \tag{3.45}$$

yielding a new shear equilibrium equation in place of Equation 3.34

$$EI\frac{\partial^3 w_1}{\partial x^3}(x_a) - EI\frac{\partial^3 w_2}{\partial x^3}(x_a) - kw_1(x_s) = 0. \tag{3.46}$$

The results of the solution of the transcendental equation of the generalized eigenvalue problem in the limit as $\frac{k}{EI} \to \infty$ as a function of x_a, x_s are displayed in Figure 3.19. The zeroes are shown in terms of the dimensionless frequency parameter,

λ, for successively increasing zero number. The collocated solutions are included for reference. The non-collocated zeroes are plotted at the spanwise location $\bar{x}$ which corresponds to the center of the S/A pair so that $x_a = \bar{x} - \frac{\Delta}{2}$ and $x_s = \bar{x} + \frac{\Delta}{2}$. Each curve represents a different fixed degree of non-collocation. Non-collocation distances of $\Delta = 5\%$ and $\Delta = 10\%$ are shown.

One of the features first noticed is the appearance of two pole-zero cancellations in the vicinity of each node location. These two pole-zero cancellations correspond to a loss first of observability when the sensor is at the node location and then to a loss of controllability when the actuator is at the node location. The pole-zero cancellations appear in Figure 3.19 to occur to either side of the node location because the zeroes are plotted at the spanwise location which corresponds to the center of the S/A pair. Naturally, if the node location occurs at a distance from the end of the structure smaller than the separation distance between the sensor and actuator only one pole-zero cancellation exists in the vicinity of the collocated pole-zero cancellation.

It is in the neighborhood of the node locations that the initially alternating pole-zero pattern of the collocated case is most likely to be destroyed. The destruction of the alternating pattern occurs when the sensor and actuator are located on opposite sides of a node so that the measurement of that mode is 180 degrees out of phase with the actuator. The spanwise region where the alternating pole-zero pattern is destroyed is given directly by the degree of non-collocation, Δ. For non-collocated S/A pairs that are originally dual and collocated, the zero corresponding to that particular unstably interacting mode does not disappear, but just moves higher in frequency. It may move well beyond the next pole if the degree of non-collocation is large enough, as is seen in the next subsection. If a non-collocated configuration is chosen and alternating pole-zero patterns are still desired for the low frequency modes, the sensor and actuator should be placed away from any node locations of the modes in the control bandwidth if possible.

The effects of non-collocation are larger at higher frequencies when the non-

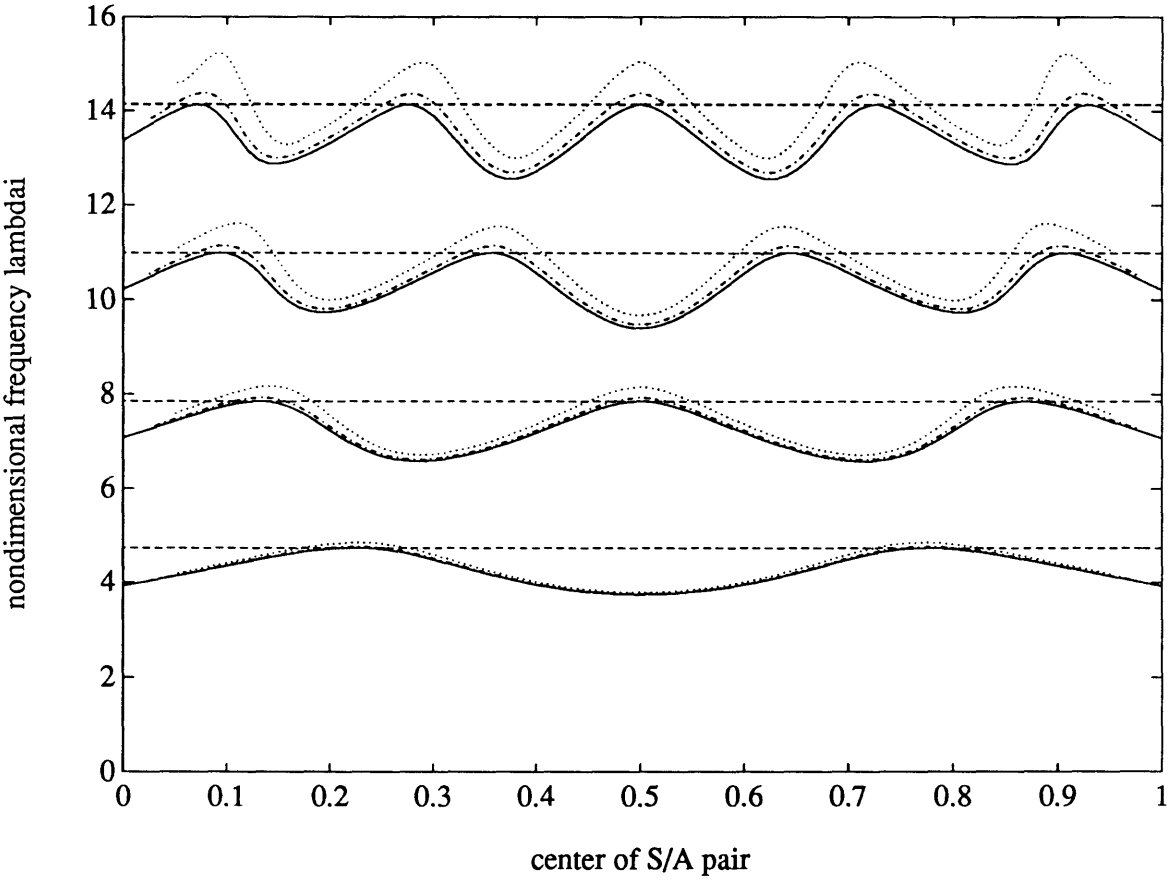

Figure 3.19: Zero trajectories for free-free beam case with non-collocated transverse forcing and displacement measurement as a function of center of spanwise location of sensor/ actuator pair, $\bar{x}$. Results are shown for the case $x_s = x_a + \Delta$, $\Delta = 5\%(dashed), 10\%$ (dotted).

collocation distance becomes an ever greater percentage of the spatial wavelength of the corresponding mode. This can be seen by observing that the maximum travel of the zero as a percentage of the pole interval grows with increasing mode number. For a given degree of non-collocation, the zero sensitivity to S/A pair location at a pole-zero cancellation increases with increasing zero number.

The sensitivity of the zero to the sensor and actuator location for the slightly non-collocated case may be seen by examining the slope of the zero trajectories in Figure 3.19. Unlike the collocated case where the sensitivity of a zero is zero at a pole-zero cancellation, for the non-collocated case this is no longer true. When the system is no longer collocated a pole-zero cancellation corresponds to either a loss of observability or controllability but not both. As a result, the sensitivity at the zero is no longer zero. This was shown in Section 2.3 for the general non-collocated case and is substantiated here by the free-free beam example. It is also evident that generally, the sensitivity is larger as the non-collocation distance becomes larger. The zero sensitivity to S/A pair location at a pole-zero cancellation increases with increasing non-collocation distance for a given zero. The slope of the zero trajectories is not largest at the pole-zero cancellations.

A tradeoff is apparent for general controlled structures problems. Sensitivity of the zero is smaller in regions near nodes but more likely to destroy the alternating pole-zero pattern. Higher sensitivity away from the nodes will not destroy the alternating pattern for small sensor and actuator spacing.

The mode shapes associated with the zeroes may be found as well. These mode shapes correspond to the initial conditions component of the zero direction (Equation 2.6). The mode shapes of the zeroes in the collocated case are given by the modes of a pinned or clamped system. For the free-free case with a displacement sensor and force actuator, the zero mode shapes are real and appear to pin the location of the sensor, irrespective of the size of the non-collocation distance. For small non-collocation distances, the mode shapes corresponding to the zeroes reported in this

section appear as slight perturbations to a truly pinned condition, or the collocated case.

Highly Non-Collocated Sensor and Actuator Pairs

The preliminary consequences of non-collocation have been discussed in the previous section. For small degrees of non-collocation the zeroes are perturbed slightly from their collocated solutions. The next step is an understanding of the effects as the degree of non-collocation is increased parametrically to the full length of the structure. As the non-collocation distance becomes large, the behavior of the zeroes may vary greatly depending on the type of structure on which the S/A pair acts.

The nature of the partial differential equation determines the characteristics of the zeroes as the non-collocation distance becomes large. The two structures studied in the collocated case are examined again here, namely a free-free and a clamped-free uniform Bernoulli-Euler beam. A uniform free-free rod governed by a second order partial differential equation is examined as well.

For the three sample structures, a force actuator is fixed at a free end and the sensor is moved along the length of the span. A trajectory of zeroes is generated as a function of the S/A pair spacing for the fixed actuator location.

Zeroes of the free-free and clamped-free beams are presented in Figures 3.20 and 3.21 as a function of the sensor location, x_s. The zeroes are represented by the frequency parameter λ. For these two structures, as the non-collocation distance is increased, non-minimum phase zeroes appear. In the case of a real zero, λ is a complex number, and the zero is plotted as the absolute value of λ. The first three poles and two zeroes are presented in Figures 3.20 and 3.21. The solid lines represent λ_i of the imaginary zeroes, the dotted lines the λ_i of the real zeroes. The poles are included as the dashed horizontal lines.

Figure 3.20 shows the zeroes of the free-free case. The actuator is fixed at $x_a = 0$. Beginning with the sensor location at $x_s = 0$ the alternating pole-zero pattern of

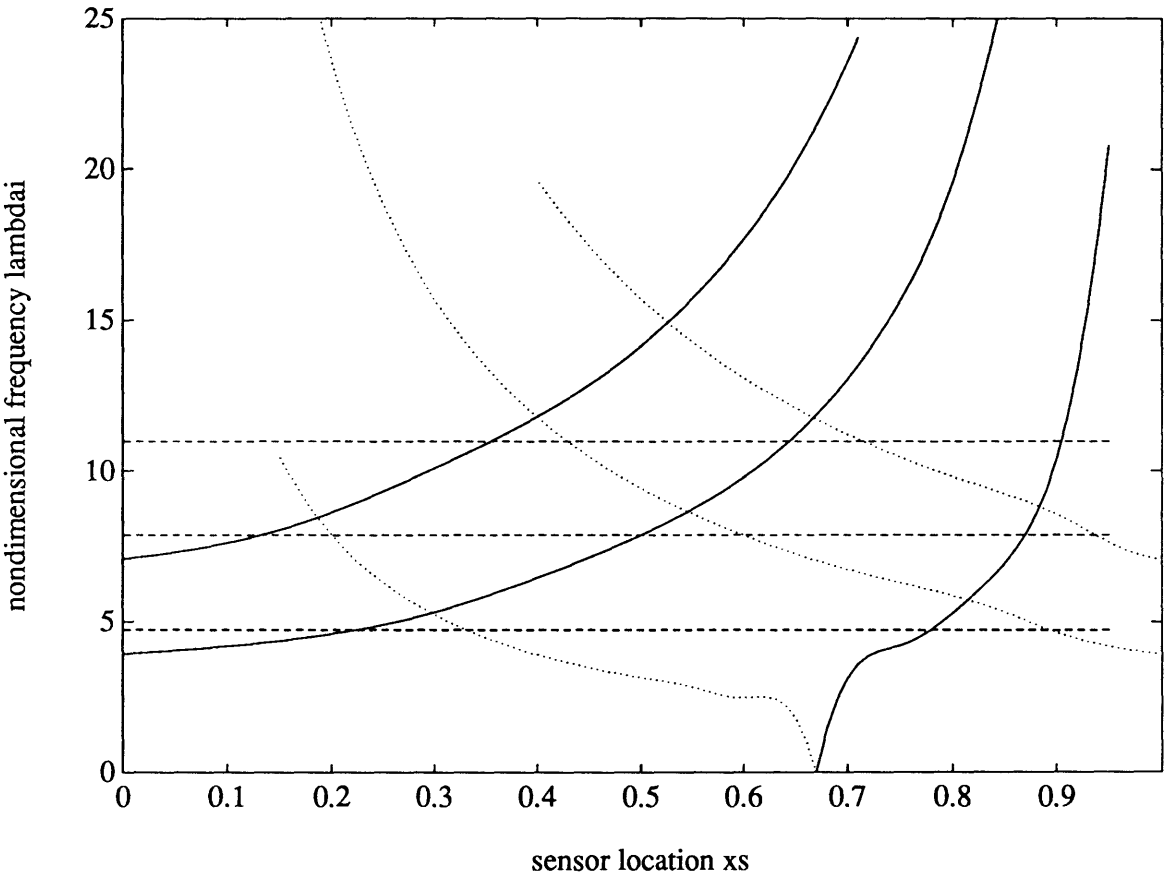

Figure 3.20: Zeroes as a function of sensor location as the actuator remains fixed at $x_a = 0$ for a free-free beam. Zeroes are plotted as a frequency parameter λ for imaginary zeroes or as $abs(\lambda)$ for real zeroes. The imaginary zeroes are given by the solid line, the real zeroes by the dotted line, the poles by the horizontal dashed line.

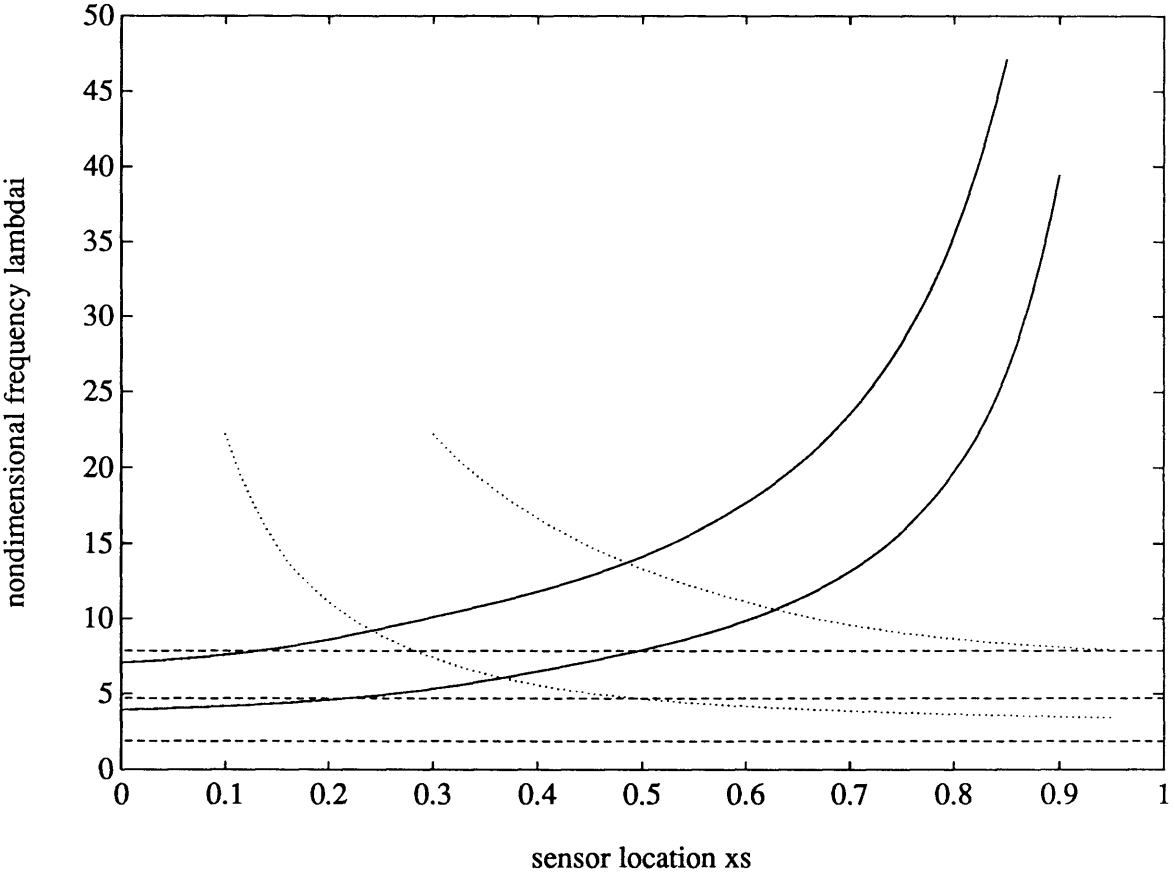

Figure 3.21: Zeroes as a function of sensor location as the actuator remains fixed at $x_a = 0$ for a clamped-free beam. Zeroes are plotted as a frequency parameter λ for imaginary zeroes or as $abs(\lambda)$ for real zeroes. The imaginary zeroes are given by the solid line, the real zeroes by the dotted line, the poles by the horizontal dashed line.

a collocated S/A pair is visible. The real zeroes are at infinity. As the sensor is moved away from the actuator, the imaginary zeroes increase in frequency as in the slightly non-collocation case. The real zeros are still very far out along the real axis although they move in quickly as the non-collocation distance becomes larger. The pole cancellation zeros are visible at the node locations. It is always the imaginary zeroes that produce the pole-zero cancellations. However, while the zero associated with the first mode produces the pole cancellation of the node nearest the actuator at $x_s = 0.225$, it is a different zero that produces the pole-zero cancellation at the far node of the first mode shape at $x_s = 0.775$.

This imaginary zero which cancels a pole when $x_s = 0.775$ originates at $\lambda_i = 0$, at $x_s = 0.67$, the center of percussion of the free-free beam. Of the two pairs of poles corresponding to the two rigid body modes of the free-free beam with high gain feedback, one pair is at the origin, while the other pair is at infinity on the imaginary axis. When the feedback is collocated, one zero is at infinity on the imaginary axis, indicating one rigid body mode is uncontrollable or unobservable. As the feedback becomes non-collocated, this zero pair at infinity circulates to the real axis and progressively nears the origin. It arrives at the origin at a sensor location given by the center of percussion of a rigid structure. With an actuator on the end and a sensor at the center of percussion, the other rigid body mode becomes unobservable or uncontrollable. As the sensor continues further, the zero pair becomes imaginary again.

In addition to the details of the figure such as the node locations and the center of percussion there are more global features to the figure worth mentioning. Although the free-free beam is a symmetric plant, there is asymmetry to the zeroes of the plant as the sensor traverses the span. The real zeroes occur at points different from the imaginary zeroes at symmetric locations. The transpose problem, a sensor at x_a and an actuator at x_s will yield equivalent zeroes to the those of the case shown when the actuator is at x_a and the sensor is at x_s.

Finally the sensitivity of both the real and imaginary zeroes are visible in the figure. As the non-collocation distance grows, the sensitivity of a particular imaginary zero increases. The sensitivity of the corresponding real zero decreases as the non-collocation distance increases. With increasing zero number, the sensitivity of a given zero to the non-collocation distance becomes larger.

The zero mode shapes for the imaginary zeroes of the free-free beam example appear to be real and pin the sensor location. For the real zeroes far away from the imaginary axis, the zero mode shapes have a real and a complex part however both are small. As the real zeroes move closer in to the imaginary axis, the zero mode shapes become predominantly real.

The effect of the two rigid body modes results in a very low frequency non-minimum phase zero when the sensor is positioned at the center of percussion and the actuator is positioned at the end. This will pose severe performance limitations on the disturbance rejection and command following given this S/A pair. The problem will not be as acute for the clamped-free case.

This zero locus as a function of the non-collocation distance was also found for the case of a clamped-free beam. The fixed end is located at $x = 1$ and the actuator location is fixed at the free end, $x_a = 0$. Figure 3.21 shows that for the clamped-free case as the degree of non-collocation is increased the imaginary zeroes rise and the real non-minimum phase zeroes become apparent. The trajectories of the zeroes for the clamped-free and the free-free case have similar characteristics in that they both have rising imaginary zeroes and decreasing non-minimum pahse zeroes as the non-collocation distance grows larger. The clamped-free case does not have a non-minimum phase zero tending towards the origin as the non-collocation distance becomes large since there are no rigid body modes of the clamped-free beam.

For these two fourth order plants, as the non-collocation distance becomes large, real zeroes appear in symmetric pairs about the imaginary axis yielding non-minimum phase zeroes. These non-minimum phase zeroes appear ever closer to the imaginary

axis. Hence, increasingly large degrees of non-collocation for such a plant produce non-minimum phase zeroes of increasingly lower frequency. This produces a fundamental limitation on the performance achievable with a non-collocated system [1]. Manipulators are plagued by such performance limitations. Torque actuators are placed at joints, far from the end point locations being controlled. An attempt to alleviate this severe non-minimum phase behavior is found in [30]. The application of a control torque on a flexible manipulator is translated by means of tensioned cables attached to the arm at points much closer to the sensed end. The non-minimum phase zeroes of this system are then much higher in frequency.

For the case of the free-free rod, all possible combinations of x_a and x_s produce solutions to the transcendental equation which are purely real values of λ_i and hence purely imaginary zeroes. Figure 3.22 shows the zeroes and poles for the case in which the actuator remains at the free end $x = 0$ and the sensor is moved successively further from the actuator. While the features of the imaginary zeroes are similar to those of the free-free beam example, this non-collocated plant is minimum phase. Spector and Flashner [16] discuss non-collocated structural systems by means of a pinned-free beam example. They claim that all non-collocated systems are non-minimum phase above some finite frequency. The free-free rod is a counter example to this claim. Another experiment conducted by Cannon and Rosenthal [4] on a lumped mass model approximating a torsional rod never found any non-minimum phase behavior.

Summary

The location of a dual sensor and actuator can substantially alter the pole-zero patterns. For the collocated case, each zero migrates relative to its neighboring pole as a function of the S/A location dominated by the controllability and observability of that mode. For small non-collocation distances, compared to the spatial wavelength of the mode in question, the zeroes migrate in a pattern still dominated by the modal controllability and observability. The alternating pole-zero pattern is destroyed in the vicinity of the nodes of the mode shapes. The effect of non-collocation has been shown

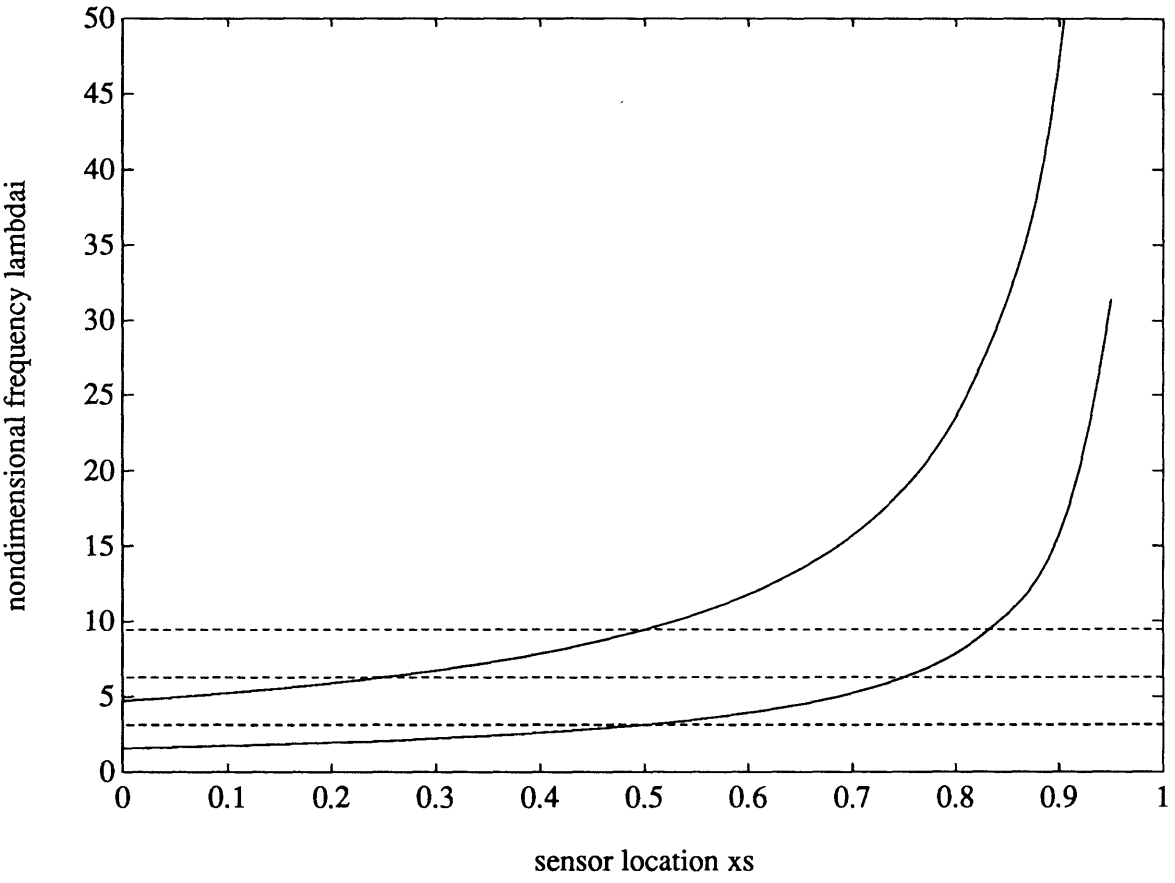

Figure 3.22: Zeroes as a function of sensor location as the actuator remains fixed at $x_a = 0$ for a free-free rod. Zeroes are plotted as a frequency parameter λ for imaginary zeroes. The imaginary zeroes are given by the solid line, the poles by the horizontal dashed line.

to increase the frequency of the imaginary zeroes. As the non-collocation distance becomes large, the imaginary zeroes become higher in frequency moving far away from their corresponding poles. Non-minimum phase zeroes may appear for certain structures with non-collocated S/A pairs. These non-minimum phase zeroes becomes of successively lower frequency as the non-collocation distance increases.

The sensitivity of the zeroes as a function of location of the sensor and actuator was also studied for the collocated case and as the S/A pair were moved apart. The sensitivity of the zero to changes in the collocated an dual S/A pair location is zero at the nodes of the mode shapes. The sensitivity of the zeroes to changes in the location of the S/A pair becomes non-zero at the nodes once the S/A pair are separated slightly, and steadily increases as the degree of non-collocation becomes larger. The sensitivity of the zero near and away from nodes generally becomes larger with increasing zero number for both the collocated and non-collocated case. It becomes particularly strong for the imaginary zeroes as the non-collocation is larger than half the span of the structure.

The solution method used in this section, which is based on the operational definition of zeroes, can be used not only for infinite order models of controlled flexible structures but for finite order models, such as finite element models, as well. A lumped stiffness corresponding to the feedback element can be included in the structural model, and incorporated into the stiffness matrix of a finite element model. For the collocated case, as this lumped stiffness is made infinitely large, the measured degree of freedom becomes pinned. This infinite order modelling technique can also be applied to MIMO systems in theory, although it would be quite a challenge as the number of sensor and actuator pairs grows.

Chapter 4

The Effect of Modelling on Zero Frequencies

The zeroes have been shown to be a complex function of the type, impedance, and location of the actuation and sensing mechanisms. Even if these actuator and sensor characteristics are precisely known and accurately modelled, the zeroes may still be incorrectly predicted due to the incomplete and /or inaccurate modelling of the structure on which the sensor and actuator pair act. The zeroes are a result of interference of the infinity of modes of the continuum. Any incomplete finite order model which attempts to capture this behavior is subject to errors associated with truncation. Inaccuracy in the calculation of mode shapes due to spatial discretization of the continuum degrades the prediction of the modes. Modal observability and controllability may be inaccurately calculated, and hence the zeroes, a function of the modal observability and controllability are thus affected by discretization.

The precision of the zeroes is susceptible to the limitations of various modelling techniques which attempt to capture the structural behavior of an infinite order system with a finite number of states. These limitations can be classified as being of two general types, truncation and discretization. Truncation consists of capturing an infinite order system by a finite set of modes. There are two aspects of truncation from an infinite set to a set of N_r retained modes. In one instance, the first N_r modes are kept in the model and the higher modes from $N_r + 1$ to ∞ are truncated. In the other instance, the "best" N_r modes are chosen for the model, where "best" is some measure used to describe the importance of a mode to the control objective. Most

control design techniques require a finite set of degrees of freedom. Truncation is an inevitable method of reducing a model to a finite order.

Discretization consists of describing the spatially varying state of the structure, the displacements, rotations, and/or internal strains, at a finite set of locations on the structure and then interpolating the state of this structure between such points by a simple function. This finite set of points need not describe the exact displacements of the structure at these points. This is because such discretization enforces constraints which tend to stiffen the model of the structure [31]. Discretization implies a decreased level of fidelity of the model globally at the finite set of sample points, and also a decreased level of fidelity locally within each element.

The errors in modelling of continuous systems, whose motion is governed by partial differential equations, can be quantified in terms of these two concepts, truncation and discretization. In turn, the effects of truncation and discretization on the zeroes can be decoupled and studied separately. A Rayleigh Ritz assumed modes model may be used to isolate truncation effects. By using a truncated finite set of continuously defined exact mode shapes, the effects of discretization are eliminated in such a model. Once these truncation effects are understood, a model based on a finite set of equal number of discretized mode shapes may be compared to a model based on a finite set of exact continuously defined mode shapes. Hence, the discretization component of the modelling process may be isolated.

There is a common basis by which these effects of truncation and discretization can be characterized. It is shown in the first section of this chapter that the zeroes, although being a complex aggregate quantity, do converge to exact values as the number of modes included in a model is increased or as the fidelity of the mode shapes is refined. For the purposes of the examples used in this chapter, these exact values are determined from a partial differential equation model of a Bernoulli-Euler beam with either clamped-free or free-free boundary conditions, as was done in chapter 3. The effects of truncation and discretization, as well as any suggested improvements

to the modelling techniques are based on convergence rates of the zeroes to the exact zeroes as a function of the number of modes included in the model or as a function of the discretization of the field.

The purpose of this chapter is to determine strategic methods for improving zero predictions. Specifically, a study of truncation effects can lead to criteria for choosing certain modes over others to include in the model. A study of discretization can determine the requirement for fidelity of the mode shapes. These methods for improving zero predictions can then be combined for more accurate low order models.

In this chapter, the convergence behavior of the zeroes is established first. It is assumed that the actuator and sensor are collocated. This convergence behavior is then used as the basis for study of the effects of truncation of infinite order systems. The two aspects of truncation are studied individually, beginning with the type of truncation which just eliminates all but the first N_r modes. The effects of such truncation are discussed and explored via a simple beam model. A method of compensating for this type of truncation is presented which is shown to be equivalent to modelling schemes used in various other disciplines. The second type of truncation which chooses the "best" N_r modes is then discussed, and the implications of such truncation for the zeroes is presented. The effects of discretization are then studied in two parts by means of a simple beam model. The effect of using higher order interpolation functions between the mesh points is presented. The level of discretization of the spatial field is then explored. Together these discretization studies help determine how to concentrate the level of fidelity for a given number of degrees of freedom to best improve the prediction of the zeroes.

4.1 Convergence Behavior of Zeroes

A study of the effects of truncation and discretization can best be made if the zeroes can be shown to converge, and to converge to their "exact" values. If the zeroes do converge, it is desirable to know how the convergence proceeds as the number of modes

included in the model or the fidelity of the modes is increased. Ideally, the convergence properties should be well behaved, and monotonic, just as the convergence of the eigenfrequencies of a consistent assumed displacement based method is assumed [31]. The objective of this section is to establish that for collocated and dual point sensor sensor and actuator pairs the zeroes converge in the same fashion as do the poles for a given modelling scheme.

Convergence of the poles may be monotonic from above as successively more modes are included in the model, with the fundamental pole converging fastest if the modelling technique guarantees this. This Rayleigh convergence behavior is true of techniques such as a Rayleigh Ritz assumed modes method or a Finite Element assumed displacement method with compatible displacements at the boundaries and a distribution of mass in the mass matrix consistent with those displacements. However, convergence of the poles may not necessarily be monotonic from above. A technique which does not assume convergence from above is a Finite Element assumed displacement method with a lumped mass matrix.

Williams [32] has proven that for collocated and dual sensors and actuators, the zeroes have Rayleigh convergence behavior as the number of modes in the model is increased for a model based on compatible assumed displacement and consistent masss. The matrix-second-order equations of motion are placed in a system matrix which becomes singular at a zero frequency. An additional mode increases the dimension of the system matrix by one. With some matrix manipulation, the system matrix is shown to have an embedding property which is characteristic of Rayleigh converging systems [33].

If an assumed displacement model with consistent displacements is not used, monotonic convergence from above is not guaranteed. A consistent mass model incorporates the displacement interpolation functions used to determine the stiffness matrix to allocate mass contributions and loads to the nodes. A lumped mass model just distributes element mass to the nodes resulting in a diagonal mass matrix. A

Table 4.1: Poles and zeroes of lumped and consistent mass models of a uniform rod with a collocated and dual S/A pair

	LUMPED	*CONSISTENT*	*EXACT*
pole #1	2.828	3.464	3.142
zero #1	1.530	1.611	1.571
pole #2	4.000	6.928	6.283
zero #2	3.695	5.629	4.712

Finite Element model based on a lumped mass matrix is not a Ritz analysis since the mass matrix is not consistent and hence does not have Rayleigh convergence properties [34,35]. An example of such non-convergence is available from Wie [15] in which an attempt was made to show the effects on zeroes of consistent versus lumped mass matrices. The poles and zeroes of a rod with a collocated, and dual axial displacement and force S/A pair at a tip are found. A consistent mass model and a lumped mass model are used for comparison. The flexible poles and zeroes are given in Table 4.1.

The poles predicted by the lumped mass model may be compared to the exact model. The poles are underpredicted for this particular number of modes. The poles are overpredicted by the consistent mass matrix model. The zeroes follow in the same pattern as the poles. For the lumped mass model, the zeroes are underpredicted, and for the consistent mass matrix model, the zeroes are overpredicted.

The proof offered here to establish that the zeroes converge in the same fashion as the poles for a given modelling technique is based on a root locus argument. The open loop zeroes of a system are in fact the poles of a closed loop system with infinite gain. This is the essence of the solution method outlined in Chapter 3 for the continuous case.

Any assumed displacement technique can result in a set of second order differential equations describing the homogeneous dynamics of N points on a structure of the

following form

$$M\ddot{q}_i(t) + Kq_i(t) = 0 \tag{4.1}$$

where M must be positive definite and K may include rigid body modes. Both M and K must be symmetric. It is assumed that the effect of the actuator inertia and compliance have already been incorporated into Equation 4.1. The forcing is assumed to always enter at a sampled location on the structure and hence it is incorporated consistently into the model. The model may or may not be completely observable and controllable. The root locus method can find the pole cancellation zeroes in addition to the transmission zeroes.

If it is assumed that the model in Equation 4.1 is described in terms of sampled point displacements or rotations, and that the collocated and dual S/A pair are located at a sampled location, a feedback form for a collocated and dual sensor and actuator pair at sampled location i would be of the form

$$f_i = -k_f q_i. \tag{4.2}$$

This feedback form may be included as a lumped stiffness, k_f along the diagonal of the stiffness matrix. The force equilibrium at the sampled location corresponding to the location of the S/A pair is augmented by a generalized force proportional to the generalized displacement at that location.

$$M\ddot{q}_i(t) + Kq_i + diag(0 \cdots 0 k_f 0 \cdots 0)q_i = 0 \tag{4.3}$$

$$M\ddot{q}_i(t) + K_R q_i = 0 \tag{4.4}$$

As k_f is taken to be infinitely large, so that the poles of the original system of Equation 4.1 approach the zeroes of the system, one diagonal element in the revised stiffness matrix, K_R, becomes infinitely large. The effect is to "pin" that degree of freedom. The remaining $N-1$ system eigenvalues of the N^{th} order system are the predicted zeroes, according to the modelling method chosen, of the original system of order N.

The zeroes of the system are given by the poles of the system given by Equation 4.4 as $K_f \rightarrow \infty$. It suffices to determine the convergence of the poles of the "pinned" system of Equation 4.4 to establish the conergence behavior of the zeroes. If a modelling method ensures a particular convergence behavior of the poles of the pinned system, the zeroes will converge in this same manner.

This proof may be extended to the MIMO case directly.

Convergence properties of the eigenfrequencies of structural dynamic systems given by a mass and stiffness matrix are well known. For Rayleigh Ritz assumed modes models, the poles of the "pinned" system will converge with Rayleigh convergence behavior. For an assumed displacement based Finite Element model with consistent displacements, there are two possible cases. The number of degrees of freedom is increased by more elements (h-type) or is increased by raising the order of the interpolation functions (p-type). Covergence theorems based on both of these cases may be found in Meirovitch [33]. Rayleigh convergence behavior governs both cases. A lumped mass model will not have monotonic convergence behavior of the poles of the "pinned" system and hence of the zeroes.

Four examples are presented to demonstrate the convergence behavior of zeroes. These examples all use consistent assumed displacement based models, either Rayleigh Ritz models or Finite Element assumed displacement models with consistent mass and compatible deflections. Hence, the zeroes should converge monotonically from above for all of the examples presented, where collocated and dual S/A pairs are used, as the number of modes included in the model is increased. The examples use a Bernoulli-Euler beam model with a collocated S/A pair. The zeroes are reported as the difference from their exact value normalized by their exact value.

These four examples are presented in Table 4.2. Examples one and two are of a clamped-free beam with a dual transverse force/displacement pair at the tip. Example one uses exact Rayleigh Ritz modes, where the accuracy on the frequency parameter λ_i is 10^{-16}, and example two uses cubic Finite Elements with compatible displacement

Table 4.2: Characteristics of plant of the examples used to show zero convergence

	EXAMPLE 1	*EXAMPLE 2*	*EXAMPLE 3*	*EXAMPLE 4*
STRUCTURE	clamped-free	clamped-free	clamped-free	free-free
S/A PAIR	dual	dual	non-dual	non-dual
MODEL	RR	FE	FE	FE

and slope at the sampled locations. Monotonic convergence of the zeroes from both models is visible in Figure 4.1. Data is plotted for the first and second zero. The errors in the second zero prediction are consistently larger than those of the first zero as expected for Rayleigh convergence. The errors predicted in these models are very small. This is due to the fact that the system is a simple uniform structure and the exact mode shapes are known. For more complicated structures, the errors are larger but the trends will be the same. The Rayleigh Ritz model for this level of accuracy in the exact mode shape yields substantially better predictions than the Finite Element model for the first two zeroes. This is explored in the next two sections as a manifestation of truncation and discretization.

Non-dual S/A pair systems appear to exhibit the same convergence properties although this has not been proven here. The author is unaware of the existence of such a proof, although a couple of examples here show the possibility. Example three is of a collocated but non-dual S/A pair, a clamped-free beam with a transverse force actuator and angular measurement collocated at the tip. A finite element model of this non-dual system has the first two zeroes converging from above as a function of the number of degrees of freedom as shown in Figure 4.2. The error in the first two zeroes is shown to steadily decrease, with the error in the first zero less than that of the second zero as expected by Rayleigh convergence behavior.

The fourth example is of a free-free beam, a system with multiple rigid body

modes and hence a pole-zero cancellation at the origin given only one S/A pair. A collocated, non-dual S/A pair, transverse force to rotation is chosen which when located at the center of the beam produces complete pole-zero cancellation. A Finite Element assumed displacement model is used. The first two zeroes are still converging from above monotonically as shown in Figure 4.3.

Convergence behavior of zeroes of collocated and dual S/A pairs is guaranteed when the modelling scheme adopted assures convergence behavior of the poles. Zeroes converge to their exact values in the same manner as the poles of the particular modelling scheme. Observability and controllability do not qualify this result. Furthermore, typical results on simple systems indicate that non-dual but collocated S/A pairs exhibit this same convergence behavior.

4.2 Model Truncation Effects

With few exceptions, truncation is a necessary step in the analysis and design of control systems for structures. However, truncation has a marked effect on the accuracy of zeroes. Consider the fact that the system response in the frequency domain is a summation of weighted modal frequency responses. This response is constructed as a Fourier series where the basis functions are the modal responses of the freely vibrating system. These basis functions contain no information regarding the nature of the forcing or sensing of the system such as actuator or sensor type or location. An exact prediction of the system response, including the zero locations, is only captured when all infinity of the modal responses are included. Truncation implies trying to reconstruct the system response with only a finite set of the basis functions. Therefore truncation necessarily implies inaccuracies in the zero locations, even if a truncated series of exact modes is used.

If the difficiencies introduced by truncation can be understood, then additional basis functions can be introduced to compensate for the truncated information. These assumed displacement functions need not be the same free vibration modes, but

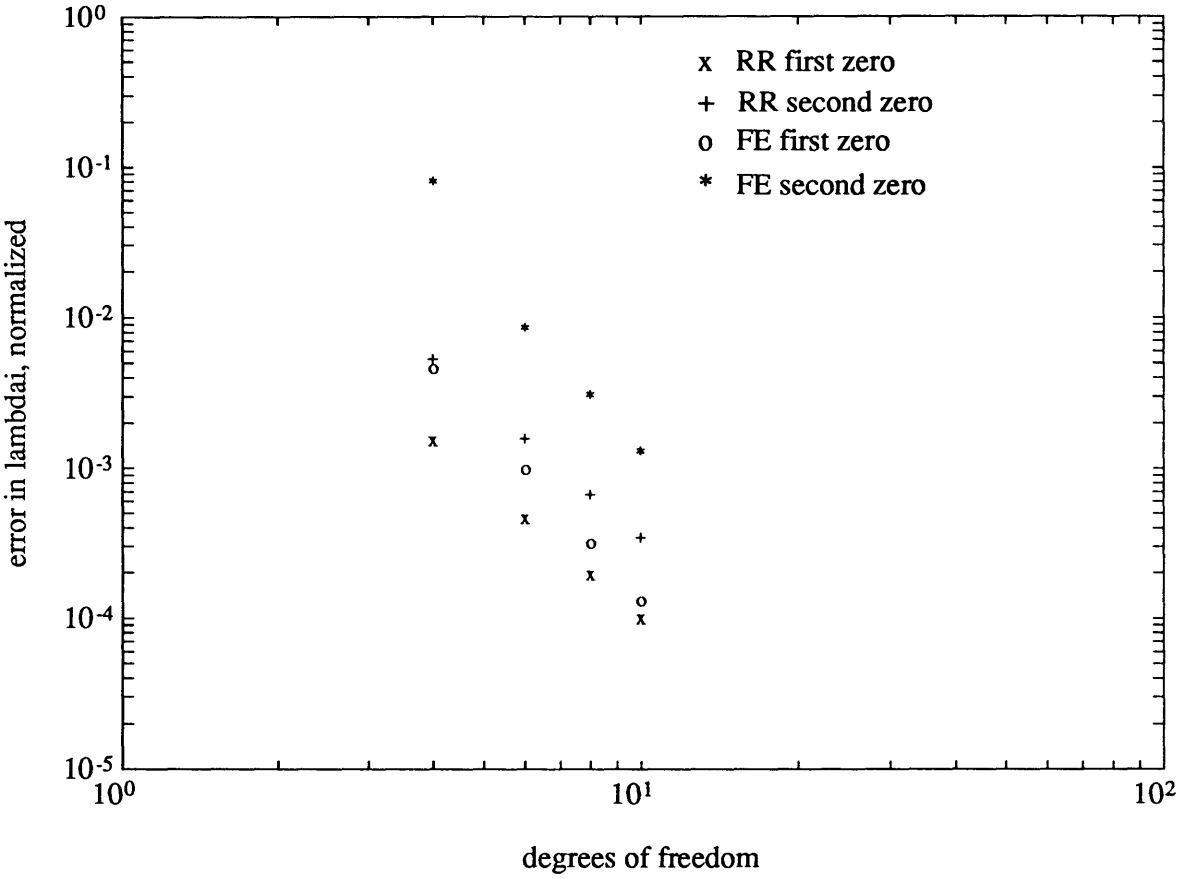

Figure 4.1: Examples 1& 2: Normalized error of the first and second zero frequencies for a clamped-free beam with a dual tip transverse displacement/force S/A pair, Rayleigh Ritz and Finite Element models. First and second zero error are given by x, + and o, * for the Rayleigh Ritz and Finite Element models respectively.

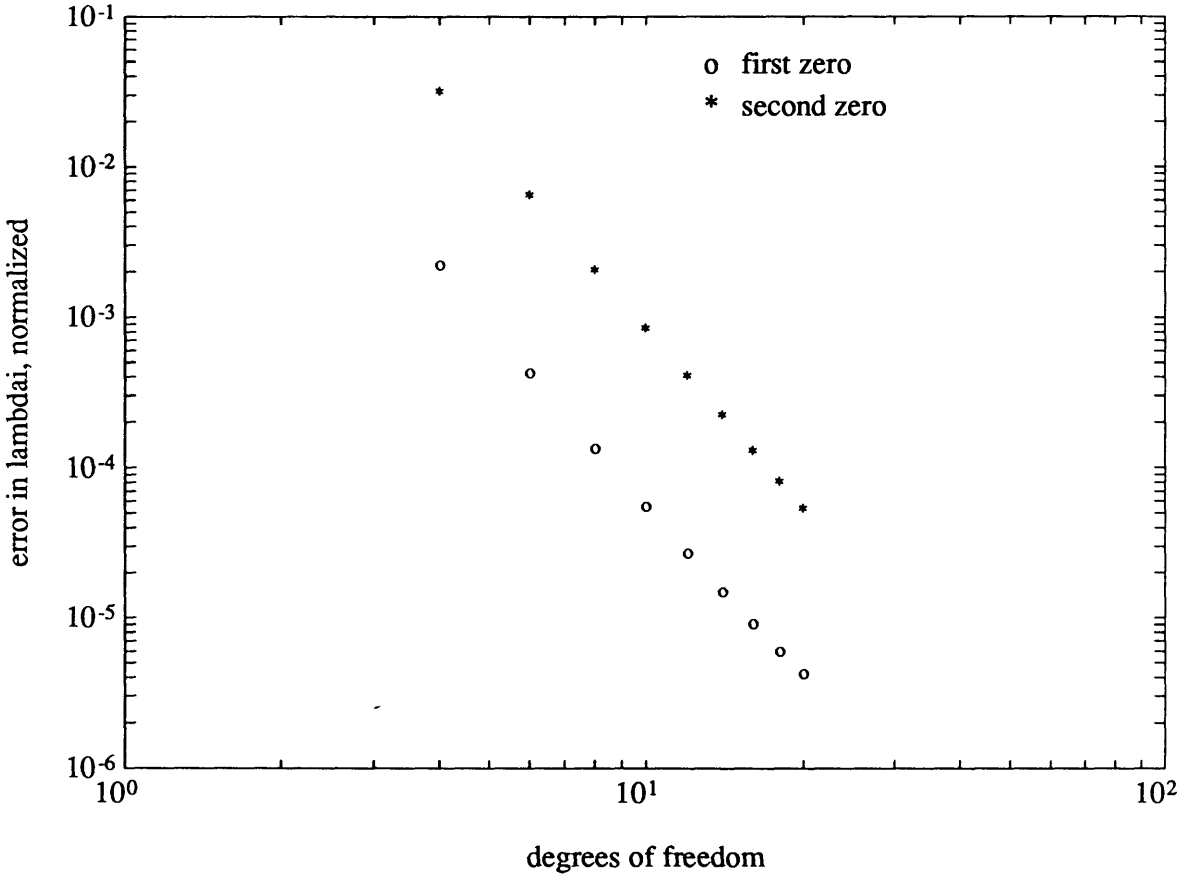

Figure 4.2: Example 3: Normalized error of the first (o) and second (*) zero frequencies for a clamped-free beam with a non-dual tip angular measurement/ transverse force S/A pair, Finite Element model

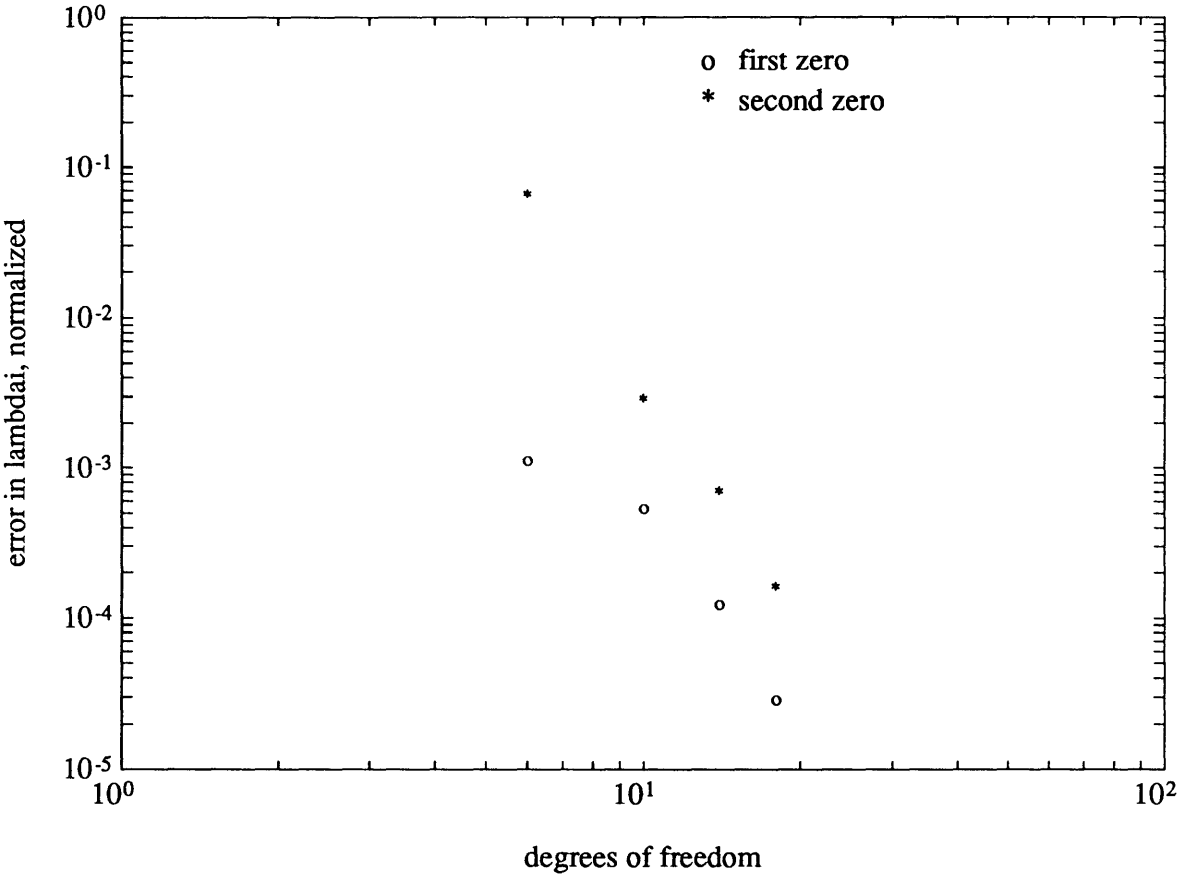

Figure 4.3: Example 4: Normalized error of the first (o) and second (*) zero frequencies for a free-free beam with a non-dual centered angular measurement/ transverse force S/A pair, Finite Element model

instead an augmented set of basis functions for constructing the forced response. A model with a fixed number of these augmented basis functions plus normal modes could then perform as well as one with a greater gross number of normal modes. It is necessary to find which displacement functions would serve this purpose.

There are two common types of truncation used in model reduction: including the first N_r of the infinite number of modes, or including the "best" N_r modes. These two types of truncation are examined separately for their effect on the zeroes. The simpler of the two types is considered first. This is the case where the first N_r modes are retained and the modes $N_r + 1$ to ∞ are truncated. These modes that are truncated each contribute something to the response. Since these modes are all well above the bandwidth of the model, these modes can be modelled as contributing only a static correction term. Each truncated mode contributes only a small static correction to the system response in the bandwidth. In fact, the example one in the last section, Figure 4.1, in which the Rayleigh Ritz model with exact mode shapes is used, isolates this effect. As successively more modes are used, the model is able to slowly build up the proper prediction of the zero, since an increasingly accurate model of the static behavior is achieved.

The static deflection shape may be a linear combination of the truncated set of mode shapes or it may not. If the static shape is completely represented by the set of mode shapes that are included in the model, then the zeroes are predicted perfectly. However, if instead the forcing is such that these static deflection shapes are a set of shapes that cannot be reconstructed completely by the modes retained in the model, the zeroes rely on the static contribution of higher modes not included in the model and are not necessarily accurately predicted. It is the nature of the spatial distribution of control inputs that determines whether the static deflection shape or shapes can be constructed from a finite set of modes.

To improve the prediction of the zeroes while still only including N_r modes, the effect of the static behavior of the actuator and structure must be incorporated into

the model. Many disciplines take this approach of ensuring that the static information is included because empirically or otherwise it yields good results for predicting necessary quantities such as internal stresses, accelerations, or deflections. These techniques are described here and they are all shown to have the same objective. First, a standard model is developed to which the varying methods are referenced. Then the various methods are compared with this standard model.

A structure may be described by an infinite number of modes with equation of motion,

$$\ddot{\xi}_i(t) + \omega_i^2 \xi_i(t) = \Xi_i(t) \tag{4.5}$$

where $\xi_i(t)$ is the orthonormalized modal coordinate, ω_i is the natural frequency and $\Xi_i(t)$ is the generalized modal force of mode i. For a general load profile $Q(x,t)$ the generalized modal force Ξ_i is given by

$$\Xi_i(t) = \int_D \phi_i(x) Q(x,t) dx \tag{4.6}$$

where $\phi_i(x)$ is the mode shape of mode i. If the actuator distribution function $Q(x,t)$ contains mode i, then $\Xi_i(t)$ is non-zero. The displacement of the structure is then given by

$$q(x,t) = \sum_{i=1}^{\infty} \xi_i(t) \phi_i(x). \tag{4.7}$$

If instead of a continuous spatial field, a spatially discretized description is used, then the modal force is

$$\Xi_i(t) = \phi_i^T Q(t) \tag{4.8}$$

where ϕ_i and Q are now vectors. The deflection at the discretization points, j, is then given by

$$q_j(t) = \sum_{i=1}^{N} \xi_i(t) \phi_{i,j} \tag{4.9}$$

The static deflection can be expressed as

$$q_{static}(x) = \sum_{i=1}^{\infty} \frac{\Xi_i}{\omega_i^2} \phi_i(x) \tag{4.10}$$

for the continuous case, or for the discretized case as

$$q_{static,j} = \sum_{i=1}^{N} \frac{\Xi_i}{\omega_i^2} \phi_{i,j}. \tag{4.11}$$

The complete static deflection is described by the summation of the static contribution of each mode.

If the model is to be truncated, then the deflections can be expressed as a sum of those contributed by the N_r retained modes and the truncated modes

$$q(x,t) = \sum_{i=1}^{N_r} \xi_i(t)\phi_i(x) + \sum_{i=N_r+1}^{\infty} \xi_i(t)\phi_i(x) \tag{4.12}$$

$$q_j(t) = \sum_{i=1}^{N_r} \xi_i(t)\phi_{i,j} + \sum_{i=N_r+1}^{N} \xi_i(t)\phi_{i,j} \tag{4.13}$$

From Equation 4.5, the solution for the modal coordinate can be written,

$$\xi_i(t) = \frac{\Xi_i(t)}{\omega_i^2} - \frac{\ddot{\xi}_i(t)}{\omega_i^2}. \tag{4.14}$$

Substituting for the spatially continuous case gives

$$q(x,t) = \sum_{i=1}^{N_r} [\frac{\Xi_i(t)}{\omega_i^2} - \frac{\ddot{\xi}_i(t)}{\omega_i^2}]\phi_i(x) + \sum_{i=N_r+1}^{\infty} [\frac{\Xi_i(t)}{\omega_i^2} - \frac{\ddot{\xi}_i(t)}{\omega_i^2}]\phi_i(x) \tag{4.15}$$

or for the spatially discrete case

$$q_j(t) = \sum_{i=1}^{N_r} [\frac{\Xi_i(t)}{\omega_i^2} - \frac{\ddot{\xi}_i(t)}{\omega_i^2}]\phi_{i,j} + \sum_{i=N_r+1}^{N} [\frac{\Xi_i(t)}{\omega_i^2} - \frac{\ddot{\xi}_i(t)}{\omega_i^2}]\phi_{i,j} \tag{4.16}$$

Equation 4.15 and 4.16 clearly identify four terms: the static and dynamic contributions of the retained modes and the static and dynamic contribution of the truncated modes. Simple model truncation methods retain only the first two of these terms. It will be shown that all the methods discussed in this section retain the first three.

Combining the static deflections due to retained and truncated modes gives,

$$q(x,t) = \sum_{i=1}^{\infty} \frac{\Xi_i(t)}{\omega_i^2}\phi_i(x) - \sum_{i=1}^{N_r} \frac{\ddot{\xi}_i(t)}{\omega_i^2}\phi_i(x) - \sum_{i=N_r+1}^{\infty} \frac{\ddot{\xi}_i(t)}{\omega_i^2}\phi_i(x) \tag{4.17}$$

$$q_j(t) = \sum_{i=1}^{N} \frac{\Xi_i(t)}{\omega_i^2}\phi_{i,j} - \sum_{i=1}^{N_r} \frac{\ddot{\xi}_i(t)}{\omega_i^2}\phi_{i,j} - \sum_{i=N_r+1}^{N} \frac{\ddot{\xi}_i(t)}{\omega_i^2}\phi_{i,j} \tag{4.18}$$

where the first term is the total static response due to all the modes, the second is the dynamic "correction" due to the retained modes and the third the dynamic "correction" due to the truncated modes. Alternatively, from Equations 4.12 and 4.13, if only the truncated modes are broken into their static and dynamic parts, and the motion is assumed sinusoidal,

$$q(x,t) = \sum_{i=1}^{N_r} \frac{\Xi_i(t)}{\omega^2 - \omega_i^2}\phi_i(x) + \sum_{i=N_r+1}^{\infty} \frac{\Xi_i(t)}{\omega_i^2}\phi_i(x) - \sum_{i=N_r+1}^{\infty} \frac{\Xi_i(t)\omega^2}{\omega_i^2}\phi_i(x) \quad (4.19)$$

$$q_j(t) = \sum_{i=1}^{N_r} \frac{\Xi_i(t)}{\omega^2 - \omega_i^2}\phi_{i,j} + \sum_{i=N_r+1}^{N} \frac{\Xi_i(t)}{\omega_i^2}\phi_{i,j} - \sum_{i=N_r+1}^{N} \frac{\Xi_i(t)\omega^2}{\omega_i^2}\phi_{i,j} \quad (4.20)$$

where the first term represents the total response of the retained modes, the second the static response of the truncated modes, and the third the dynamic "correction" due to the truncated modes.

What Equations 4.17, 4.18, 4.19, and 4.20 have in common is that the last term of each represents a dynamic correction to due to the truncated modes, which if the frequencies of interest are small compared to the frequencies of the truncated modes, will be small. Thus the use of the first two terms of Equation 4.17, 4.18 or 4.19, 4.20 represent two approaches to calculating the response of a system which are in fact identical in all but algebra, but which are considerably more accurate than just considering the response of the retained modes. The first approach (Equations 4.17, 4.18) calculates the static response of all the modes, and corrects for the dynamic response of the retained modes. The second (Equations 4.19, 4.20) calculates the total response of the retained modes and corrects with the static response of the truncated modes.

Various methods have evolved in dynamic modelling to retain some information for the modes truncated from a model. It is desired then to show that all these methods reduce exactly to one of the two approaches presented. In aeroelasticity, a method known as the Mode Acceleration Method (MAM) [36] is used to predict the deflections, accelerations and stresses on the wings and fuselage due to disturbances. The philosophy behind the MAM is to begin with a solution corresponding to the static case and then add a dynamic correction term.

The Mode Acceleration Method predicts a displacement field with N_r retained modes by

$$q_{N_r}(x,t) = q_{static}(x) - \sum_{i=1}^{N} \frac{1}{\omega_i^2} \ddot{\xi}_i(t)\phi_i(x) \tag{4.21}$$

$$= \sum_{i=1}^{\infty} \frac{\Xi_i}{\omega_i^2}\phi_i(x) - \sum_{i=1}^{N_r} \frac{1}{\omega_i^2} \ddot{\xi}_i(t)\phi_i(x) \tag{4.22}$$

By comparison with Equation 4.17, it is clear that the MAM is just an example of the first approach which calculates total static response and corrects for the dynamic response of the retained modes.

In finite element solutions of structural dynamics, models are often truncated to only a few low frequency modes, and a component known as the residual stiffness is included in the model [34]. If only N_r of N modes are maintained in a model then the equilibrium between the external loading, $Q_j(t)$ and the inertia and elastic loading is not met. The response to a part of the external load vector has not been included in the model. This portion of the external load vector is given by

$$\Delta Q_j(t) = Q_j(t) - \sum_{i=1}^{N} (M\phi_{i,j})\Xi_i \tag{4.23}$$

$$\Delta Q_j(t) = Q_j(t) - Q_{N_r,j}(t) \tag{4.24}$$

where ΔQ is the excluded portion of the external load vector, and M is the mass matrix of the system. The correction term removed from the load vector is the portion of the load vector which is in equilibrium with the inertia and elastic loads associated with the retained modes. This portion of the load vector is originally given by the modal force vectors, Ξ_i, of the retained modes, and is then transformed back into physical coordinates such that it is a linear combination of the retained modes. The static correction known as the residual stiffness is then added to the model, since the response to ΔQ should be at most a static response [34].

$$K\Delta q = \Delta Q \tag{4.25}$$

where K is the system stiffness matrix and Δq is the static displacement correction which is added to the displacement prediction made by the retained mode set so that

the total response is given by

$$q_j(t) = \sum_{i=1}^{N_r} \xi_i(t)\phi_{i,j} + \Delta q_j \tag{4.26}$$

where Δq_j is calculated from Equation 4.24 and 4.25. The equivalence to other approaches can be found by expanding the content of Δq in terms of the modes of the full system

$$\Delta q = \phi \Delta \xi. \tag{4.27}$$

Replacing Δq with $\phi\Delta\xi$ in Equation 4.25, then substituting in Equation 4.24 and premultiplying by ϕ^T yields for ϕ orthonormal

$$diag(\omega_i^2)\Delta\xi_j = \phi^T Q_j - \phi^T Q_{N_r,j} \tag{4.28}$$

Letting $\Lambda = diag(\omega_i^2)$ Equation 4.28 becomes

$$\begin{aligned} \Delta\xi &= \Lambda^{-1}\Xi - \Lambda^{-1}\phi^T Q_{N_r} && (4.29)\\ &= \sum_{i=1}^{N} \frac{1}{\omega_i^2}\Xi_i - \sum_{i=1}^{N_r} \frac{1}{\omega_i^2}\Xi_i && (4.30)\\ &= \sum_{i=N_r+1}^{N} \frac{1}{\omega_i^2}\Xi_i && (4.31) \end{aligned}$$

which is to say the $\Delta\xi$ associated with the retained modes is zero. Substituting Equations 4.31 and 4.24 into 4.26 gives the displacement prediction via this residual stiffness method with N_r modes retained in the model and a static correction term Δq as

$$\begin{aligned} q_{N_r,j}(t) &= \sum_{i=1}^{N_r} \xi_i(t)\phi_{i,j} + \sum_{i=N_r+1}^{N} \Delta\xi_i(t)\phi_{i,j} && (4.32)\\ q_{N_r,j}(t) &= \sum_{i=1}^{N_r} \xi_i(t)\phi_{i,j} + \sum_{i=N_r+1}^{N} \frac{\Xi_i(t)}{\omega_i^2}\phi_{i,j}. && (4.33) \end{aligned}$$

From Equation 4.33 it is clear that this residual stiffness corresponds to an approach of the second type, Equation 4.20, which calculates the total response of the retained modes and corrects with the static response of the truncated modes.

In system identification, prediction of the frequency response is always performed in a specific frequency window. Residual terms are defined as contributions due to those modes which exist outside of the frequency range to be identified. It is found that correlation is improved greatly by including residual terms, [37] for modes both above and below the frequency window of interest. Since the discussion here focuses on truncation of modes of higher frequency, the residuals due to higher frequency modes are the focus of the remainder of this discussion.

While the two previous methods, the Mode Acceleration Method and the Finite Element residual flexibility, expressed the displacement in the time domain, identification of this kind treats the displacement expressed in the frequency domain as a transfer function from a certain loading. If all the modes were included, the transfer function would have the form

$$\frac{q_x, j}{Q_x} = \sum_{i=1}^{\infty} \frac{(\phi_x^T \phi_x)_i}{\omega_i^2 - \omega^2} \tag{4.34}$$

where the actuator and sensor are collocated at x.

In order to have a model that matches the data well when only N_r modes are identified, a residual stiffness is included

$$\frac{q_{N_r}}{Q_x} = \sum_{i=1}^{N_r} \frac{(\phi_x \phi_x)_i}{\omega_i^2 - \omega^2} + \frac{1}{K_{R_{xx}}} - \frac{1}{m_{R_{xx}} \omega^2}. \tag{4.35}$$

In this instance the residual inertia [37] of modes below the bandwidth have been included as well where $m_{R_{xx}}$ is the residual mass. Comparison with Equation 4.19 indicates that the identified residual stiffness, $K_{R_{xx}}$, is just the static contribution of the truncated modes. For collocated and dual sensors and actuators, the effect of modes below a certain freqeuncy will always appear as a contribution of a pure inertia or as a constant.

One final way to ensure inclusion of the complete static information is in a Rayleigh Ritz assumed modes model where instead of including only the dynamic mode shapes the static deflection shape or shapes are included in the set of comparison functions.

This static deflection shape, assuming the SISO case, in most instances adds information from the space spanned by the truncated modes. This method was used by Anderson [23] in building a two-dimensional model of induced strain actuation.

The Rayleigh Ritz method begins with a representation of the physical displacements by a summation of assumed shape functions. This set of assumed displacement functions must satisfy the displacement boundary conditions and may include the static deflection shape. If the assumed shape functions, save the static deflection shape, are in fact chosen to be the exact mode shapes of the N_r retained modes then the shape function representation of the displacement is

$$q(x) = \sum_{i=1}^{N_r} b_i \phi_i(x) + c_i \psi(x) \tag{4.36}$$

where $\psi(x)$ is the static deflection shape. $\psi(x)$ need not be orthogonal to the other assumed displacement shape functions. The Rayleigh Ritz method produces orthogonal estimates for the first $N_r + 1$ mode shapes, since $N_r + 1$ shape functions were initially assumed. Any Ritz mode shape, $\Phi(x)$, may be expressed as a linear combination of the assumed shape functions

$$\Phi_k(x) = \sum_{i=1}^{N_r} a_{i,k} \phi_i(x) + \psi(x) \qquad k = 1, 2, \cdots, N_r + 1 \tag{4.37}$$

Clearly, the first N_r mode shapes will be given by the exact mode shapes so that

$$\Phi_1(x) = \phi_1(x) \tag{4.38}$$

$$\Phi_2(x) = \phi_2(x) \tag{4.39}$$

$$\cdots \tag{4.40}$$

$$\Phi_{N_r}(x) = \phi_{N_r}(x) \tag{4.41}$$

Finally, in addition to the N_r dynamic mode shapes, there is an additional mode which by the Rayleigh Ritz method is made orthogonal to the other modes yielding

$$\phi_i^T M \Phi_{N_r+1} = 0 \qquad i = 1, 2, \cdots, N_r \tag{4.42}$$

which produces an expression for a_{i,N_r+1}

$$a_{i,N_r+1} = -\phi_i^T M \psi \qquad i = 1, 2, \cdots, N_r + 1 \tag{4.43}$$

Using Equation 4.10 or 4.11 to substitute for the static deflection shape in terms of all the modes

$$a_{i,N_r+1} = -\phi_i^T M \sum_{m=1}^{N} \frac{\Xi_m}{\omega_m^2} \phi_m = -\frac{\Xi_i}{\omega_i^2} \tag{4.44}$$

and hence solving Equation 4.37 for Φ_{N_r+1}

$$\Phi_{N_r+1}(x) = \sum_{i=1}^{N_r} -\frac{\Xi_i}{\omega_i^2}\phi_i(x) + \sum_{i=1}^{N} \frac{\Xi_i}{\omega_i^2}\phi_i(x) = \sum_{i=N_r+1}^{N} \frac{\Xi_i}{\omega_i^2}\phi_i(x) \tag{4.45}$$

Expressing q in terms of the Ritz predicted modes

$$q(x,t) = \sum_{k=1}^{N_r+1} \Phi_k \xi_k \tag{4.46}$$

$$= \sum_{k=1}^{N_r} \phi_k \xi_k + \Phi_{N_r+1}\xi_{N_r+1} \tag{4.47}$$

$$= \sum_{k=1}^{N_r} \phi_k(x)\xi_k + \sum_{i=N_r+1}^{N} \frac{\Xi_i}{\omega_i^2}\phi_i(x) \tag{4.48}$$

which shows that using a static deflection shape in a Ritz method is just another implementation of the second approach given by Equation 4.19. The $(N_r+1)^{th}$ mode retains the static deflection information from all the truncated modes.

The same procedure can be used with a Finite Element model. If N modes are calculated and N_r retained, the static correction mode can be found by calculating the static deflection ψ_j and orthogonalizing it to the retained modes using Equations 4.37 and 4.43.

The previous three methods correct the response fro the static behavior of the truncated modesby means of a static feedthrough term that is added to the transfer function response so that the static behavior, the dc response, is correct at the sensor location. In a state space model description, this would correspond to adjusting the D matrix given the system of equations

$$\dot{x} = Ax + Bu \tag{4.49}$$

$$y = Cx + Du. \tag{4.50}$$

Note that this method does not augment the system order.

The inclusion of the static behavior can not improve convergence in the case of a distributed load that can be decomposed into a finite set of mode shape basis functions which all lie in the set of retained modes. One other instance where the static deflection does not help convergence is when the truncated mode shape contributing to the static deflection shape is unobservable from the sensor.

The effect of truncating modes well above the bandwidth, without taking steps to retain their static correction, is to remove a small static contribution of that truncated mode to the predicted system response. The effect on the zero is to over- or underpredict it, depending on the type of modelling scheme being used. An example is now given to show the improved zero convergence achieved by including the static information in the models. A clamped-free Bernoulli-Euler beam with a collocated transverse displacement/force S/A pair at the free end is the system to be modelled. A Rayleigh Ritz assumed modes method is used. This problem is therefore identical to example one of Section 4.1, except that one of the assumed modes is now the static deflection shape of the clamped-free beam with a tip force. The results of the zero predictions are shown for the first two zeroes in Figure 4.4. The zero predictions for the Rayleigh Ritz model without the static mode shape is included for comparison. The zeroes are plotted as a function of the number of assumed modes. For the case of the static deflection shape included, $N_r - 1$ dynamic mode shapes are included along with the static deflection shape. The RR model including the static deflection shape predicts the zeroes extremely well. There is an approximate improvement of four orders of magnitude between the Rayleigh Ritz model without and with the static deflection shape. The convergence *rate* of the RR assumed modes model which includes the static deflection shape is also much faster than that of the model without. The convergence rate of the zero prediction does not decrease as the zero number increases. The effect of the complete static information appears to improve the zero predictions uniformly for successive zero number.

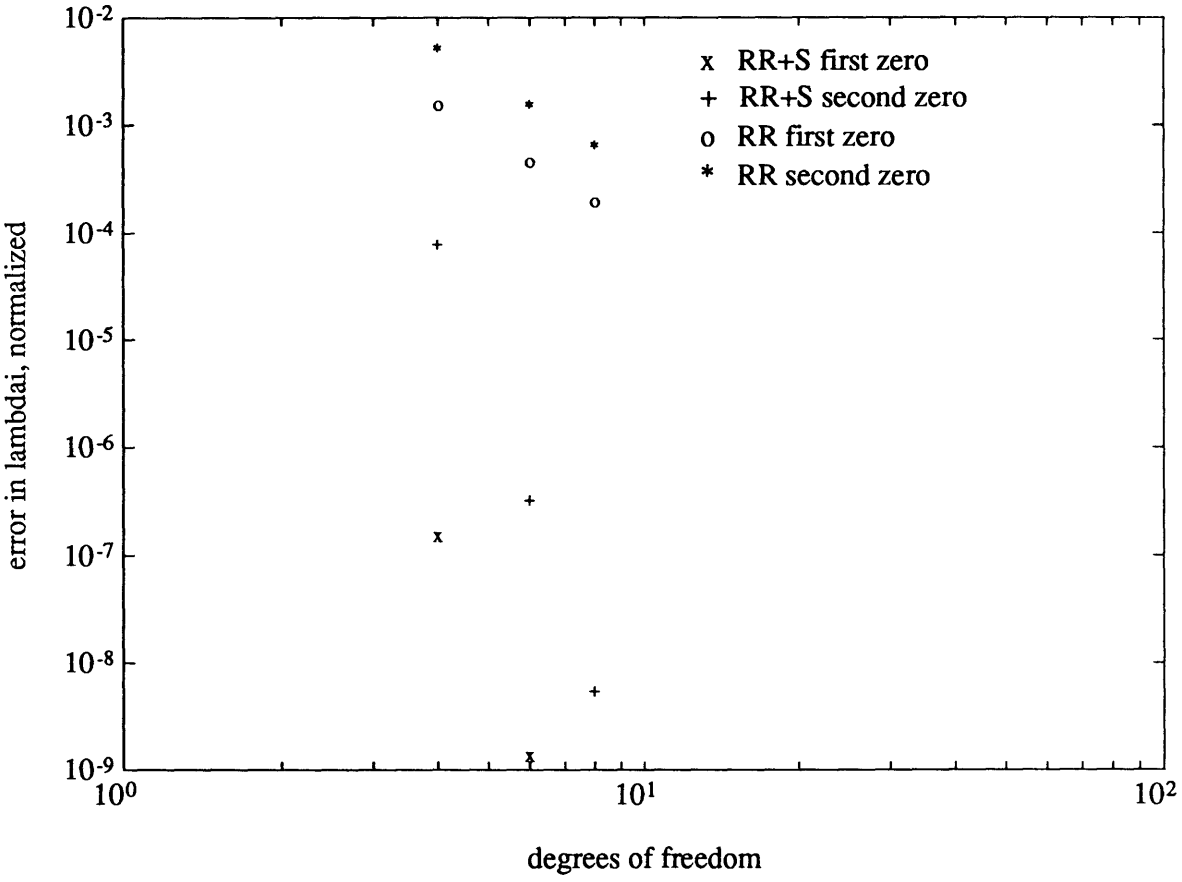

Figure 4.4: First and second zero of a clamped-free beam with collocated tip tranverse displacement/force S/A pair, Rayleigh Ritz model with (x,+) and without (o,*) static deflection shape incorporated as an additional assumed mode shape.

The ability to improve the zero convergence rate by including the deflection shape corresponding to the static deflection given a load entering at the actuator location, motivates a look at the adjoint system. A deflection shape corresponding to imposing a unit displacement at the sensor location could be included in the model, which would correspond in a sense to the observability properties. For the collocated case these coincide. For the non-collocated case they would not. The inclusion of the static deflection shape corresponding to a unit load at the actuator location is only appropriate when the actuator is a low impedance actuator. A high impedance actuator would require a static deflection shape corresponding to a unit displacement deflection at the actuator location.

Truncating higher modes without retaining the static contribution of the truncated modes removes residual stiffness of these modes and adversely influences the prediction of zeroes. The solution for such truncation is straightforward and can be done using one of the two generalized approaches outlined provided the truncated modes are above the frequency range of interest. The second type of truncation, where the "best" N_r modes are chosen for a model, may result in modes which are truncated which fall below, within, and above the bandwidth within which the zeroes need to be well predicted.

To determine the effect of such truncation it is necessary to evaluate why certain modes would not be included in a model. Modal Cost Analysis (MCA) [38] is a method for evaluating modes for truncation. The cost of mode i, V_i is given by

$$V_i = \frac{1}{4\zeta_i\omega_i^3}[p_i^T Q p_i + r_i^T Q r_i \omega_i^2](b_i^T W b_i) \tag{4.51}$$

where Q is the output penalty matrix, ω_i is the frequency of mode i, ζ_i is the modal damping of mode i, W is the intensity of the zero mean uncorrelated white noise at the control input location, b_i is the control influence vector, and p_i, r_i are the measurement vectors of the displacement and rate states. For control system design, modes which have a low disturbability, low observability, high damping, or high frequency can be seen to have low modal cost and hence are candidates for truncation. The question

is then, does a low modal cost also mean that the contribution of that mode to the zero predictions in the bandwidth is also negligible. This is clearly not the case. The modal cost is not a measure of the importance of the mode for zero predictions. A mode which may have low disturbability from a disturbance location may be highly observable and controllable and have a non-negligible modal residue. A mode which is only slightly observable may indeed have a low modal residue but depending on the rate of change of the transfer function or singular values with respect to frequency, a small modal residue could alter the frequency of the zero by a worthwhile amount. Modes with high damping are just as likely to affect zeroes away from their corner frequencies as modes with low damping.

The issue in this type of truncation however is no longer a simple question of the residual stiffness. There are three zones where modes can be truncated, modes occuring above, below, and within the bandwidth. Modes above the bandwidth contribute a static stiffness term which can be compensated for by explicitly ensuring that the static contribution of the truncated modes is included in the model as was shown in Equations 4.17, 4.18 and 4.19, 4.20. Truncation of modes below the bandwidth removes an inertia contribution as described in Equation 4.35. Modes truncated within the bandwidth however are more difficult to correct for.

Such truncation in the bandwidth does not affect all zeroes equally. Pole cancellation zeroes, the limiting case of a transmission zero are due to the loss of observability or controllability of a particular mode and not on a summation of the contributions of other modal responses. Transmission zeroes however will be affected by such truncation methods.

Figure 4.5 shows a typical mode in the bandwidth that is to be truncated. For frequencies well below its natural frequency, it acts like a pure stiffness and for frequencies well above it, it behaves as a pure inertia. If the mode is modelled as providing a pure static contribution, its effect is mismodelled for frequencies above its natural frequency. It could be modelled as having a pure static contribution below

its natural frequency and having no contribution above its natural frequency. The effect of a direct feedthrough from the input to the output like a residual stiffness would be captured in the state space form by the D matrix. Modelling this truncated mode in the bandwidth by a step change in the static stiffness corresponds to a D matrix that is a function of frequency, in this case, a step function. For frequencies below the truncated mode, the D matrix would have a certain value to match the static stiffness including the mode, and above the truncated mode, the D matrix would be discounted by the static contribution of that mode. These two methods of truncating a mode within the bandwidth ensure that the model order is reduced but it is hoped that the ability to improve the accuracy of the zero prediction is still improved.

The effects on the zeroes of the two types of truncation have been explored. For any type of truncation, as more modes are included in the model, the zeroes predicted approach the exact zeroes. The truncation type corresponding to the retension of the first N_r modes results in the truncated modes contributing a simple stiffness to the response in the bandwidth. By fourier arguments, or based on experience from other disciplines, it was shown that inclusion of the complete static deflection information speeds both the convergence and the convergence rate of the zeroes. The convergence rate of the zeroes is improved for all the zeroes by the inclusion of the complete static information. If however truncation does not occur above the bandwidth, compensation for such lost modes is necessary to ensure quick convergence of the zeroes. Such compensation may involve a frequency dependent D term. Model order reduction for control system design is not necessaarily consistent with the objective of accurate prediction of the zeroes.

4.3 Model Discretization Effects

Both truncation and discretization result in errors in the prediction of zeroes. For example, in the case of an assumed displacement based model with compatible dis-

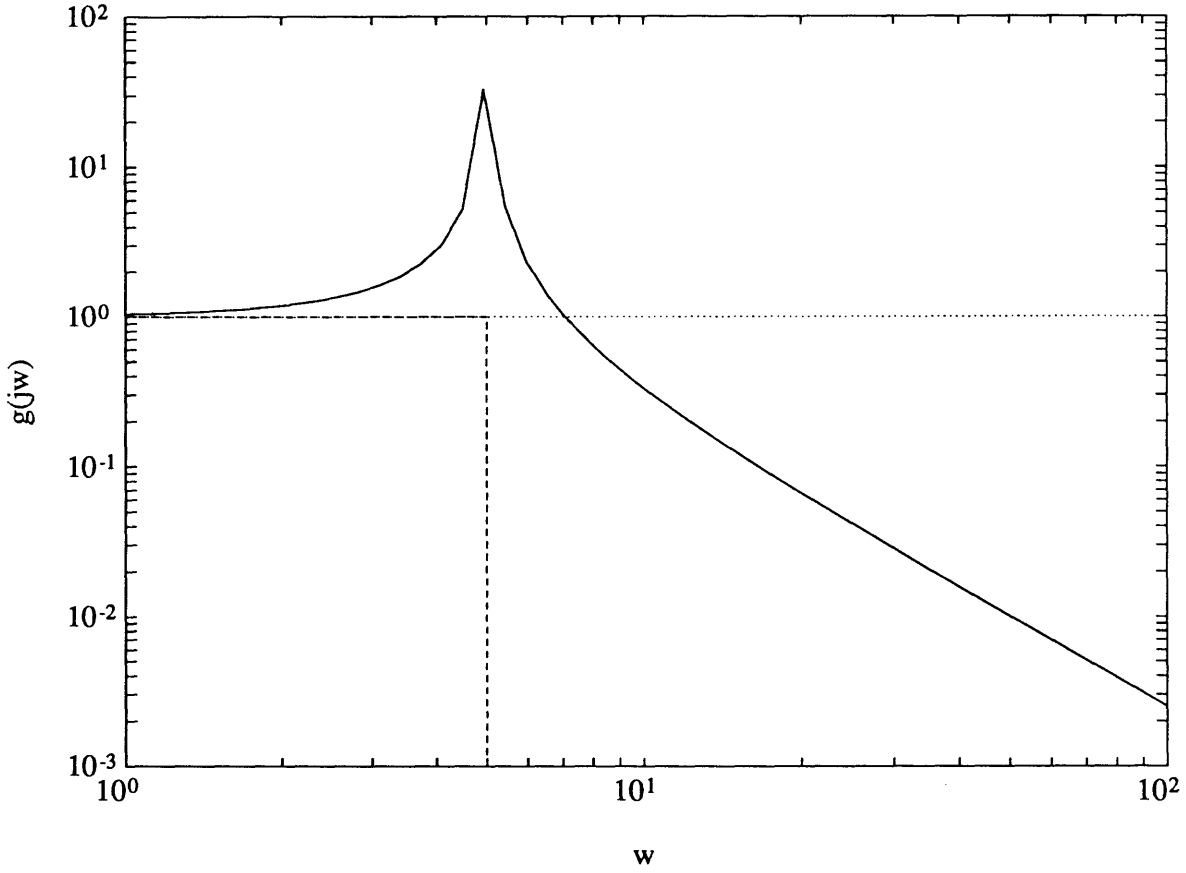

Figure 4.5: Compensating for a Mode Truncated in the Bandwidth

placements and consistent masses, the zeroes will be overestimated due to constraints on the allowable displacements. A Rayleigh Ritz assumed modes model allows only certain constrianed displacements. A compatible displacement based Finite Element model describes the system by only a finite set of points, producing further constraints. These constraints tend to stiffen the system and hence overestimate the eigenfrequencies. The zeroes, being the eigenfrequencies of the infinite gain closed loop system, are overpredicted as well.

Discretization has two constraining influences, a local constraint, and global constraint. One aspect of discretization involves the fidelity of assumed distribution functions within. The second aspect of discretization is that the continuum to be modelled is described by a finite set of points on the structure. This is the global constraint of discretization, the description of the spatial field by a finite set of sampled points and parameters. The influence of these two constraints on the calculation of zeroes are the focus of this section.

The effects of such discretization are studied by means of an example. The effect of local fidelity is studied by considering two different interpolation functions, and comparing the convergence behavior of the zero predictions. Compatible, consistent, cubic and quintic assumed displacement function elements are assumed for a uniform clamped-free Bernoulli-Euler beam with dual displacement /force S/A pair at the tip. For loads entering the structure at the nodes, the cubic beam element can capture the static information exactly. Unlike a Rayleigh Ritz assumed modes model which only includes dynamic modes, a Finite Element model inherently contains static information, if not exactly then at least approximately over each element. By comparing the performance of these two element types with a Rayleigh Ritz assumed modes model including a static deflection shape, the effect of the local fidelity may be isolated.

To make such a comparison equitable, models of the same number of unconstrained degrees of freedom (or states) must be compared. For the Finite Element models, the

zero predictions are plotted as a function of the number of degrees of freedom (dofs). For the Rayleigh Ritz model, $N_r - 1$ dynamic modes and one static modeare used, and the results are plotted as a function of N_r.

The results are shown in Figure 4.6 for the Rayleigh Ritz model, the cubic and quintic Finite Element models. The convergence rate of the quintic beam element is faster than that of the cubic. This may be seen by the average slope of the zero predictions as a function of the number of degrees of freedom. Looking at the fundamental zero prediction, an order of magnitude improvement in the error is visible for low order models when the cubic and quintic are compared. Due to the higher convergence rate of the quintic, the improvement grows with increasing number of dofs. Using a cubic element, the second zero prediction has an error of 10%. While the higher order interpolation functions allow a more accurate approximation to the mode shape locally, the higher order polynomials make the system matrices less banded and increase the computation required for solution. [39].

The effect of discretization of the field, or global fidelity, may also be seen in Figure 4.6. The Finite Element and Rayleigh Ritz models both contain the exact static deformation shape, and are compared for the same number of degrees of freedom. The remaining discrepancy between the models' zero predictions is due solely to the discretization of the spatial field and the nature of the assumed displacement functions. For a given interpolation function, as the number of degrees of freedom is increased, the convergence of the Rayleigh Ritz model is consistently better than the Finite Element. The performance of the zero prediction clearly increases as the fidelity of the representation of the spatial field increases.

The two types of discretization effects on the zeroes, namely, fidelity on the global level by number of nodal points, and fidelity on the local level by order of interpolation functions have been examined. The zeroes predicted from a model are improved as both the number of degrees of freedom is increased, and as the order of the interpolation functions used is increased.

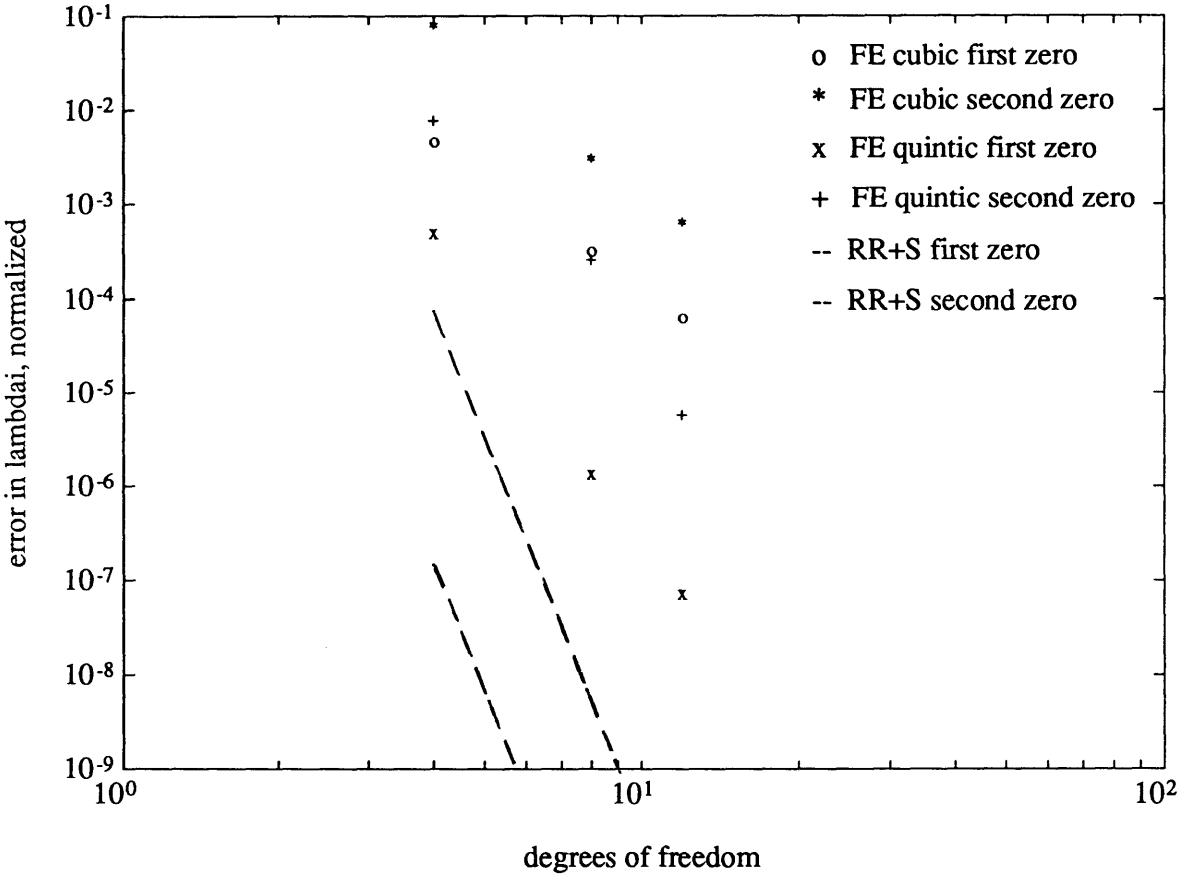

Figure 4.6: First and second zero predictions of Finite Element cubic and quintic displacement function models, and Rayleigh Ritz exact assumed modes with a static mode model

Now that the effects of truncation and discretization have been explored, it is desirable to show that a truncated low order model can effectively capture the zeroes by incorporating both high fidelity modes and the complete static information. The same clamped-free beam with transverse displacement/force tip S/A pair is used again. A cubic assumed displacement Finite Element model is adopted which includes the residual stiffness to ensure that the complete static information is maintained in the model even as the modes are truncated from the model. A 20 unconstrained degree of freedom (ten element) model is used to discretize the structure. This 20 degree of freedom model produces an initial set of 20 dynamic mode shapes. This set of 20 modes is then truncated to N_r retained modes, the residual stiffness is included in the model, and the first and second zero are calculated. Figure 4.7(a) shows the first and second zero as a function of the number of retained modes. At most 20 modes are included and hence there is a lower limit to the error in the zero prediction at about 10^{-5} and 10^{-4} for the first and second zero respectively. This limit is represented by dashed lines. The first and second zero predictions for the truncated models quickly approach the value predicted by a model of 20 modes. A model with only six retained modes with a fidelity of 20 nodal dofs and the residual stiffness included performs as well in predicting the first two zeroes as a model with 20 modes.

In this chapter, the effects of modelling on the zeroes have been examined. The zeores converge in the same manner as the poles for a given modelling scheme. This convergence property of the zeroes is valid for a system with collocated and dual sensors and actuators, and for systems with unobservable or uncontrollable modes. The effects of truncation of modes above the bandwidth removes a static stiffness contribution. Including the complete static deflection information improves fourier convergence of the system response and the zeroes in particular. This can be done via an additional assumed mode or modes corresponding to the static deflection or by including the residual stiffness correction as a feedthrough term in the D matrix.

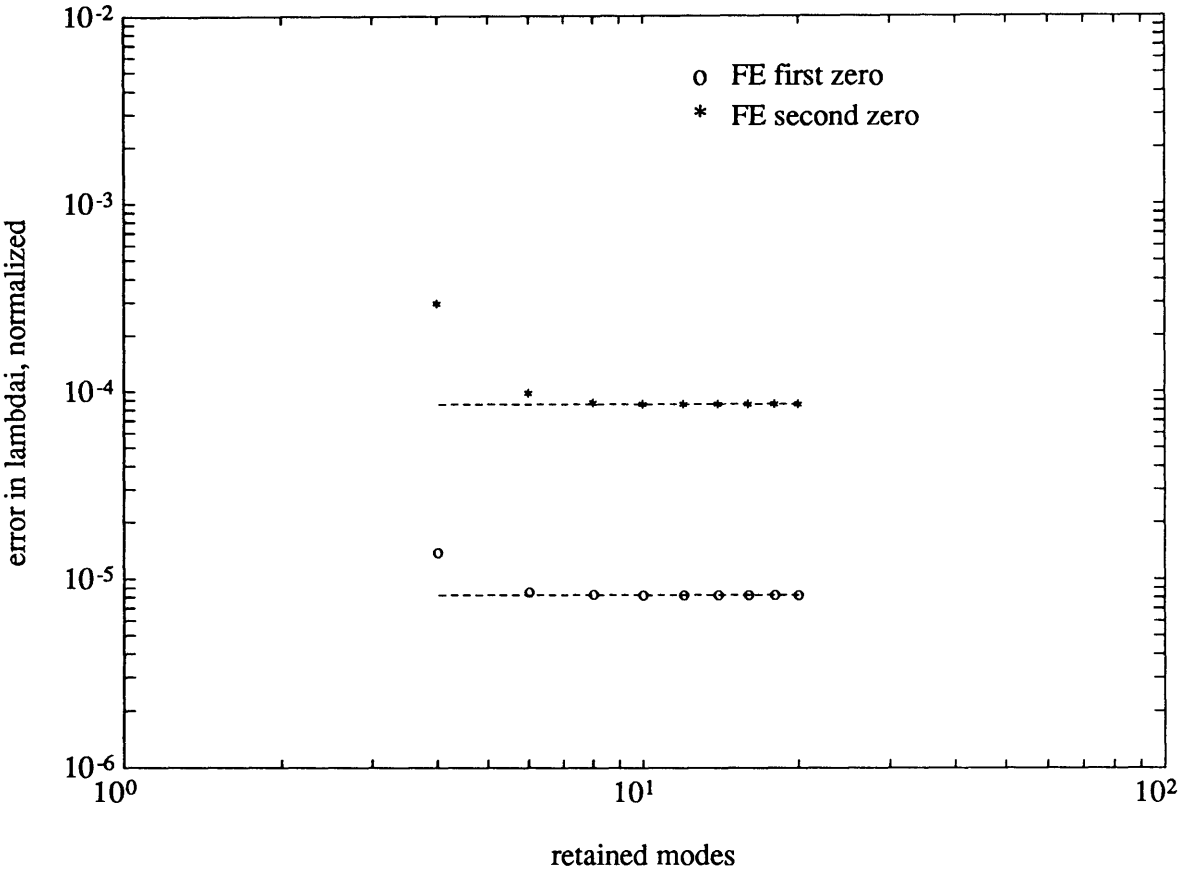

Figure 4.7: Zero predictions of Finite Element cubic displacement function model as a function of number of retained modes, N_r, with residual stiffness included. The number of modes in the original model, N is twenty.

Truncation in the bandwidth of modes deemed unimportant in the control design problem are not necessarily unimportant in the accurate prediction of system zeroes. Modes truncated in the bandwidth needs to be compensated for by a D matrix that may be frequency dependent. The effects of discretization showed that both higher frequency sampling of the spatial field and higher fidelity of the interpolation functions improve zero predictions. Zeroes can be well predicted with a few high fidelity dynamic modes and the static behavior of the structure to the control inputs.

Chapter 5

Conclusions and Recommendations

Conclusions

The effects on the zeroes of both physical design of the actuation and measurement schemes as well as structural modelling methods have been explored. The relative position of the zeroes to the poles is an easily measurable and physically significant measure of the modal observability and controllability. There are two types of zeroes for the square case, pole-cancellation zeroes and transmission zeroes where the pole-cancellation zeroes are the limiting case of the a transmission zero as the observability or controllability tends to zero.

The definition of a zero may take several forms and for the square case, four definitions of the transmission and pole-cancellation zereos were given and shown to be equivalent. Any of these zero definitions may be used to study the characteristics of zeroes, whichever tends to be most convenient. The definitions were evaluated for their ability to provide additional information such as controllability and observability. Both SISO and MIMO definitions were presented.

After using the various definitions in different studies, the definitions may be classified for utility in addressing issues. The residue expansion definition of a zero is in a convenient form for exploring zero characteristics in terms of modal contributions. The transmission blocking zero definition has the advantage of an explicit solution to the zero in addition to the zero direction information. The root locus definition is a convenient form for physical understanding of the interaction of input and output.

By using the transmission blocking definition, a sensitivity analysis was performed on the zeroes. The zeroes for a collocated and dual sensor and actuator pair are insensitive to changes in the actuation and measurement locations in the vicinity of a node, or a pole-zero cancellation corresponding to a simultaneous loss of observability and controllability. The sensitivity of the zeroes for non-collocated and /or non-dual sensor and actuator pairs is non-zero at pole-cancellation zeroes. The tests for modal observability and controllability given by the zero directions become more sensitive when the zero spacing is close.

All of the zero definitions specify that the zeores are a function of the actuation and measurement mechanisms in addition to the structure to which they are coupled. Sensors and actuators were then evaluated as input /output pairs by considering three characteristics of a sensor or actuator: type, impedance of the actuator or sensor relative to the structure, and location.

While collocated and dual sensors and actuators are guaranteed to produce alternating poles and zeroes for any structure on which they act, another set of collocated sensors and actuators called pseudo-dual can guarantee such pole-zero patterns on particular structures. Collocated and dual sensors and actuators which operate on modes separated by two spatial derivatives will produce alternating pole-zero patterns on both purely sinusoidal and purely exponential structures. Collocated and dual sensor and actuator pairs which operate on modes separated by one spatial derivative can never produce alternating pole-zero patterns on structures governed by purely sinusoidal mode shapes, although may produce alternating pole-zero patterns on structures governed by exponential mode shapes, if the exponential behavior is always consistently increasing or decreasing. The residue expansion definition of a zero was used.

The impedance of the actuator and impedance of the sensor relative to the structure were studied parametrically via a simple reduced order model. All dual, and collocated pairs produce alternating pole-zero patterns in the most general sense.

Dual, positive complementary, and collocated S/A pairs ensure alternating pole-zero patterns, save pole-zero cancellation at the center of the spectrum. Increasing the impedance of positive complementary, dual, and collocated S/A pairs from low impedance complementary extremes causes all of the zeroes to decrease. The relative pole-zero spacing is largest at the complementary extremes, and is smallest (pole-zero cancellation) when the complements are at the center of the spectrum. Positive non-complementary, dual, and collocated S/A pairs still yield alternating pole-zero patterns, save pole-zero cancellations. Negative complements and non-complements may produce alternating pole-zero patterns as well. However, for certain combinations of measurement, a non-minimum phase plant may arise. The non-minimum phase zero is furthest away from the imaginary axis when d' is small. Traversing the positive sensor spectrum of a dual S/A pair while leaving the relative impedance of the actuator fixed, or vice versa, produces this same effect of stiffening or destiffening all of the zeroes consistently. The average slope of the transfer function may be altered by varying relative spacing of the poles and zeroes in such a manner.

A study of sensor and actuator location was performed as the dual sensor and actuator positions were varied parametrically on a variety of structures. An infinite order model was used to remove truncation effects. The zero trajectories as a function of spanwise location of the collocated sensor and actuator pair appear similar to the mode shape squared. The migration of the zeroes for collocated and dual S/A pairs are bounded by the poles immediately above and below, irrespective of the rigid body or constrained behavior of the system. The zero migrations for the unconstrained structure are smaller relatively to the pole spacing than those for corresponding constrained systems.

As the sensor and actuator pair become non-collocated, the zeroes increase in frequency, and for certain structures become non-minimum phase. The non-minimum phase zeroes become of lower freqeuncy as the non-collocation distance increased. The root locus definition of a zero was used to determine the zeroes for both the collocated

and non-collocated cases.

The zeroes have increased sensitivity to the collocated sensor and actuator pair location with increasing zero number. The zeroes also have zero sensitivity to sensor and actuator pair location in the vicinity of a pole-zero cancellation, i.e., a node location when the sensor and actuator are collocated.

In addition to the actuation and measurement mechanisms and the nature of the structure, the zeroes are a function of the modelling scheme used to predict the behavior of the structure. It was proven that for collocated and dual point sensors and actuators that the zeroes converge in the same manner as the poles for a given structural modelling method as the number of degrees of freedom in the model is increased. Improvement in the zero predictions for a given number of modelled modes may be accomplished by including the static deflection information into the model. High fidelity mode shapes improve the zero predicitions for a given order of the system. In particular, higher order interpolation functions improve the zero predictions for a given number of degrees of freedom. Hence for a high fidelity model in the control bandwidth, a low order model with high fidelity mode shapes and the complete static information should be used. Model order reduction accomplished by truncating modes in the bandwidth is not necessarily compatible with accurate prediction of the zeroes in the bandwidth.

Recommendations

The issues of type, impedance of the sensor and actuator relstive to the structure, and location may be explored further. Distributed sensors and actuators as well as high order dual pairs should be investigated. Non-dual sensor and actuator pairs may be investigated for their ability to induce missing zeroes to allow a possible gain stabilized controller roll off.

The impedance of sensor and actuator can be extended by a more detailed structural model as well as a dynamic model of the actuator. The full effect of controlling the relative spacing of the poles and zeroes for controlling hte backbone of the transfer

function may be the basis of a verification and control design experiment.

The parametric dependence of the zeroes on location may be extended to collocated and but non-dual systems. Will the relative pole-zero spacing be some coupling of both mode shape types? Will there be non-minimum phase zeroes? Sensor and actuator pairs on particular structures will need ot be classified into categories whcih would or would not produce non-minimum phase zeroes.

The tradeoff between sensitivity of the zero to sensor and actuator locations at particular structural locations and modal controllability and observability may be incorporated into an optimization problem to place sensors and actuators most effectively.

For large non-collocation distances it would be useful to generalize a test for the type of structure which will yield non-minimum phase zeroes and which not. The behavior of these real zeroes as a function of the damping level in the structure should be investigated.

As for the modelling methods and errors introduced in predicting the zeroes, it is recommended to investigate in particular the non-collocated and non-dual sensor and actuator pair cases. Finite order modelling of a non-collocated system may predict non-minimum phase zeroes which are actually only a product of truncation.

Truncating modes in the bandwidth should be studied to produce viable methods for ensuring minimal disruption of the other dynamics in the model.

Modelling was approached for force type actuators and displacement type sensors. Issues involved with displacement type actuators and force sensors may be investigated as well.

Bibliography

[1] Freudenberg and Looze, "Right Half Plane Poles and Zeroes and Design Tradeoffs in Feedback Systems," IEEE Transactions on Automatic Control, Vol. AC-30, No. 6, January, 1985.

[2] Gevarter, W. B., "Basic Relations of Flexible Vehicles," *AIAA Journal*, Vol. 8, No. 4, April, 1970, pp. 666-672.

[3] Martin, G.D., "On The Control of Flexible Mechanical Systems, "Ph.D. Dissertation, Department of Aeronautics and Astronautics, Stanford, CA, SUDAAR 511, May, 1978.

[4] Cannon, R.H. and D.F. Rosenthal, "Experiments in Control of Flexible Structures with Non-Collocated Sensors and Actuators," Journal of Guidance Control and Dynamics, Vol. 7, No. 5, Sept.-Oct., 1984, pp. 546-553.

[5] Safonov, M. G. and H. Flashner, "Modeling and Robustness Issues in Control Design for Flexible Structures," ACC, 1989, pp. 2527-2531.

[6] Stieber, Michael, E., "Sensors, Actuators, and Hyperstability of Structures," *AIAA Guidance, Navigation and Control Conference, 1988.* Paper No. 88-4047-CP.

[7] Blackwood, G. H., C.-C. Chu, J. L. Fanson, and S. W. Sirlin, "Uncertainty Modelling for the Control of an Active Structure," presented at the Winter Annual Meeting of the American Society of Mechanical Engineers, San Francisco, CA, Dec., 1989.

[8] Kosut, R. L., Salzwedel, H., and A. Emami-Naeini, "Robust Control of Flexible Spacecraft," *Journal of Guidance Control and Dynamics*, Vol. 6, No. 2, March-April, 1983, pp. 104-111.

[9] Stein, G., and M. Athans, "The LQG/LTR Procedure for Multivariable Feedback Control Design," *IEEE Transactions on Automatic Control*, Vol. AC-32, No. 2, February, 1984.

[10] Aubrun, J.-N., Ratner, M. J., and M. G. Lyons, "Structural Control for a Circular Plate," *Journal of Guidance, Control, and Dynamics*, Vol. 7, No. 5, Sept.-Oct., 1984, pp. 535-545.

[11] Juang, J.-N., Horta, L. G., and H. H. Robertshaw, "A Slewing Control Experiment for Flexible Structures," *Journal of Guidance Control and Dynamics*, Vol. 9, No. 5, Sept.-Oct., 1986, pp. 599-607.

[12] deLuis, J. et. al., "Design and Implementation of Optimal Controllers for Intelligent Structures Using Infinite Order Structural Models", Space Systems Laboratory Report #3-89, Ph.D. Thesis, Massachusetts Institute of Technology, Jan., 1989.

[13] Fanson, J. L., G. H. Blackwood, and C.-C. Chu, "Active Member Control of Precision Structures," *Proceedings of the 30th Structures, Structural Dynamics, and Materials Conference*, Mobile, AL, 1989, Paper No. 89-1329, pp. 1480-1494.

[14] Williams, Trevor, "Transmission-Zero Bounds for Large Space Structures, with Applications," *Journal of Guidance, Control, and Dynamics*, Vol. 12, No. 1, Jan.-Feb., 1989, pp. 33-38.

[15] Wie, B., "On the Modelling and Control of Flexible Space Structures," Guidance and Control Laboratory, Department of Aeronautics and Astronautics, Stanford University, Stanford, California, SUDAAR report no. 525, June, 1981.

[16] Spector, V. A. and H. Flashner, "Modeling of Non-Collocated Structural Control Systems," AIAA Guidance Navigation and Control Conference, 1988, Paper No. 88-4060.

[17] Hughes, P. C. and R. E. Skelton, "Controllability and Observability of Linear Matrix-Second-Order Systems," Journal of Applied Mechanics, Vol. 47, No.2, June, 1980, pp. 415-420.

[18] Schrader, C. B., and M. K. Sain, "Research on System Zeros: A Survey," *International Journal of Control*, Vol. 50, No. 4, 1989, pp. 1407-1433.

[19] Kwakernaak, H., and R. Siven, *Linear Optimal Control Systems*, Wiley-Interscience, New York, NY, 1972.

[20] Emami-Naeini, A., and S. M. Rock, "On Asymptotic Behavior of Non-Square Linear Optimal Regulators," *Proceedings of 23rd Conference on Decision and Control*, Las Vegas, NV, December 1984, pp. 1762-1763.

[21] Hallauer, W. L., Jr., nad G. R. Skidmore, "Experimental-Theoretical Study of Active Damping with Dual Sensors and Actuators," *Proceedings of AIAA Guidance, Navigation and Control Conference*, 1985, Paper No. 85-1921, pp. 433-442.

[22] Lazarus, K. B., "Induced Strain Actuation of Composite Plates," Gas Turbine Laboratory Report #197, S.M. Thesis, Massachusetts Institute ofTechnology, March, 1989.

[23] Anderson, E., "Piezoceramic Actuation of One- and Two- Dimensional Structures," Space Systems Laboratory Report #5-89, S.M. Thesis, Massachusetts Institute of Technology, Jan., 1989.

[24] Blackwood, G. H., and F. M. Fleming, "Characterization of Transverse Field-Induced Strain in PMN:BA Electroceramic Plates," Space Engineering Research Center Report #7-90-I, Massachusetts Institute of Technology, July, 1990.

[25] Liang, C., Jia, J., and C. Rogers, "Behavior of Shape Memory Alloy Reinforced Composite Plates Part II: Results," *Proceedings of the 30th Structures, Structural Dynamics, and Materials Conference*, Mobile, AL, 1989, Paper No. 89-1331-CP, pp. 1504-1513.

[26] Hagood, N. W., "Experimental Investigation into Passive Damping Enhancement for Space Structures," *Proceedings of the AIAA Guidance Navigation and Control Conference*, August, 1989, Paper No. 89-3436, accepted JGCD

[27] Warkentin, D., "Embedded Electronics for Intelligent Structures," Massachusetts Institute of Technology S.M. Thesis, January, 1991.

[28] Chen, G.-S., Lurie, B. J., and B. K. Wada, "Experimental Studies of Adaptive Structures for Precision Performance," *Proceedings of the 30th Structures, Structural Dynamics, and Materials Conference*, Mobile, AL, 1989, Paper No. 89-1327, pp. 1462-1472.

[29] Williams, T. and Jer-Nan Juang, Pole/Zero Cancellations in Flexible Space Structures," *Journal of Guidance, Control, and Dynamics*, Vol. 13, No. 4, July-Aug., 1990, pp. 684-690.

[30] Park, J.-H., and H. Asada, "Design and Analysis of Flexible Arms for Minimum-Phase Endpoint Control," *Proceedings of the American Control Conference*, 1990, pp. 1220-1225.

[31] Meirovitch, L., *Analytical Methods in Vibrations*, MacMillan Publishing Co., Inc., New York, NY, 1967.

[32] Williams, T., "Model Order Effects on the Transmission Zeros of Flexible Space Structures," *Proceedings of the American Control Conference*, 1990, pp. 876-877.

[33] Meirovitch, L., *Elements of Vibration Analysis*, 2d ed., McGraw-Hill Book Co., New York, NY, 1986.

[34] Bathe, K.-J., *Finite Element Procedures in Engineering Analysis*, Prentice-Hall, Inc., Englewood Cliffs, NJ, 1982.

[35] Desai, and Abel, *Introduction to the Finite Element Method*, Van Nostrand Reinhold Co., New York, NY, 1972.

[36] Bisplinghoff, R. L., Ashley, H., and R. L. Halfman, *Aeroelasticity*, Addison-Wesley Publishing Co., Reading, MA, 1955.

[37] Ewins, D. J., *Modal Testing: Theory and Practice*, John Wiley and Sons, Inc., New York, NY, 1984.

[38] Skelton, R. E., P.C. Hughes and H.B. Hablani, "Order Reduction for Models of Space Structures Using Modal Cost Analysis," *Journal of Guidance, Dynamics, and Control*, Vol. 5, No. 4, July-Aug., 1982, pp. 351-357.

[39] Strang, G., *Introduction to Applied Mathematics*, Wellesley-Cambridge Press, Wellesley, MA:1986.

[40] Blevins, R. D., *Formulas for Frequency and Mode Shape*, Robert Krieger Publishing Co., Inc., Malabar, FL:1979.

[41] Craig, Jr., R. R., *Structural Dynamics:An Introduction to Computer Methods*, John Wiley and Sons, Inc., New York, NY:1981.

[42] Atluri, S. N., and A. K. Amos, editors, *Large Space Structures: Dynamics and Control*, Springer-Verlag:1988.

[43] Kailath, T., *Linear Systems*, Prentice-Hall, Inc., Englewood Cliffs, NJ:1980.